UKAEA FUS 546

EURATOM/UKAEA Fusion

Revisions and improvements of neutron capture cross sections for EAF-2009 and validation of TALYS calculations

R.A. Forrest, J Kopecky and A.J. Koning

March 2008

EURATOM/UKAEA Fusion Association

Culham Science Centre

Abingdon

Oxfordshire

OX14 3DB

United Kingdom

Telephone: +44 1235 466586

Fax: +44 1235 466435

UKAEA

Fusion Working in Europe


UKAEA
Fusion
Working
in Europe

Revisions and improvements of neutron capture cross sections for EAF-2009 and validation of TALYS calculations

R. A. Forrest[1], J. Kopecky[2] and A.J. Koning[3]

[1]EURATOM/UKAEA Fusion Association, Culham Science Centre, Abingdon, Oxfordshire, OX14 3DB, UK.
[2]JUKO Research, Kalmanstraat 4, 1817 HX Alkmaar, The Netherlands.
[3]NRG Group, P.O. Box 25, NL-1755 ZG Petten, The Netherlands

Abstract

The European Activation File EAF-2007 forms a comprehensive data library for activation cross sections covering all stable and radioactive targets (including isomers) with half-lives > 6 hours (816 targets in total) with cross sections in the energy range between 10^{-5} eV and 60 MeV. The underlying capture cross sections file is unique for its completeness, including 1,054 reactions on 812 targets. The summed reactions on 475 targets are supported by experimental data (differential or integral) with the remaining 337 reactions having no experimental support. It is a primary goal of any data library to assign a degree of quality assurance and to justify the expected level of cross section predictability. The tools used for capture cross section calculations or validations are reviewed. The completeness of the neutron capture data with no experimental support forms a perfect object for testing the global performance of the available calculation tools and based on this to assign the cross section uncertainty to the above 337 reactions in a quantitative way. The recent version of EAF (EAF-2007) has been used for a detailed data quality survey and further the recent data source, calculated by the modelling code TALYS-1.0, has been tested and validated. Conclusions are drawn about the predictability power of the TALYS calculations with global parameters and suggestions for improvements for the EAF-2009 release are included.

1. Introduction

The most straightforward validation of calculated neutron capture cross sections is a direct comparison with differential data. These data can be divided into five major energy regions: the thermal cross section at 0.0253 eV, the resolved resonance region up to the energy E_H, the 30 keV data point measured primarily for astrophysical applications, averaged cross sections measured in the region of the smooth statistical component (E_H to several MeV) and finally the pre-equilibrium region around 14 MeV. For cross section data with no experimental information, three cross section estimates or systematic have been derived; σ_{th} - an estimate at 0.0253 eV, σ_{30} - the systematic at 30 keV and $\sigma_{14.5}$ - the systematic at 14.5 MeV and these have been used for validation.

Special attention has always been devoted to the (n,γ) reactions within the EAF project, due to the experience of one of the EAF team members. This resulted in two earlier reports describing the unique methods of data treatment (calculations and/or validations) for this reaction channel (see the references given in [1]). The recent release of the European Activation File EAF-2007 [2] includes the most comprehensive (n,γ) subfile among all recent libraries. The adopted data sources can be divided into two categories: *detailed evaluations*, usually taken from other libraries and based on calculations and/or evaluations with local parameter sets and *mass-produced calculations* mostly based on global input parameterisation. The present report concentrates on the latter group of data and use recent TALYS calculations for comparison and also as a source for data improvement. This exercise also allows a validation of the TALYS calculations, using comparisons with EAF and experimental data.

The set of (n,γ) reactions can be divided into two groups: the first covers reactions with differential and/or integral experimental data, for which the best possible existing evaluation is adopted. These evaluations are usually based on *detailed evaluations* and are often adjusted to fit the experimental data. In the EAF quality classification [2], Scores of 1 to 6 are used for these reactions and in EAF-2007 this set contains 475* reactions. These reactions can be further subdivided into those with *single-energy information* at energies of 0.0253 eV or at 30 keV and classified with Scores of 1 or 2. The other subgroup has experimental data in a *broad-energy range*, typically averaged cross sections in the unresolved resonance range up to several MeV with Scores from 3 to 6. Here it should be noted that resolved resonance data are reconstructed from the experimental resonance parameters into a point-wise resonance region and so also should be regarded as broad energy range information.

The second group, containing 337 reactions has no experimental information (Score = 0) and the adopted excitation curves are typically based on *mass-produced calculations* (with global parameters) although in some cases these have been renormalized to cross section systematics.

An additional validation approach has been proposed and applied in recent work for Score = 0 reaction channels. Besides the comparison with cross section systematics, an inter-comparison of independent calculations, carried out by different codes with different input parameters, can give additional information. For some conflicting cases a new visual tool can be used, this enables the (n,γ) cross sections of the whole isotopic chain of a target element to be plotted in a single graph, where the σ(n,γ) behaviour and expected trend with increasing neutron number can be studied.

* In this report reactions refer to total reactions ($\sigma_{total} = \sigma_g + \sigma_m + \sigma_n$) unless stated otherwise.

2. Available tools

2.1 Calculational tools

2.1.1 MASGAM / SIG-ECN

The MASGAM code was developed at ECN Petten in the early nineties to calculate (n,γ) cross sections for a wide range of targets. The calculated cross section consists basically of three components: the 1/*v* component, the statistical part (calculated by the FISPRO code) and the pre-equilibrium contribution. FISPRO [3] is a statistical Hauser-Feshbach code including width fluctuations but with the competing particle channels neglected. The Lane, Lynn and Brown formalism [4] for the direct/semi-direct component is used in FISPRO for the pre-equilibrium representation. Available information on the resolved resonance region, if available, was reconstructed with the MLBW formalism in a point-wise file by the code SIG-ECN.

If the resolved resonance region cannot be not included, then the statistical part is extended down to the energy E_H = 0.5 D_0 (D_0 is the s-wave average level spacing derived from the level density) and discontinuously coupled to the 1/*v* term. This low energy part is renormalized at 0.0253 eV either to available experimental data or to a simple estimate described below. This choice of the E_H energy is arbitrary; however, inspection of available data (see Figure 1) suggests that this choice is acceptable. The pre-equilibrium component in MASGAM, contrary to the direct/semi-direct approach in FISPRO is based on the systematics of the pre-equilibrium capture process [5]. Each of the three components, separately calculated, can be examined at an appropriate energy (0.0253 eV, 30 keV and 14.5 MeV) and renormalized either to an experimental value or to a value from systematics.

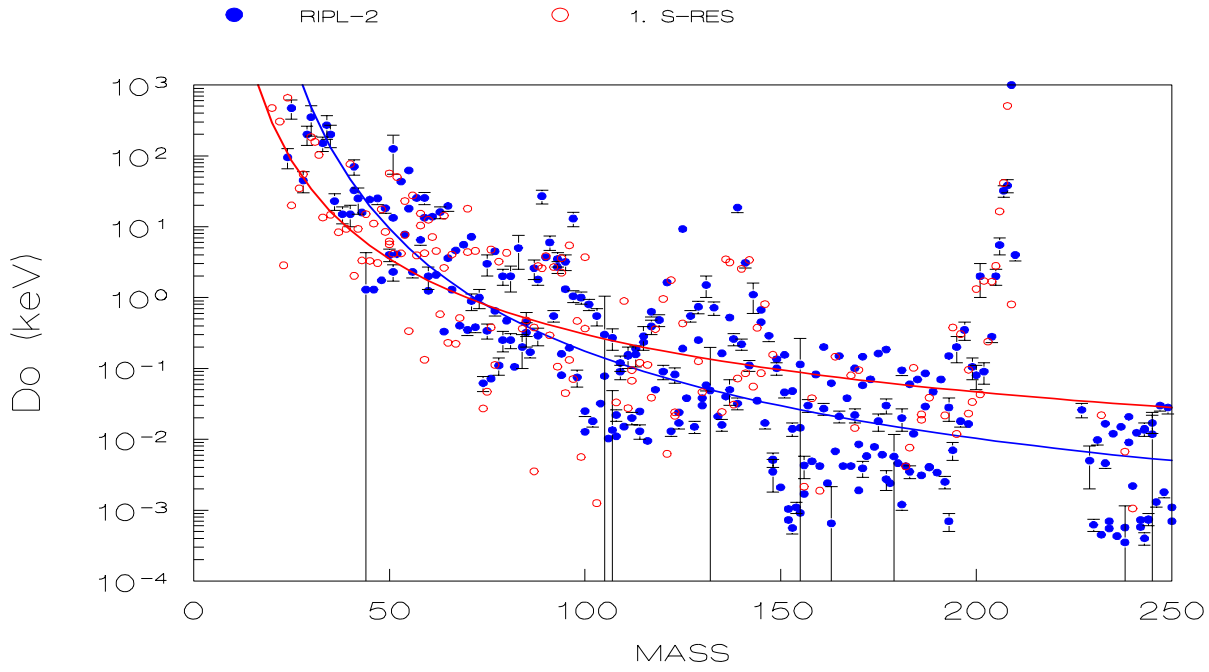

Figure 1. The experimental values of D_0 taken from the RIPL [18] compilation compared with the energy of the first s-wave resonance extracted from reference [6].

The main input parameters are derived from:

Optical model. Standard global neutron optical model parameters of Moldauer [7] were adopted for the calculation. The reasoning for this choice was that at that time the quantities

of S_0, S_1 and R′ were best reproduced (at lower incident energies) by this choice. The largest deviations have been found in the rare earth region where the nuclear deformations are large.

Discrete levels and level density. Discrete levels have been extracted from compilations published in Nuclear Data Sheets. The composite Gilbert-Cameron formula has been used to extend these values. For the parameterisation of the continuum, the level density parameter *a* and the matching energy *U*, data have been taken from the global systematic of Reffo as compiled in references [8] and [9].

E1, M1 and E2 strength function models and giant resonance parameters. For the energy dependence of the radiative strength function the traditional expression, based on the Brink hypothesis [10], with Lorentzian shape and energy independent width was assumed. In order to simplify the input data, only E1 radiation has been considered. The expression shown in equation (1) for the resonance energy, taken from reference [11] fits the experimental data rather well and the neglect of the double humped peak for deformed nuclei was justified in this simplified global parameterisation.

$$E_R = 31.2A^{-1/3} + 20.6A^{1/6} \quad \text{.....(1)}$$

For a description of the giant resonance width, the ratio of Γ_R/E_R was found to be approximately constant and the value of 0.3 (see [9]), was applied. The calculated total radiative width has been, if necessary, normalized to semi-experimental values, deduced in a tabular form from a spline eye-guiding fit to experimental data points as shown in Figure 2.

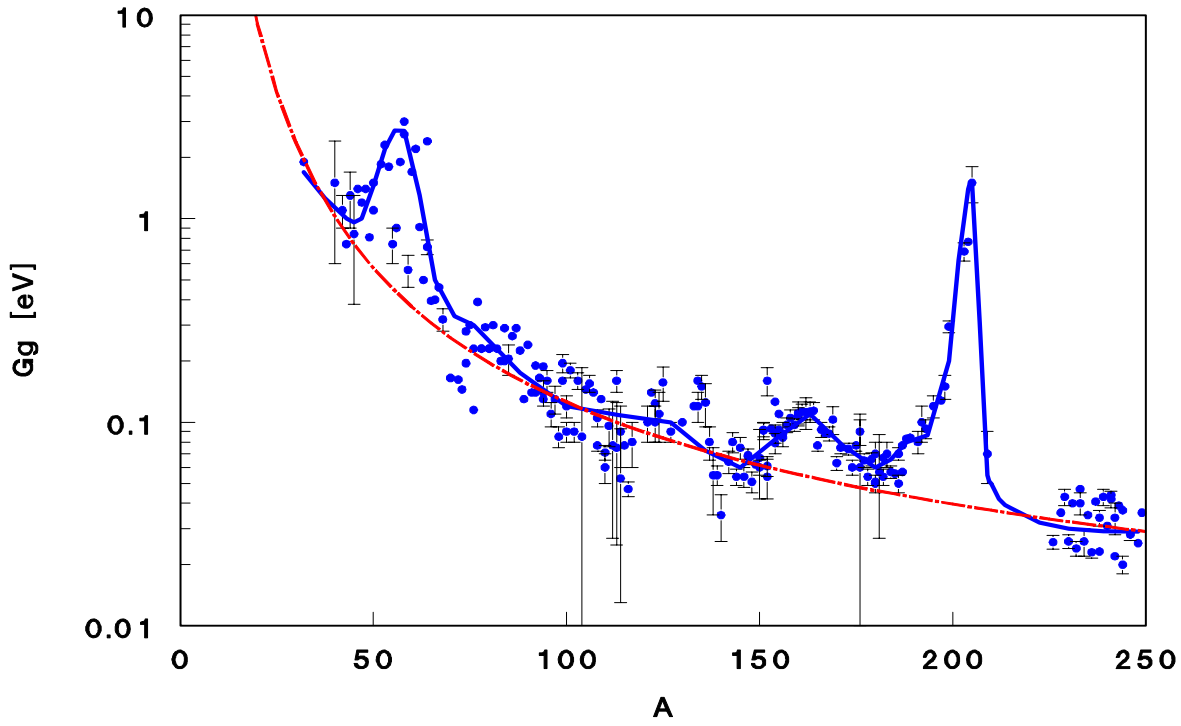

Figure 2. Total radiative width Γ_γ taken from reference [6] plotted as a function of the mass. An eye guiding spline fit to these data is represented by the blue curve and is used as a tabular form for targets with no experimental Γ_γ values. The red curve is a power fit to these data and has been used for targets with $A < 40$.

2.1.2 NGAMMA

NGAMMA was the next fast (n,γ) code developed at Petten. It is based on the spherical optical model, the Hauser-Feshbach formula with width fluctuation correction, the exciton model [12] and the unified model [13] in which equilibrium and pre-equilibrium emission mechanisms are unified and angular momentum conservation is taken into account. This exact treatment of pre-equilibrium processes replaced the systematic approximation applied in MASGAM. Besides the radiative capture channel, the code also handles the competing particle emissions, including neutrons, protons and alphas. The possibility to normalize the calculation to experimental data or to systematics is maintained (see [14]). The construction of the $1/v$ component is similar to MASGAM, but is performed manually, assigning E_H energies either from D_0 experimental values or by estimation from the trend of neighbouring nuclei.

The main input parameters are derived from:

Optical model. Standard global neutron optical model parameters of Moldauer [7], Wilmore-Hodgson [7], Buck-Perey [15,16] and Uhl [17] have been tested on several nuclei ranging from A = 90 - 205 and the parameters of Uhl, giving the best results, were finally adopted for the calculations.

Discrete levels and level density. The discrete levels have been taken from compilations published in Nuclear Data Sheets. The newly evaluated set of BSFG (back shifted Fermi gas) level density model parameters of the Beijing group (recommended by RIPL-1 [18]) have been used. In cases where no data were available and in the absence of any recommendations in reference [18] for nuclei without experimental values, an extrapolated estimate from neighbouring nuclei was applied.

E1, M1 and E2 strength function models and giant resonance parameters. The generalized Lorentzian formulation [19] has been adopted for the E1 resonance, except for deformed nuclei in the mass range above A = 150, for which the classical Lorentzian was used (based on conclusions in [20,21]). The giant E1 resonance parameters have been taken from [22] and checked against the very recent compilation of Varlamov [23]. If the experimental data on the E1 giant resonance were missing, the value from a neighbouring target has been used for extrapolation. The spin-flip M1 resonance has been adopted for M1 radiation with the standard parameterisation [19], the cross section $\sigma_{R(M1)}$ has been renormalized against the systematic (for details see reference [19]). The single-particle model is used for E2 radiation.

Since the NGAMMA code has been mainly used for improvement of data of the statistical component (for energies > E_H) for targets with resolved resonance regions and experimental information, the renormalization of calculated data against 30 keV cross sections has been applied. The renormalization factor k is displayed in Figure 3 as a function of A for the target nuclei. The majority of calculated results are well within the uncertainty factor band of 2, except for the deformed region with $160 < A < 180$, in which the generalized Lorentzian underestimates the capture cross section, as discussed above. The accuracy of NGAMMA calculations with an uncertainty factor k = 2 is surprisingly good considering the simplifications and global parameters used. The targets between A = 160 and 180 are underestimated ($k > 2$), and the use of standard Lorentzian (red data points in Figure 3) gives a good agreement. However, this agreement is probably accidental (see extensive discussion in [20,21]). Recently these calculations have been repeated with an enhanced generalized Lorentzian, which is a more physical description for deformed targets, and the results agree very well with the experimental 30 keV data.

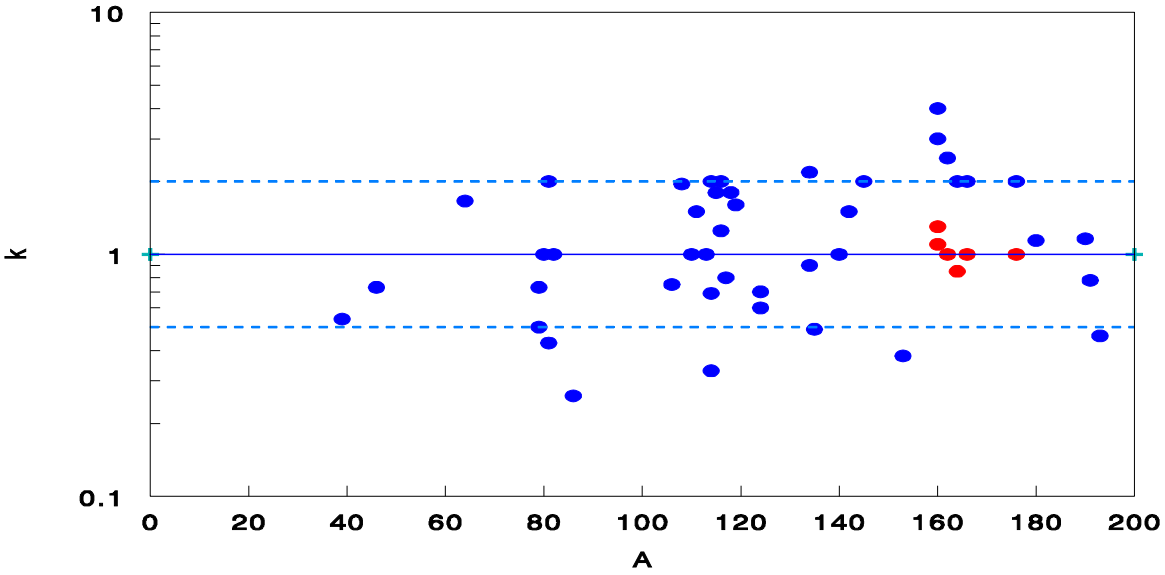

Figure 3. The renormalization factor *k* applied on NGAMMA calculations displayed as a function of *A*.

2.1.3 TALYS

TALYS [23] is a computer code system for the prediction and analysis of nuclear reactions. TALYS considers reactions that involve neutrons, gammas, protons, deuterons, tritons, helions, alpha-particles and fission, in the 1 keV - 200 MeV energy range and target nuclides of mass $A \geq 12$. This is achieved by implementing a suite of nuclear reaction models into a single code system. It enables the evaluation of nuclear reactions from the unresolved resonance region up to intermediate energies. Generally, there are two different ways to use TALYS. Firstly, *very detailed calculations* with various adjusted parameters, and choices of nuclear models, so that specific experimental data for a single nucleus are reproduced. Secondly, *large scale, default calculations* for many nuclides, in which case adjustment to experimental data is impossible or, for the moment, not practical. While the first method is generally used for detailed isotopic evaluations, it is clear that for the EAF-2007 project the second method must be used.

All results for the activation library are created using a script, which runs TALYS with default input parameters for a set of targets. This means that the data in these calculations have not been tested against individual experimental data for each isotope, and so are only as good as the global parameters of the TALYS code at the present time. The mutual quality of these isotopic evaluations is thus relatively consistent. The construction of the $1/v$ component is slightly different to MASGAM or NGAMMA. The lower energy of validity of a TALYS model calculation, E_H, is again arbitrarily chosen as the value D_0. The D_0 value is either taken from the RIPL data base or, if not present, derived from the applied level density. The thermal capture cross section is based on experimental values or, if not available then on the EAF estimate shown in equation (2). The upper energy of the $1/v$ cross section dependence is set, again arbitrarily, to $0.2E_H \equiv 0.2D_0$.

Nuclear models available in TALYS:

Optical model All optical model calculations are performed with the optical model potentials of Koning and Delaroche [24]. For compound nucleus reactions the model of Moldauer, *i.e.* the Hauser-Feshbach model corrected for width fluctuations, is used. Coupled-channels calculations are automatically invoked when a coupling scheme is available.

Discrete levels and level density For the level density, the composite formula proposed by Gilbert and Cameron, consisting of a constant temperature law at low energies and a Fermi gas expression at high energies is applied. Energy-dependent shell effects are included.

E1, M1 and E2 strength function models and giant resonance parameters Gamma-ray transmission coefficients are generated using the Kopecky-Uhl generalized Lorentzian for strength functions [19]. For pre-equilibrium reactions, which become important for incident energies above about 10 MeV, the two-component exciton model is used. In particular the pre-equilibrium emission model of Akkermans and Gruppelaar [25] is implemented. Multiple pre-equilibrium emissions up to any order of particle emission are included.

2.1.4 Remarks on the effect of applied models and input parameters on (n,γ) calculations

Several authors have devoted quite some effort to the study of the sensitivity of the calculated statistical component to the choice of assumed model. An extensive investigation was carried out by Uhl [19,20,26,27], where the choices of various *optical models* (OMP), *level density models* and *gamma-ray strength functions* were investigated. The unique aspect of this approach was that the influence of different models was studied for the different calculated results, such as the capture cross section, gamma-ray spectra and the total radiative width Γ_γ. A detailed discussion can be found in reference [26]. Kopecky, using the NGAMMA code, studied the sensitivity to the choice of various OMPs and the role of the E1 strength function parameterisation (standard and generalized Lorentzian). Herman [28], using the EMPIRE-II code, presented observations on the sensitivity to various OMP and level density approaches based on a large number of cross section calculations. All these studies were applied on capture reactions which had solid experimental support for comparison.

The conclusive observations can be summarized as:

1. The general dependence on different OMP is rather weak and influences the magnitude of the statistical component insignificantly. Only in reactions where the capture cross section represents a large fraction of the absorption cross section, is the choice of OMP likely to be important. The reasoning behind this conclusion is given in detail in reference [26].

2. There is a strong influence of the different level density models and in particular their parameters on the magnitude of the cross section especially above the inelastic scattering threshold. The completeness of discrete level information is also essential. Even if the same information on discrete levels and resonance spacing is used, different models can give significantly different cross sections. A definite recommendation is therefore difficult and good agreement is obtained for different mass regions for the different models. This is demonstrated in references [19,20,26-28] and has been especially extensively studied with the TALYS code.

3. The choice of gamma-ray strength function models, in particular for the E1 mode, also influences the magnitude of the cross section. The gamma-ray spectra are the most sensitive test [20,27] of strength functions, especially for the energy dependence of f(E1).

For targets with good experimental information, the results can always be adjusted to fit the experimental values *e.g.* of Γ_γ and D_0. This has been applied in the past for many calculations using different codes. However, for targets with no experimental data, the predictive power of calculated cross sections has to be judged using other means of comparison, such as cross section systematic data, inter-comparisons of independent calculations and visual semi-empirical tools. The basic physical constrain is that if no local parameters exist, then global parameters have to be used as the input for calculations.

In Table 1 an overview is given of three major codes used within the EAF libraries to calculate neutron capture data with an indication of the adjustable parameters (denoted as RN) used by each.

Table 1. Relevant input parameters and renormalizations (in **bold**) for σ(n,γ) calculations of targets with no experimental support for three codes used in EAF calculations.

	MASGAM	**NGAMMA**	**TALYS**
1/*v* component	10^{-5} eV - E_H **RN-EXP/SYS**	10^{-5} eV - E_H **RN-EXP/SYS**	10^{-5} eV - E_H **RN-EXP/SYS**
Optical model	Moldauer (global)	Uhl (global)	Koning-Delaroche (global)
Level density	CTGC (global) $E_H = D_0/2$, D_0 from CTGC	BSFG (global) $E_H = D_0$, **D_0 estimate from Figure 2**	CTGC (global) $E_H = D_0$, D_0 from CTGC
Gamma-ray strength functions	E1 (SLO)	E1(GLO), M1(SLO), E2 (SP)	E1(EGLO)
Statistical component	Limited **RN σ_{30} systematics**	No RN	No RN
Pre-equilibrium component	**RN $\sigma_{14.5}$ systematics**	**Exciton component adjustable**	No RN

CTGC=Constant Temperature Gilbert Cameron, BSFG=Back Shifted Fermi Gas, SLO= Standard Lorentzian, GLO=Generalized Lorentzian, EGLO=Enhanced Generalized Lorentzian, SP=Single particle.

2.2 Cross section systematics

2.2.1 Systematic at 0.0253 eV

The formula $\sigma_{n\gamma} = C_1(aU)^{C_2}$ (for derivation see next paragraph) is certainly not theoretically justified for thermal energies, due to the influence of the resonance region, which may dominate and the dependence on aU can be masked by large Porter-Thomas fluctuations. Nevertheless a least-squares fit to thermal cross sections compiled in reference [6] has been applied with the level density parameters a and U taken from database included in the MASGAM input section (see above). The result is shown in equation (2).

$$\sigma_{n\gamma} = C_1(aU)^{C_2} \text{ with } C_1 = 1.50 \times 10^{-6},\ C_2 = 3.5 \quad \text{.....(2)}$$

Figure 4 shows the raw data with the fit given by equation (2). As expected, the scatter of the data around the fitted curve remains large, with deviations of around a factor of 50. This very simple estimate seems, however, the only way possible to predict and normalize the 1/*v* component for the targets with no measured thermal cross section. The large uncertainty associated with such an estimate must always be taken into account.

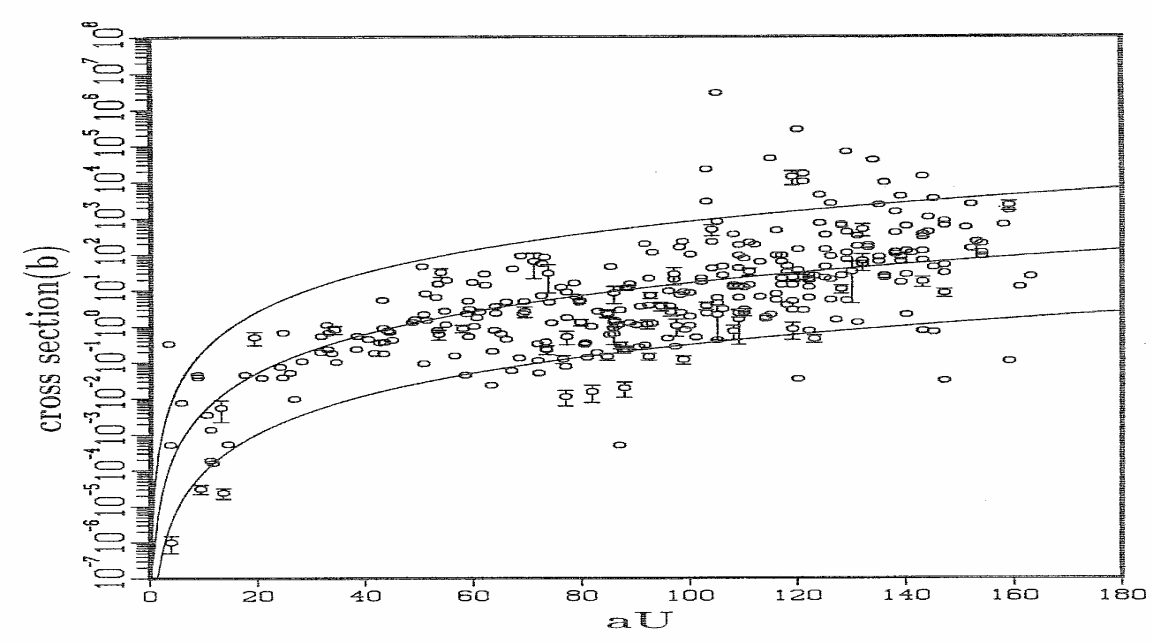

Figure 4. Thermal capture cross sections (taken from [6]) plotted against aU together with the fitted curve in equation (2). The uncertainty band with $f = 50$ is indicated. This plot is taken (scanned) from reference [1].

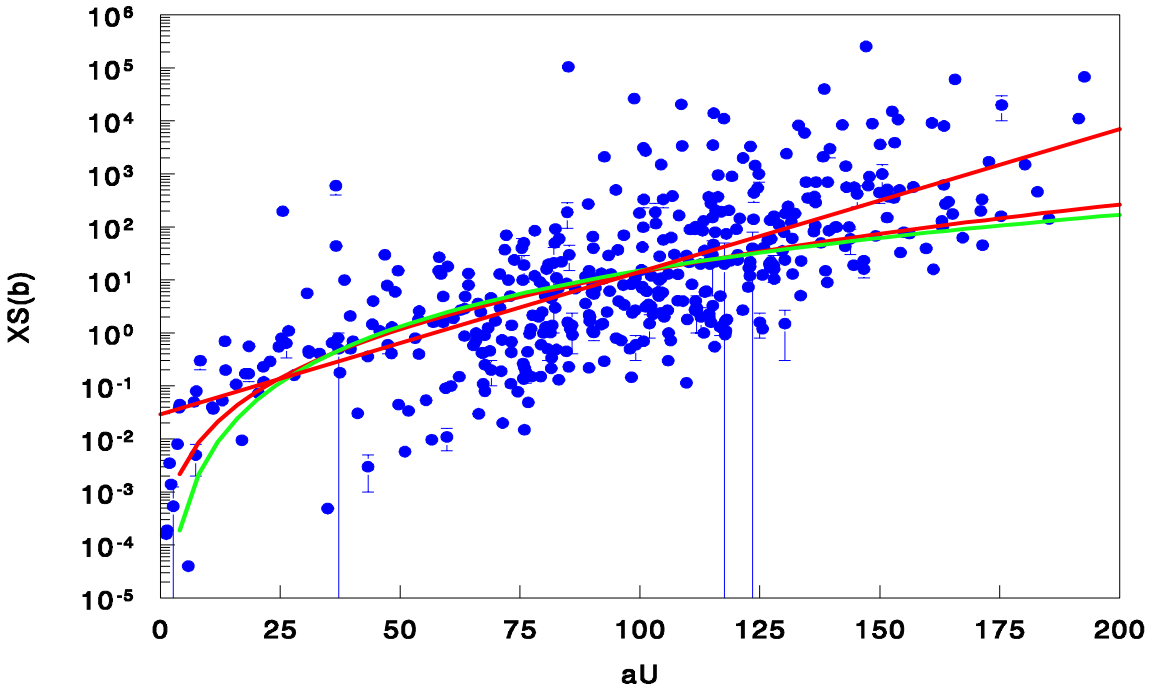

Figure 5. Thermal capture cross sections (recent data taken from [29] plotted against aU). The old systematic of equation (2) is shown as the green curve. The newly fitted curves, both linear and power fits, are shown in red.

Updated thermal cross sections are included in the EAF experimental data-base (see [2] based on the recent [29]), are plotted in Figure 5. The previous fit shown in equation (2) is compared with a new fit of the same form as well as a linear fit. The new fitting coefficients are shown in equation (3).

$$\sigma_{n\gamma} = C_1(aU)^{C_2} \text{ with } C_1 = 1.10 \text{ x } 10^{-5},\ C_2 = 3.12 \quad \text{.....(3)}$$

A slight shift to larger cross sections for targets with $aU > 100$ can be seen; however, this is compensated by a large number of data with lower cross sections values for $60 < aU < 120$. The linear fit shown in equation (4) could also be considered, especially in conjunction with equation (3) in particular mass regions. These new forms will be used for future EAF evaluations.

$$\ln \sigma_{n\gamma} = C_1 + C_2 aU \text{ with } C_1 = -1.186,\ C_2 = 0.023 \quad \text{.....(4)}$$

2.2.2 Systematic at 30 keV

The cross section at a neutron energy of 30 keV was used for the first time in MASGAM calculations to validate and/or normalize the statistical Hauser-Feshbach component. A systematic formula for the average (n,γ) cross section at 30 keV has been derived by Kopecky [1]. The capture cross sections at kT = 30 keV, compiled by the group of Kaeppeler in 1987 [30], were used for the derivation. The cross section at this energy is an important quantity for astrophysical studies (nucleosynthesis), in particular for the s-neutron capture process. The quoted values are Maxwellian averaged cross sections $<\sigma_{30keV}>$, which in the case of approximately $1/v$ dependence is close to the point-wise σ_{exp} (within 10%). This condition is also satisfied for the unresolved resonance regions. The cross section at 30 keV can be approximately described by equation (5).

$$\sigma_{n\gamma} \approx ((2I+1)/D)\Gamma_\gamma \quad \text{.....(5)}$$

The first term corresponds to the level density (D is the average level spacing) and the second is the total radiative width. If the Fermi gas approximation for the level density is made (a is the level density parameter and U is the effective excitation energy) and a standard parameterisation of Γ_γ is applied then equation (5) can be rewritten as equation (6).

$$\sigma_{n\gamma} \approx \exp(aU)^{1/2} AaU \quad \text{.....(6)}$$

Equation (6) can be shown as a formula with 5 adjustable parameters in equation (7).

$$\sigma_{n\gamma} = C_1 \exp C_2 (aU)^{1/2} C_3 A C_4 a C_5 U \quad \text{.....(7)}$$

This formulation has been used [31,32] for a limited data set, but it was shown [2,33] that the simplification to equation (8) using only 2 parameters gives a fit of comparable accuracy.

$$\sigma_{n\gamma} = C_1 (aU)^{C_2} \quad \text{.....(8)}$$

For level density parameters the tabulated approximate values of a from reference [8] have been used together with the Gilbert-Cameron prescription for U, defined in terms of the Q-value and the pairing energies (P) by equation (9) with $P(Z)$ and $P(N)$ values taken from reference [35].

$$U = Q(n,\gamma) - P(Z) - P(N) \quad \text{.....(9)}$$

Using these values for a and U, based on a spline fit to the experimental a values, and dividing the targets into odd and even Z, gives the fitting parameters shown in (10) and (11).

$$C_1 = 3.346 \times 10^{-6},\ C_2 = 4.025 \qquad Z \text{ odd} \quad \text{.....(10)}$$

$C_1 = 2.461 \times 10^{-7}$, $C_2 = 4.410$ Z even.....(11)

The capture-cross sections at $kT = 30$ keV were compiled again in 2000 [34]. Following this publication, it was decided to include the σ_{30} systematic in the validation procedures contained in the SAFEPAQ-II code. The cross sections from this updated compilation were used to update the systematic formula. The aU values were adopted from the recommended values given in the RIPL-1 report [18], based on fits to experimental level density parameters for the BSFG model. Only those cross sections which are supported by the RIPL-1 experimental aU values were considered. Since RIPL-1 does not include any systematic approximation of aU values for targets with no experimental level density parameters, the previous approach, applied successfully for MASGAM calculations, was used and the resulting parameters are shown in (12) and (13).

$C_1 = 8.236 \times 10^{-8}$, $C_2 = 4.827$ Z odd .....(12)

$C_1 = 6.995 \times 10^{-7}$, $C_2 = 4.287$ Z even.....(13)

These σ_{30} systematic equations were introduced for the production of EAF-2001 [36].

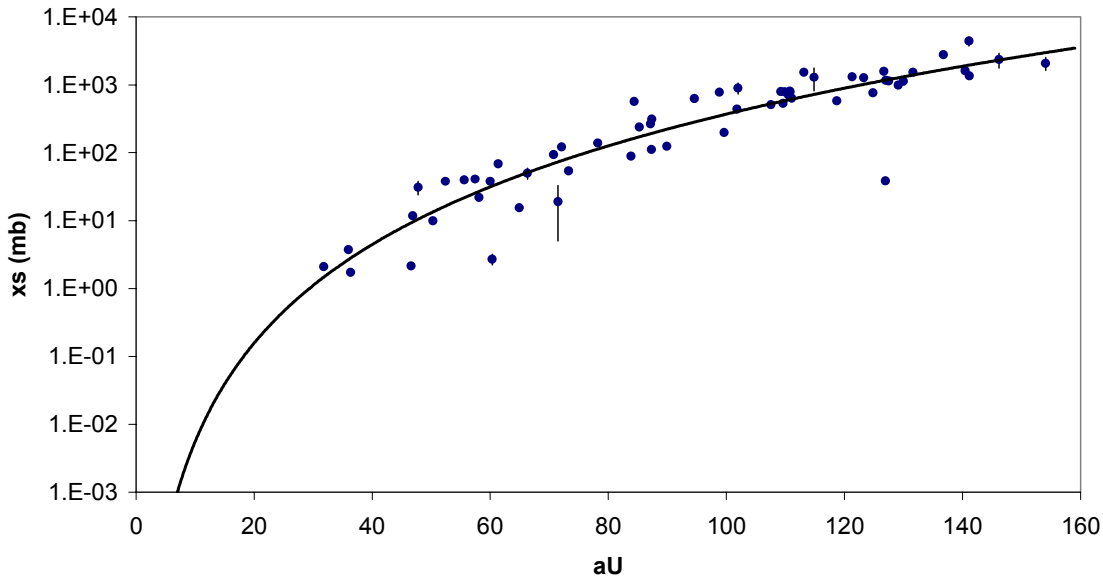

Figure 6. 30 keV cross sections for even Z targets showing the fit of a systematic formula using RIPL-1 aU values.

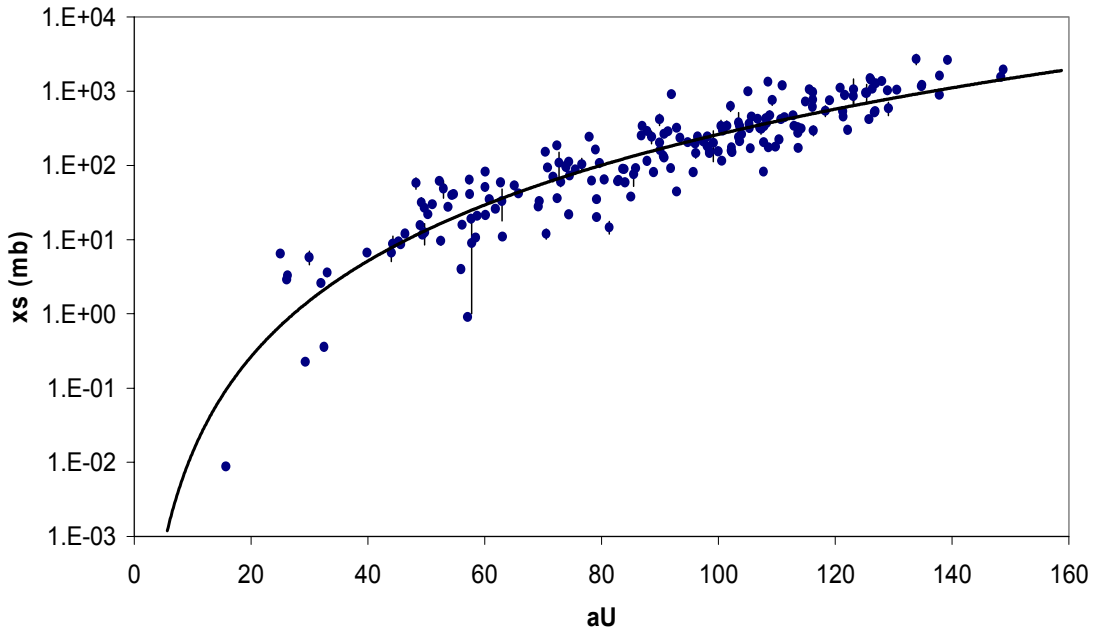

Figure 7. 30 keV cross sections for odd *Z* targets showing the fit of a systematic formula using RIPL-1 *aU* values.

When these equations were used for the C/S validation on the EAF-2001 data, a small over prediction of the calculated values in the C/S histogram was observed, by about a factor of 2. At that time this was assumed to be due to an under-prediction of the σ_{30} systematic values caused by the spread of experimental data seen in Figures 6 and 7, and to a large uncertainty of adopted data for Score = 0 targets. However, it was later realized, that an inconsistency between the two sets of *aU* values, derived from the RIPL-1 experimental recommendation and from the MASGAM tabulated data, could be the cause.

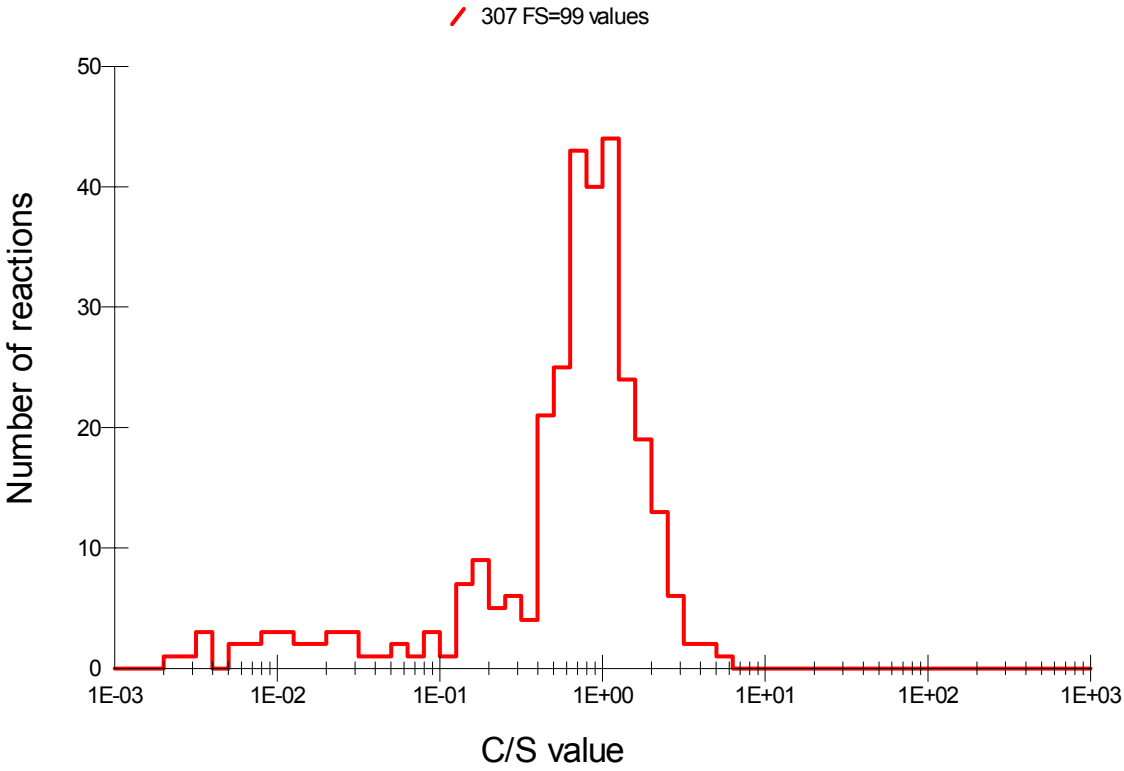

Figure 8. C/S at 30 keV for EAF-2007 (n,γ) data. Only reactions (summed reactions) with Score = 1 - 6 are used and compared with the systematics given in equations (12) and (13).

This explanation was supported by the C/S validation performance for Score = 1 – 6 targets, using tabulated aU values, with the majority of these targets also used for the σ_{30} derivation. This comparison is shown in Figure 8 for EAF-2007 and a similar over-prediction of calculated values can be observed, in contrast to the C/E comparison shown in Figure 9 where the curve is centred around C/E = 1.

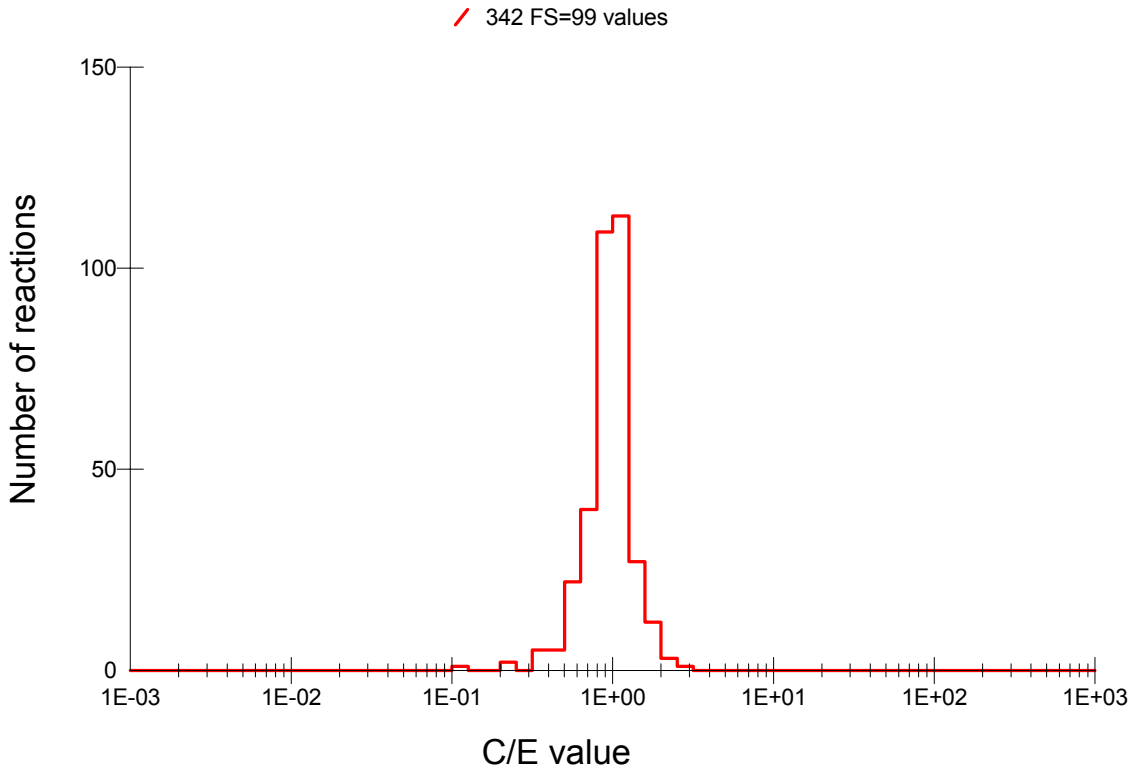

Figure 9. C/E at 30 keV for EAF-2007 (n,γ) data. The same experimental cross sections were used for the derivation of the σ_{30} systematic. Note summed reactions are shown.

This was also the reason, that the σ_{30} systematic was never used for any renormalization modifications in previous EAF libraries and served only as indicative information.

The recent edition of the RIPL-2 TECDOC [37] now includes more experimental values for level density parameters a and U compared to RIPL-1 and also gives an explicit systematic formula for targets with no experimental data (missing in RIPL-1), so it was expected that an analysis using it would give better results. The recommended values of Ignatchuk, which include also a systematic for the level density parameter (Fermi gas) a and $U = B_n - \Delta$ with the following values was used.

$$a = 0.1337A - 0.06571A^{2/3}$$
$$\Delta = 12/A^{1/2} \quad \text{for even-even nuclei}$$
$$\Delta = 0 \quad \text{for odd nuclei}$$
$$\Delta = -12/A^{1/2} \quad \text{for odd-odd nuclei}$$

The consistency of a values, for those taken from experiments and those derived from the above systematic, has been tested in reference [37] and was shown to be good. Therefore it was decided to repeat the derivation of the σ_{30} systematic using these new aU values. This resulted in new fitted equations with $C_1 = 1.846 \times 10^{-7}$ and $C_2 = 4.699$ for odd targets and $C_1 = 2.924 \times 10^{-7}$ and $C_2 = 3.797$ for even targets. However, the consistency of RIPL-2 experimental aU values with those from the systematic proved to be less good than expected.

In fact, in reference [37] only the consistency of the level density *a* parameter was tested (see Figure 6.7, page 95 of reference [34]) and not the representation of the pairing corrections through the estimation of Δ. This means that *U* values determined experimentally and from systematics do not form a consistent data set. This effect has been demonstrated in a C/S analysis and is shown in Figure 10. A huge overestimation is clearly present, showing the sensitivity of the product *aU* on the source of *U* values and indicates that those derived from experiments and systematics cannot be mixed.

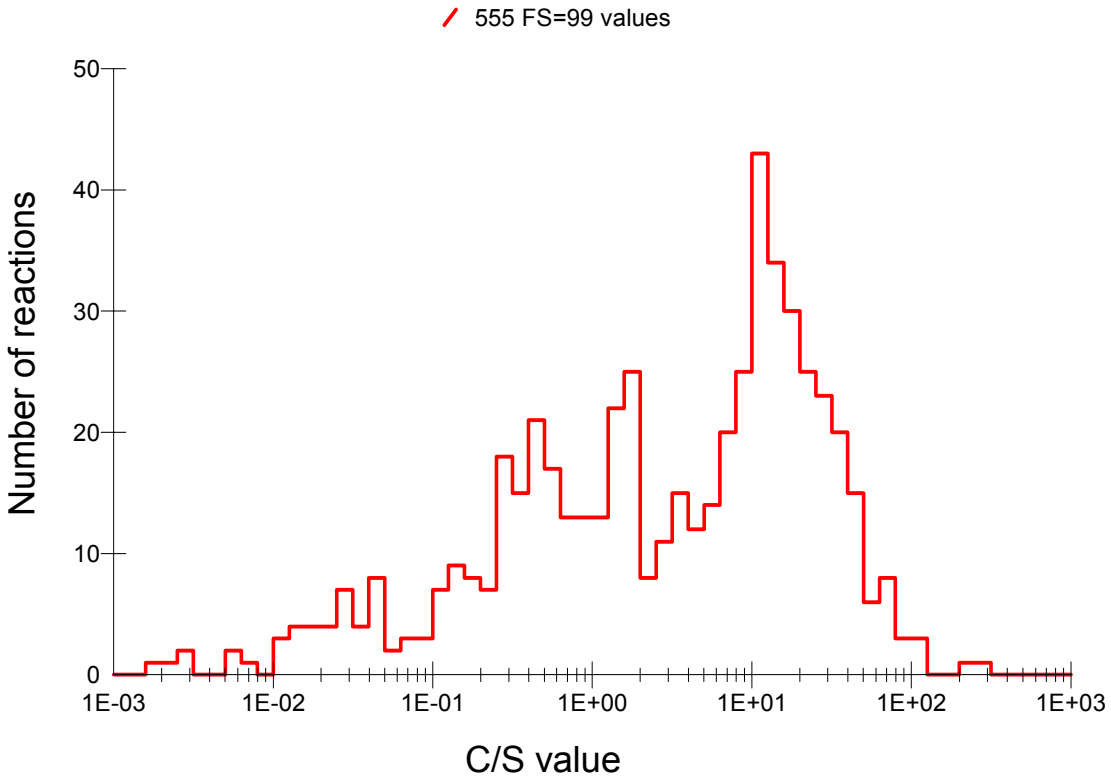

Figure 10. C/S at 30 keV from EAF-2007 for all targets compared with a new systematic derived using RIPL-2 *aU* values.

After the negative experience with the use of both RIPL-1 and -2 derived sets of *aU* values in experimental level density fits and difficulties with extension of these data to targets with no experimental level density information, it was decided to return to the original approach as applied in reference [1], namely to use the tabulated approximate values of *a* from reference [8] together with the Gilbert-Cameron prescription for the effective excitation energy *U*. An important extension of the approach is the use of the same *aU* data sets for the derivation of the σ_{30} cross section equations as well as in the C/S validation procedure for all targets. The results of such a cross section fit procedure, again using cross section data from reference [34], and final *a*, *U* tabulated values, are shown in Figures 11 and 12 and result in a new version of equation (5) with the following parameters.

$C_1 = 1.940 \times 10^{-8}$, $C_2 = 3.553$ *Z* odd ..... (14)

$C_1 = 1.041 \times 10^{-8}$, $C_2 = 3.769$ *Z* even..... (15)

The parameters shown in (14) and (15) have been included in the validation option of the SAFEPAQ-II code [2] and will be used further in this study. The use of consistent *aU* values, both for the cross section fit as well for the C/S analysis, result in a symmetric distribution of C/S seen in Figure 13, centred around C/S = 1 with an uncertainty of about two at the half-width maximum.

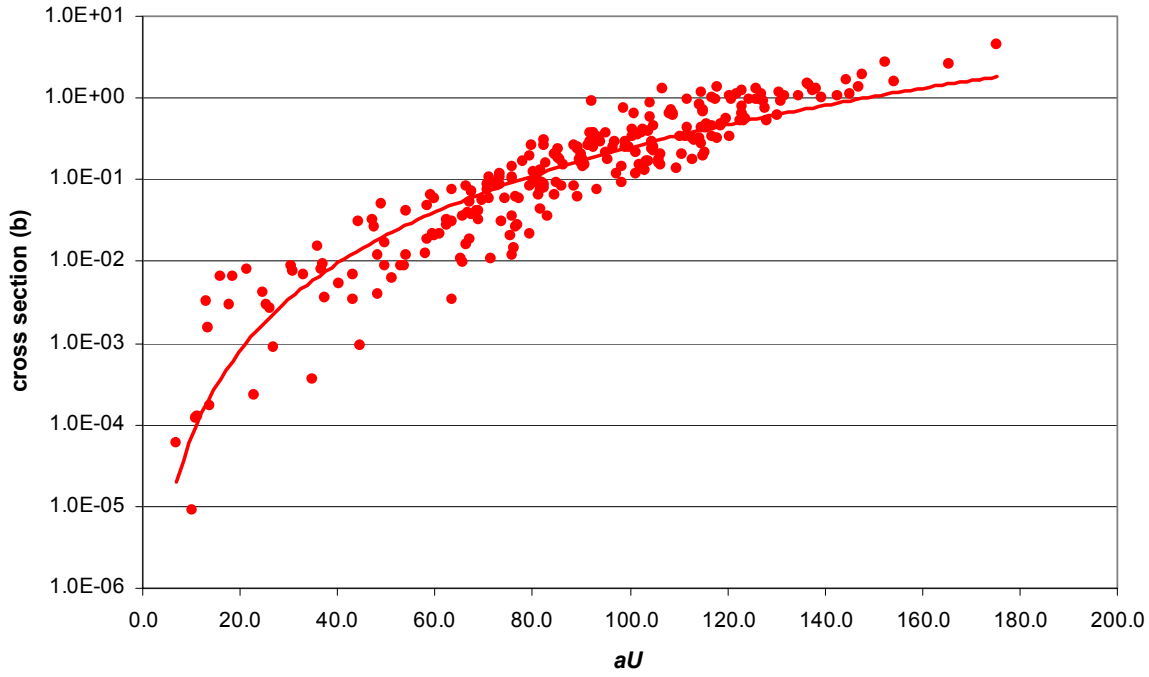

Figure 11. 30 keV cross sections for even Z targets showing the fit of the new σ_{30} systematic equation from reference [34] using the original MASGAM level density aU parameterization. The scatter of data points is reasonably covered by an uncertainty factor of $f = 3$.

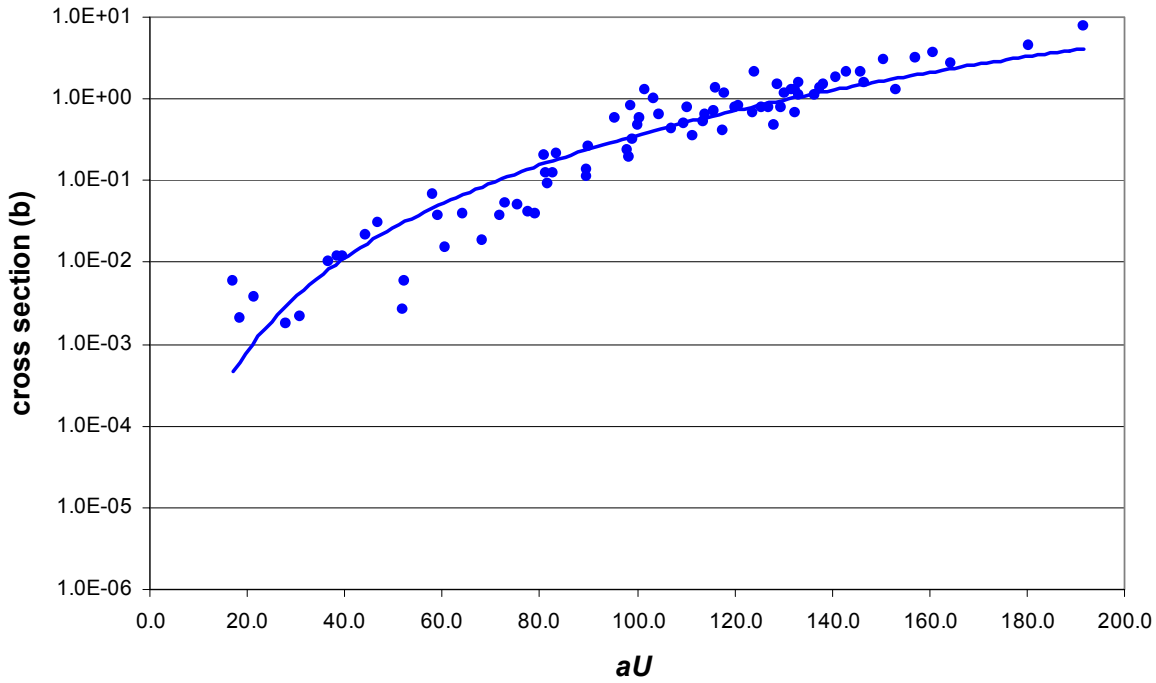

Figure 12. 30 keV cross sections for odd Z targets showing the fit of the new σ_{30} systematic equation from reference [34] using the original MASGAM level density aU parameterization. The scatter of data points is reasonably covered by an uncertainty factor of $f = 2$.

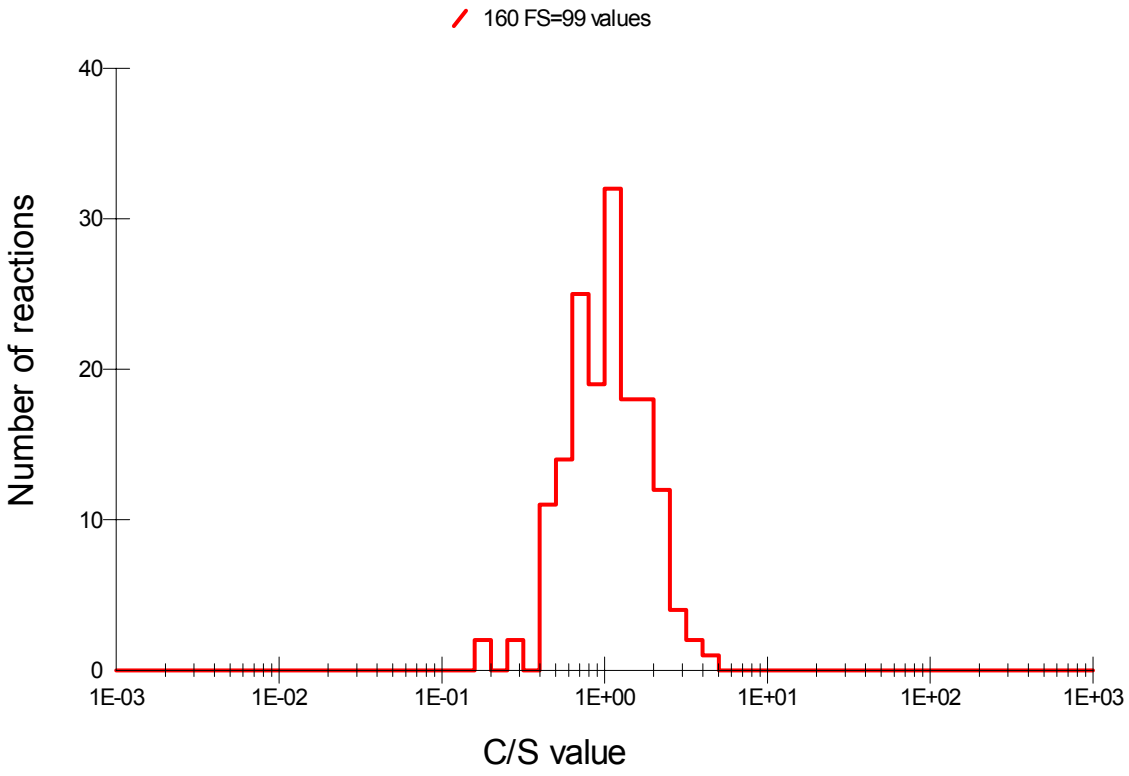

Figure 13. C/S at 30 keV using data from EAF-2007. Only targets with Score = 1-6 and used in the derivation of the 30 keV cross section systematic have been considered.

2.2.3 Systematic at 14.5 MeV

A systematic at 14.5 MeV was proposed in reference [38] by Kopecky *et al.* based on a revised cross section compilation from reference [39]. The data are shown in Figure 14 and the least squares fit is given in equation (16).

$$\sigma_{n\gamma} = 1.18 - 1.13\exp(-0.01338A) \quad \text{..... (16)}$$

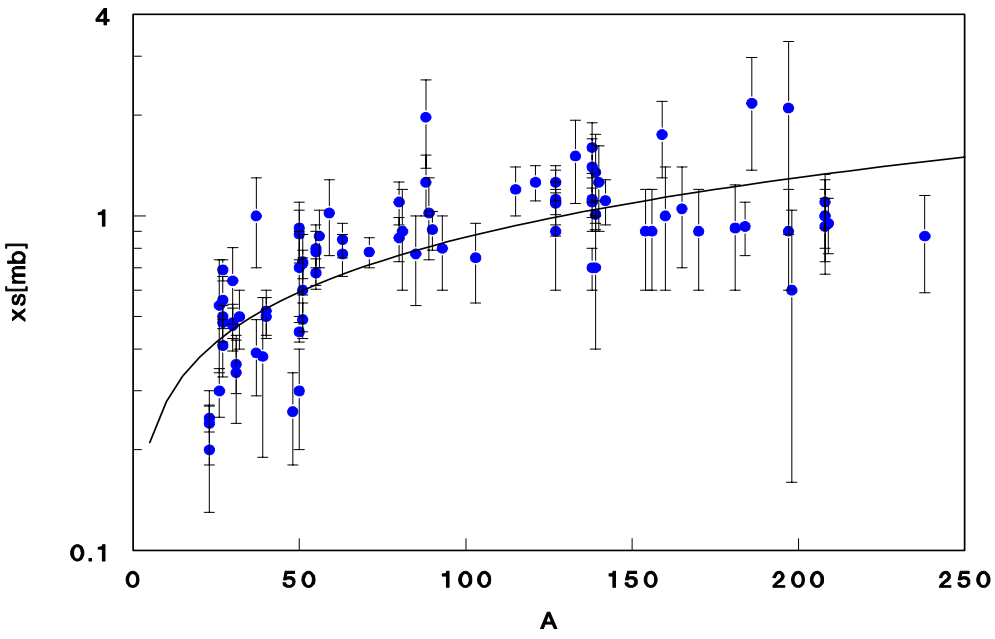

Figure 14. Systematics of radiative neutron capture cross sections at 14.5 MeV as a function of A, the curve shows the fit described by equation (16).

The dominant direct mechanism is best described by a dependence on A, instead of aU which was used at lower incident energies. The scatter of data points is reasonably covered by an uncertainty factor of $f = 1.5$.

2.3 Visualization tools

A semi-empirical visual tool has been developed and included in the processing code SAFEPAQ [2]. This enables available (n,γ) cross sections for all targets of the same element to be plotted as a function of incident energy. As the asymmetry parameter s (= $(N\text{-}Z)/A$) increases with the atomic number of the isotope for the same Z, the cross section follows a definitive trend and such a plot may be used for an indirect validation of the data. For (n,γ) reactions, a decreasing cross section trend is expected with increasing $(N\text{-}Z)$, as the number of neutrons is increasing and consequently the increase by 1 involved in capture is increasingly difficult. An example is given in Figure 15, which shows cross section data for Ni isotopes from EAF-2007. The largest cross section is for ^{56}Ni, the 'shortage' of neutrons favours an easy capture, and the excitation curves decrease gradually to the lowest cross section, which occurs for ^{66}Ni which has a large neutron excess.

This procedure can be applied in particular cases, especially if the calculated cross section for a particular target strongly deviates from the systematic cross section value, to check whether the calculation fits or violates the trend described above.

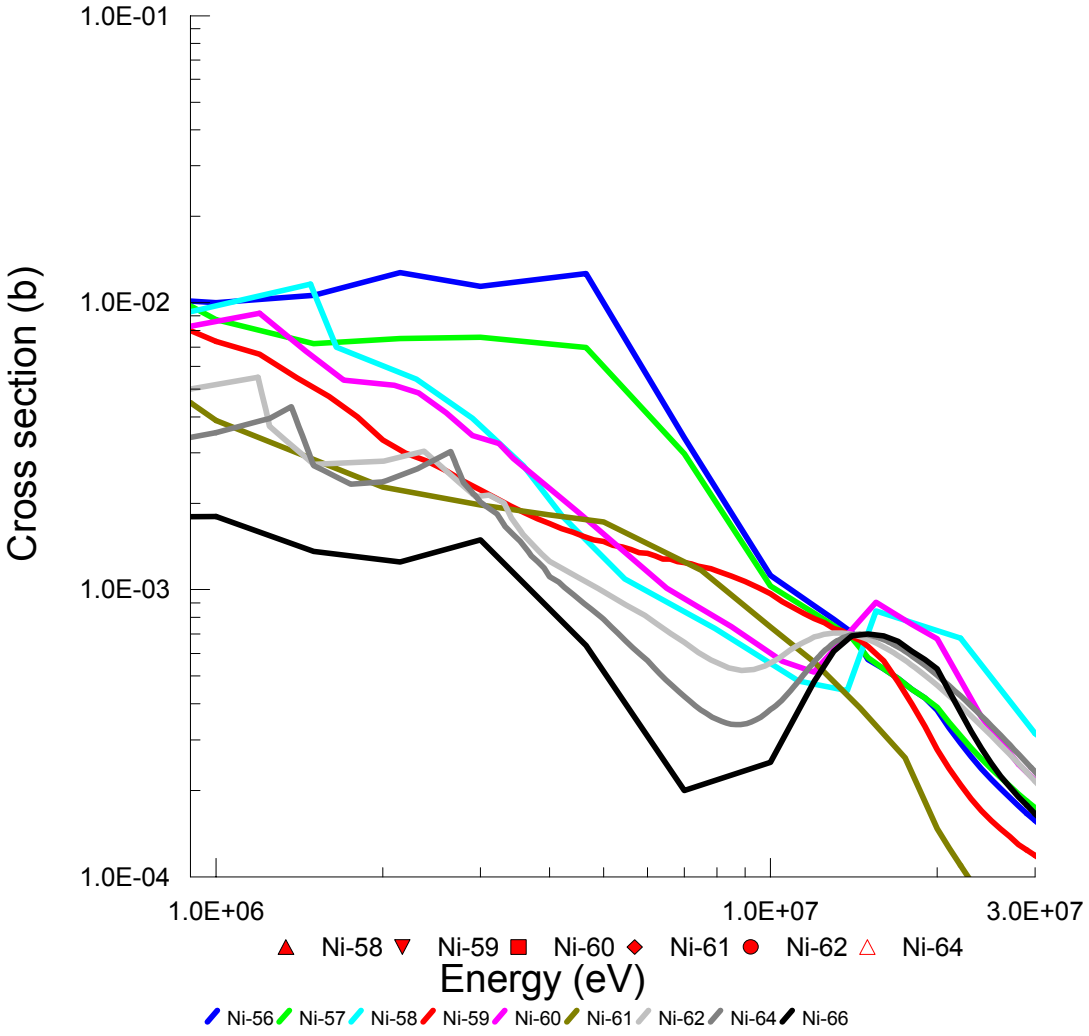

Figure 15. The extended plot of capture cross sections of Ni isotopes using data from EAF-2007. This plotting procedure has been included as a standard visual tool in the latest version of the code SAFEPAQ-II.

3. Data validation – EAF-2007

3.1 Data with experimental support (Score = 1 – 6 reactions)

The main validation procedure applied in EAF projects has always been the visual comparison of the adopted cross sections against available *differential data* in the whole energy range (from 0.0253 eV up to 60 MeV). For the (n,γ) reaction experimental data are typically only available up to about 15 MeV. For the present visual validation EAF-2007 data with experimental support (Score = 1-6) are subdivided into two groups with Scores = 1-2 and 3-6. The reason for that is that the first group can only be validated at two single energy points, namely 0.0253 eV and 30 keV while the reactions with Score = 3-6 can be compared to experimental data in broad energy ranges. In reactions with experimental information on the resolved resonance region, the point-wise file is reconstructed in the PENDF formalism and stored as such. The best available data sources (libraries) have been chosen and sometimes evaluation or calculation from different data sources are merged together (usually low energy and high energy components are merged at the end of the resolved energy range at the energy E_H). In some cases, experimental data have been used to renormalize the adopted data from one of the sources to make a better fit. For data sources with cross section extending only up to 20 MeV, the TALYS calculation has been used and merged with the existing evaluation usually at the 20 MeV energy point. For a small number of reactions, where *integral* activation experiments involve capture reactions [40], the corresponding integral data have been included for validation purposes (to assign the score) but never for a direct renormalization. Two typical examples of a visual comparison are shown in Figures 16 and 17 for EAF-2007, TALYS-5 and TALYS-6 calculations. Cross section plots of all the 475 reactions with data are available from the authors. In the present validation analysis only total cross sections (FS = 99) have been addressed, because there is little experimental information for cross sections to isomeric states, except in the thermal region. All reactions have been reviewed and for many of them modifications are proposed for the next release of EAF (EAF-2009), primarily using TALYS calculations as replacements. The lists of reactions with proposed actions are included in Appendices 1 and 2.

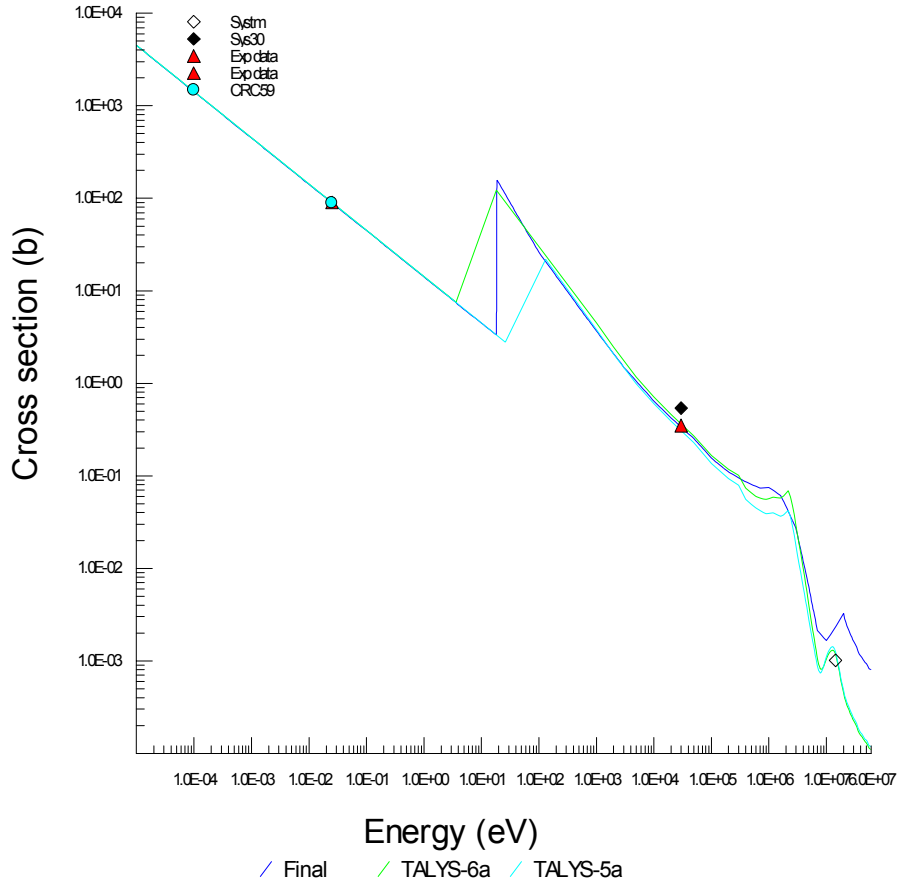

Figure 16. An example of the visual validation plot for $^{143}Pr(n,\gamma)^{144}Pr$ from EAF-2007 (Final) and TALYS.

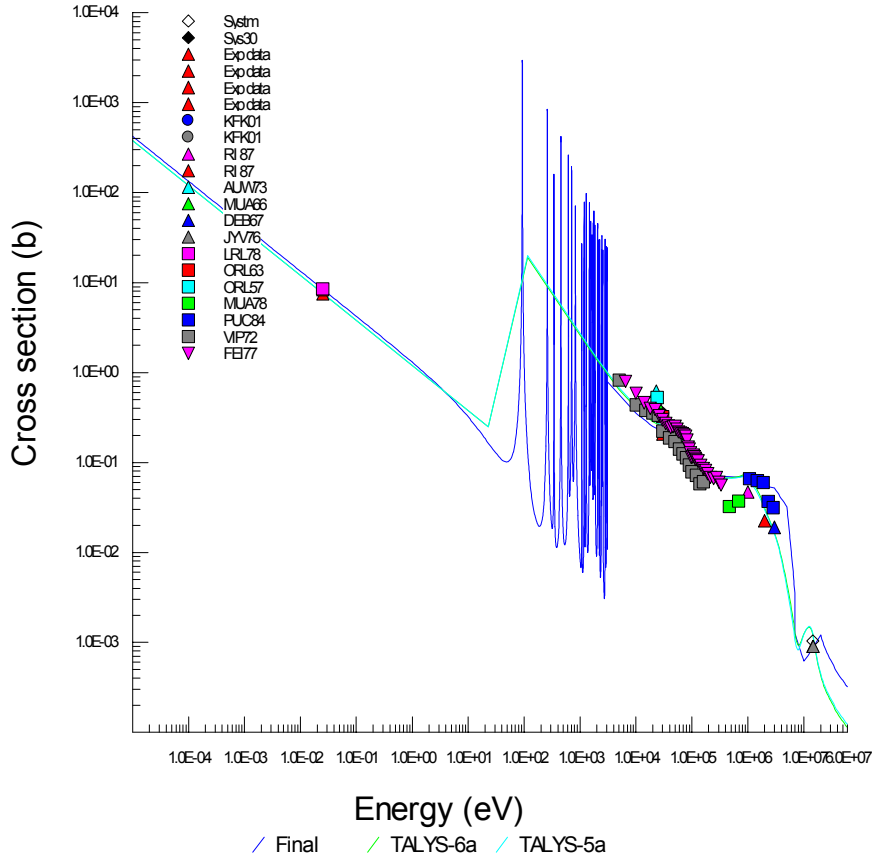

Figure 17. An example of the visual validation plot for $^{154}Sm(n,\gamma)^{155}Sm$ from EAF-2007 (Final) and TALYS.

Another validation procedure, involving comparison to experiment at a single energy is the C/E analysis performed at three distinct energies, namely the thermal cross section energy at E = 0.0253 eV and representing the $1/v$ component, the averaged E = 30 keV cross section (statistical component) and E = 14.5 MeV (pre-equilibrium component). Recommended data selected from the EXFOR compilation and other references have been stored in a SAFEPAQ-II experimental database and these are available for the C/E comparison. The results of such validation for EAF-2007 are shown in Figures 18, 19 and 9 which show very good agreement at all three energies.

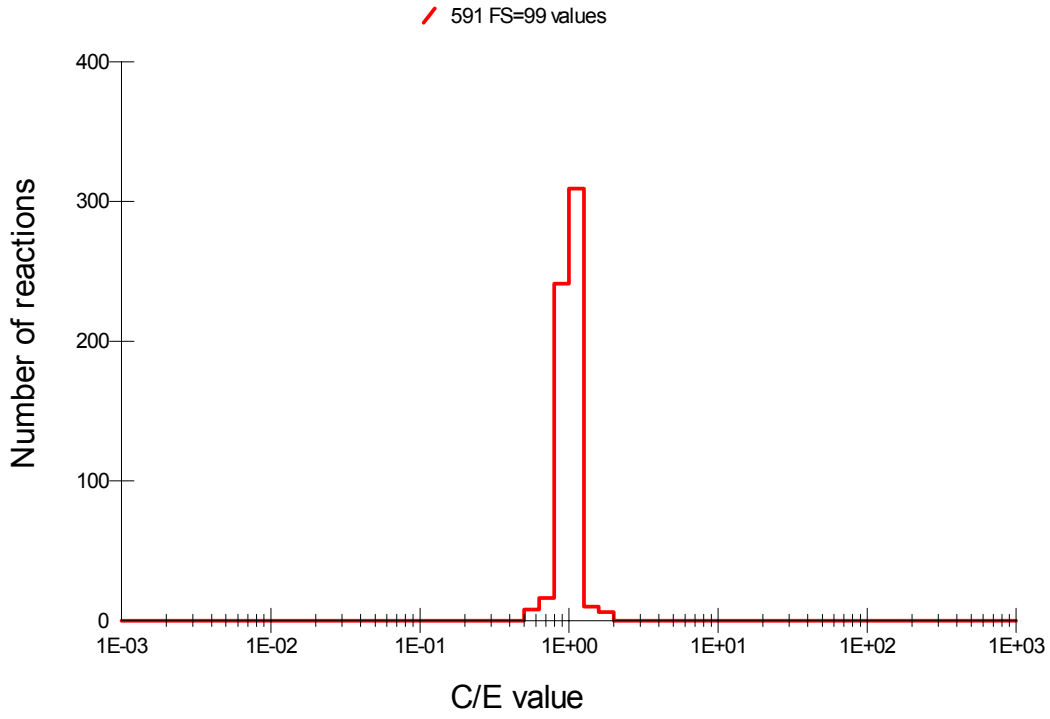

Figure 18. C/E values at 0.0253 eV for the EAF-2007 library, all targets and summed reactions are shown.

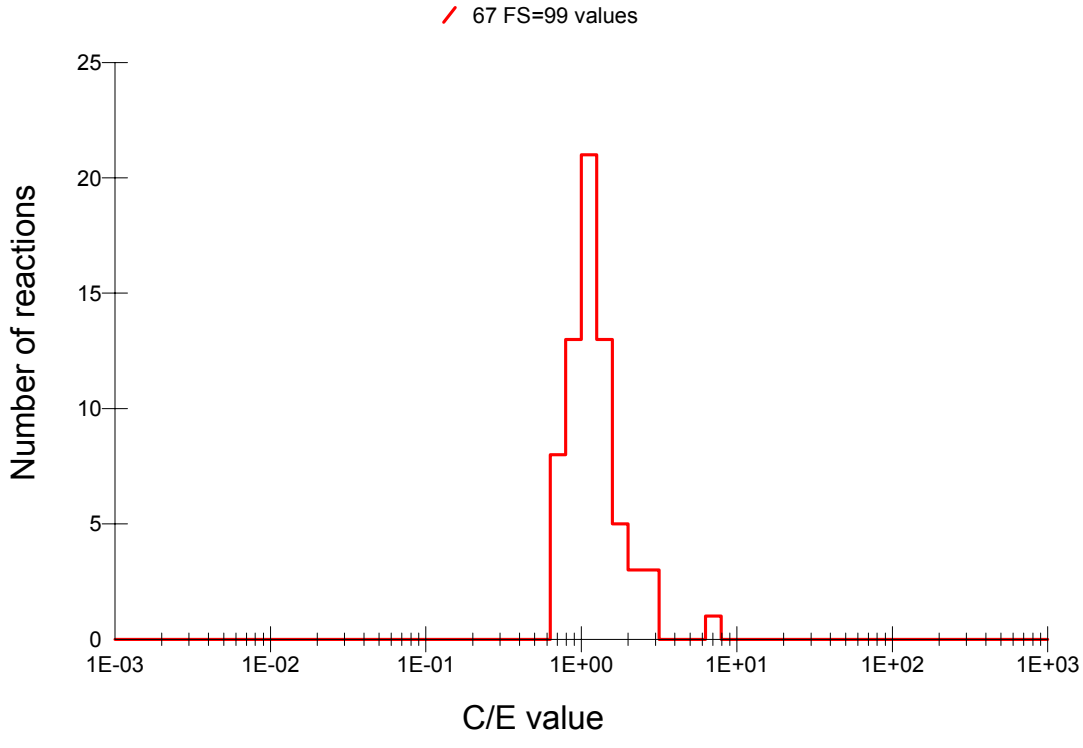

Figure 19. C/E values at 14.5 MeV for the EAF-2007 library, all targets and summed reactions are shown.

A similar approach is used for the validation based on the experimental resonance integrals. Note that for reactions with no resolved resonance region but with experimental values of the resonance integral the Single Resonance Approximation (for details see [2]) has been used to give a cross section with a representative resonance and a better resonance integral. The improvement achieved in C/E results is shown in Figure 20.

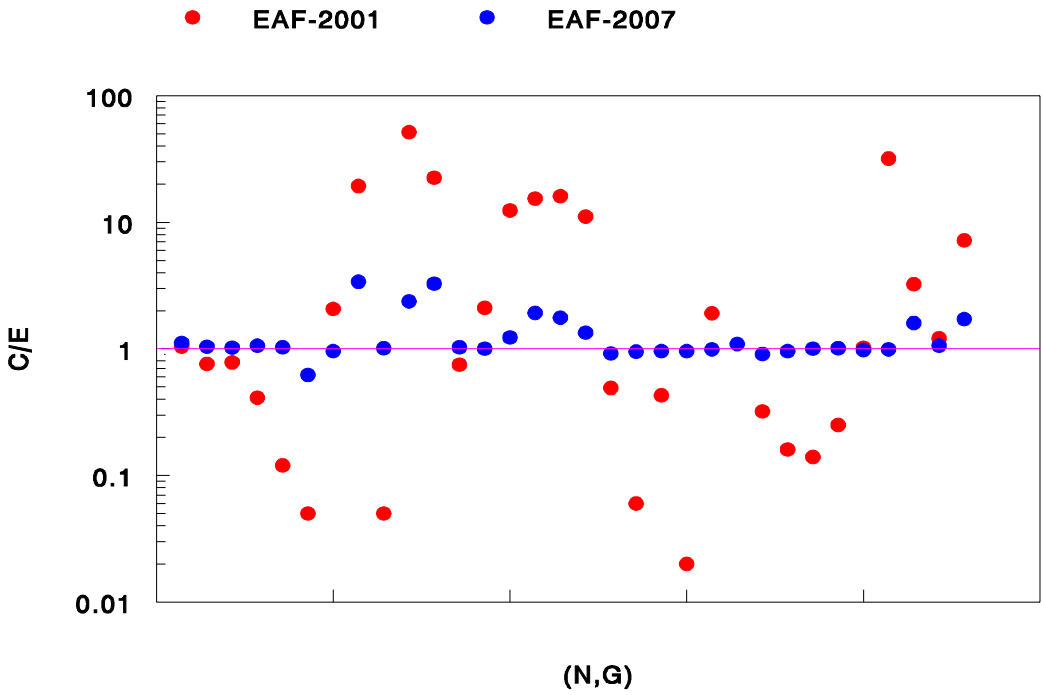

Figure 20. Improved C/E for resonance integrals for reactions in EAF-2007 where the Single Resonance Approximation was applied compared to EAF-2001 data.

3.2 Data with no experimental support (Score = 0 reactions)

In the absence of any experimental information, the cross section systematic relations are the only semi-experimental tool available to compare the calculated cross section with and to enable a confidence level to be assigned to the adopted excitation curves. For previous EAF libraries C/S analysis at two distinct energies, 30 keV and 14.5 MeV, has been used to give a visual representation of the quality of the EAF data. However, the present improvement of the σ_{30} systematic (see Section 2.2.2) and the availability of TALYS calculations with two different input parameters (TALYS-5 and -6) enables for the first time an attempt to improve the Score = 0 reaction data. This will be discussed in detail in section 5. Here only the standard C/S analysis is presented.

3.2.1 Validation at 30 keV

All 337 reactions without experimental support have been visually reviewed, comparing the EAF-2007 data with TALYS-6 calculations which use global parameters. There is typically no or only a very small difference between TALYS-5 and -6 for these reactions. The listing, with some comments for modifications for these reactions, is given in Appendix 3. Note that Appendix 3 lists reactions where there are no experimental data for the total and in cases where the reaction is split none for any of the final states.

For a direct validation of the excitation curves (above the resolved resonance region threshold E_H), ratios of C/S (comparisons of calculated data with the systematic cross sections at 30 keV) have been considered in this study, and are now based on the final improvement of the 30 keV systematic, as discussed in detail in Section 2.2.2. Since the validation at incident energy of 30 keV has turned out to be rather effective and the only one check of the statistical component of the excitation curve for targets with no experimental data, we have performed the C/S analysis as detailed below.

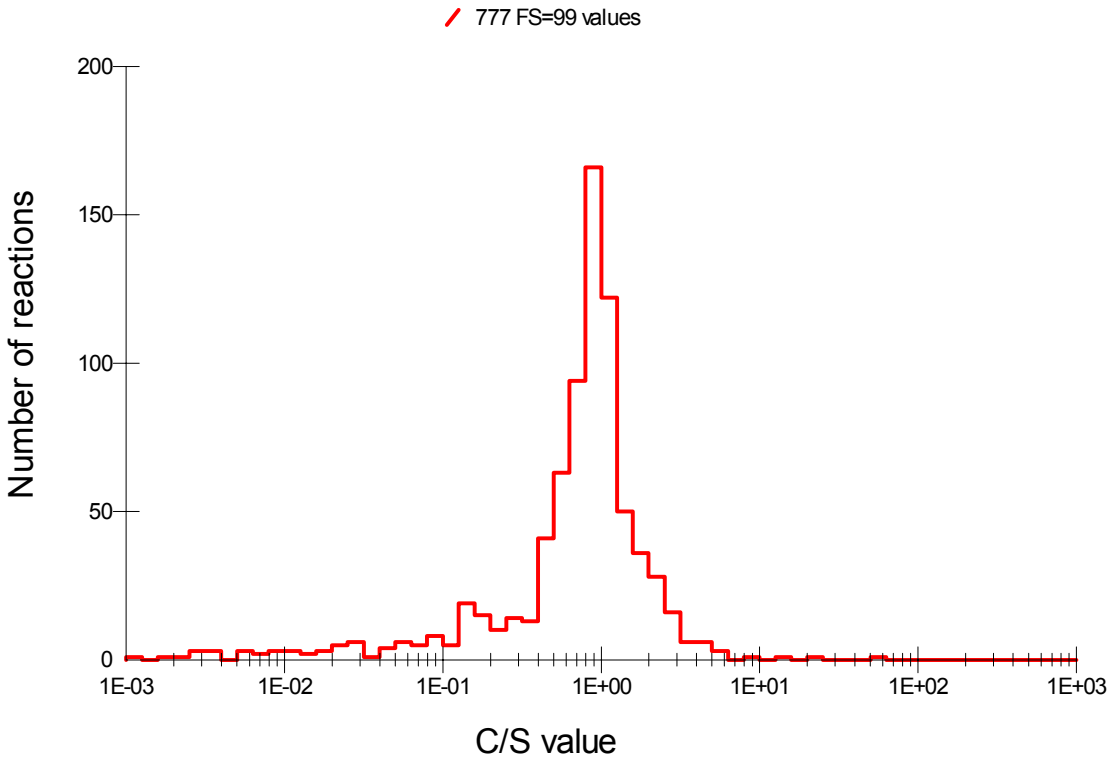

Figure 21. C/S at 30 keV for the EAF-2007 library. Reaction data for all targets are plotted. The C/S < 0.1 originate from reactions where the 30 keV data point lies in the resolved resonance region, and the C/S value depends on the location of the nearest resonance to 30 keV.

Firstly the C/S analysis has been applied to all targets and the corresponding plot of C/S (30 keV) data for EAF-2007 is shown in Figure 21 using the new systematic implemented in the SAFEPAQ-II code. An inspection of this plot shows that the mean value of the histogram lies close to but slightly below C/S = 1, which is a very satisfactory result. The broadness of the distribution is due to two facts; firstly due to the uncertainty of the σ_{30} systematic and secondly when the 30 keV data point lies in the resolved resonance region, C/S has no real physical meaning.

In order to clarify this result in more details, we have carried out the C/S analysis for targets supported by experimental data (Score = 1-6), and where the *aU* values have been taken from the tabular approximation. The results are shown in Figure 22, in which targets with Score = 1-6 are compared to the cross section systematic predictions. It can be seen, that the peak of the C/S ratio is well centred around C/S = 1. For these reactions the calculations are usually made with local input parameters and adjusted to local values of D_0 and Γ_γ and a good agreement is expected. This result supports the correct derivation of the σ_{30} systematic, reproducing the experimentally validated cross sections of EAF-2007. As before the values below C/S = 1 are largely due to resonances occurring at the 30 keV energy.

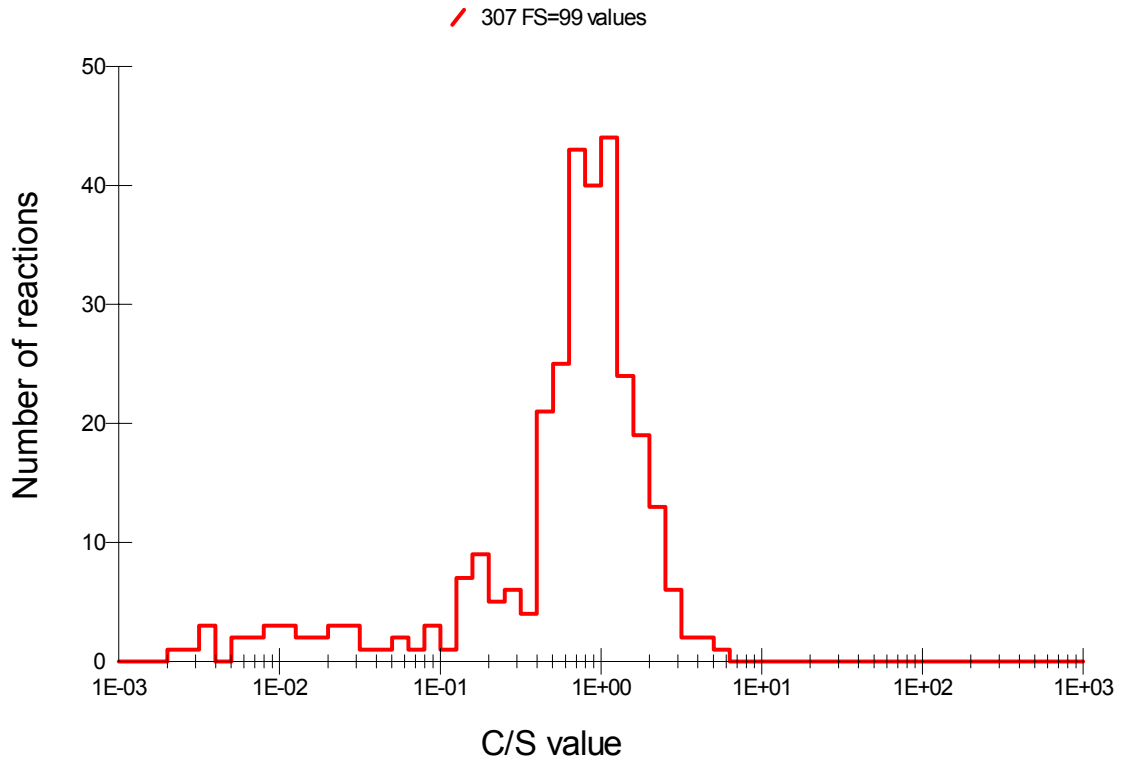

Figure 22. C/S at 30 keV again from EAF-2007. Only targets with Score = 1-6 are used for the comparison with the 30 keV cross section systematic.

Finally the C/S analysis has been applied to targets with no experimental support, having a Score = 0. For these targets validation against the 30 keV cross section systematic is rather important, because it can serve as an indirect validation of the calculated cross sections (statistical component) although this approach has not been applied yet. The results of the C/S analysis for EAF-2007 Score = 0 targets is shown in Figure 23. The obtained distribution shows a small under estimation (C/S is centred at about 0.9) with a reasonably narrow data scatter. These results demonstrate the quality of adopted capture data in EAF-2007.

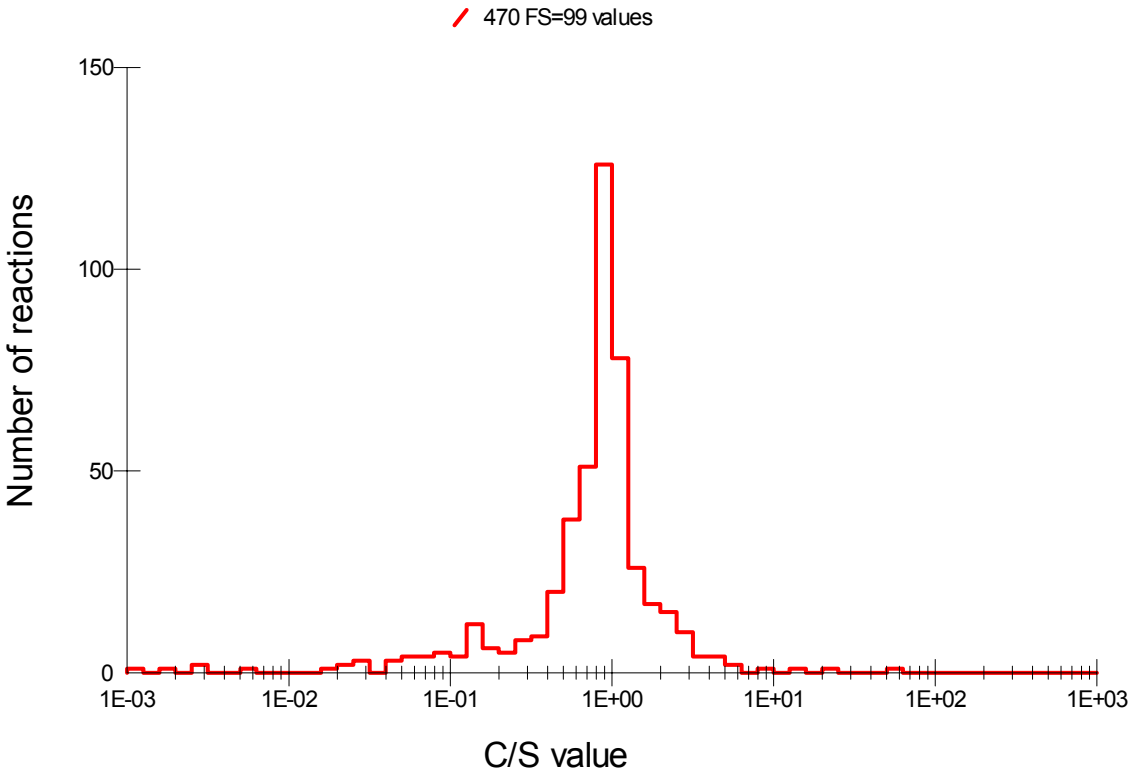

Figure 23. C/S at 30 keV from EAF-2007 for targets with Score = 0.
These results and their use for improvement of future EAF libraries are discussed in section 4.

3.2.2 Validation at 14.5 MeV

Generally the pre-equilibrium component of EAF-2007 data at about 14.5 MeV is in very good agreement with the systematic prediction of the cross section as can be seen in Figure 24. The small peak with over-estimated values around C/S = 2-3 is for a group of JEF and JENDL calculations, due to the use of the direct/semi-direct formalism [4] and the merging of the source values at 20 MeV to TALYS calculations (Section 4.2.3 discusses this further). For these reactions, replacement by TALYS data at all energies is proposed and details are listed in Appendices 1-3.

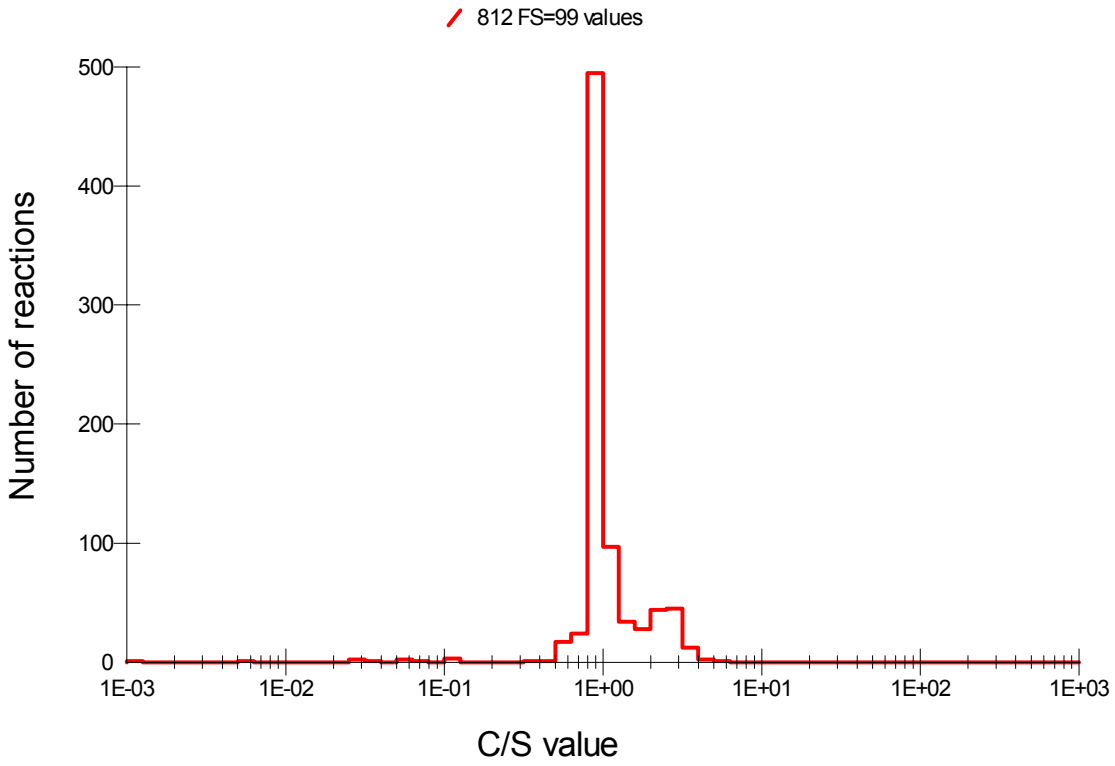

Figure 24. C/S at 14.5 MeV from EAF-2007 for all targets.

4. Data validation – TALYS calculations

TALYS calculations were carried out during 2005 and 2006 using two different sets of input parameters for level densities and these are denoted as TALYS-5 and -6 respectively. Generally TALYS calculations for EAF libraries are executed in the large-scale default calculation mode. In the TALYS-5 calculations however, an improvement to the procedure was employed, namely the derived D_0 parameters from level density models were adjusted to the recommended experimental D_0 values as compiled in reference [37]. In the compilation of TALYS plots shown on the web site www.talys.eu, they are denoted as '*with local level density parameters*', while in TALYS-6 no adjustment was applied and the D_0 values from the level density models, denoted as '*with global level density parameters*' were used. It should be noted however, that experimentally known discrete levels are used in both approaches. Since it was shown in the discussion above, that both Γ_γ(tot) and D_0 are essential ingredients for a good prediction of capture cross sections, it is interesting to investigate whether this adjustment of D_0 gives any improvement of the results for TALYS-5.

4.1 Data with experimental support

Both sets of TALYS calculations have been used in the EAF-2007 validation against differential data and the resulting TALYS-5 and -6 cross sections are included in the complete set of plots. Additionally the standard single-energy C/E validations have been applied and the results are discussed below.

4.1.1 Thermal cross sections

Both sets of calculations show an excellent C/E agreement as can be seen in Figures 25 and 26, but this is to be expected, since the TALYS code is using the recommended σ_{th} database taken from EAF. These values are applied to adjust the $1/v$ component at the energy of 0.0253 eV.

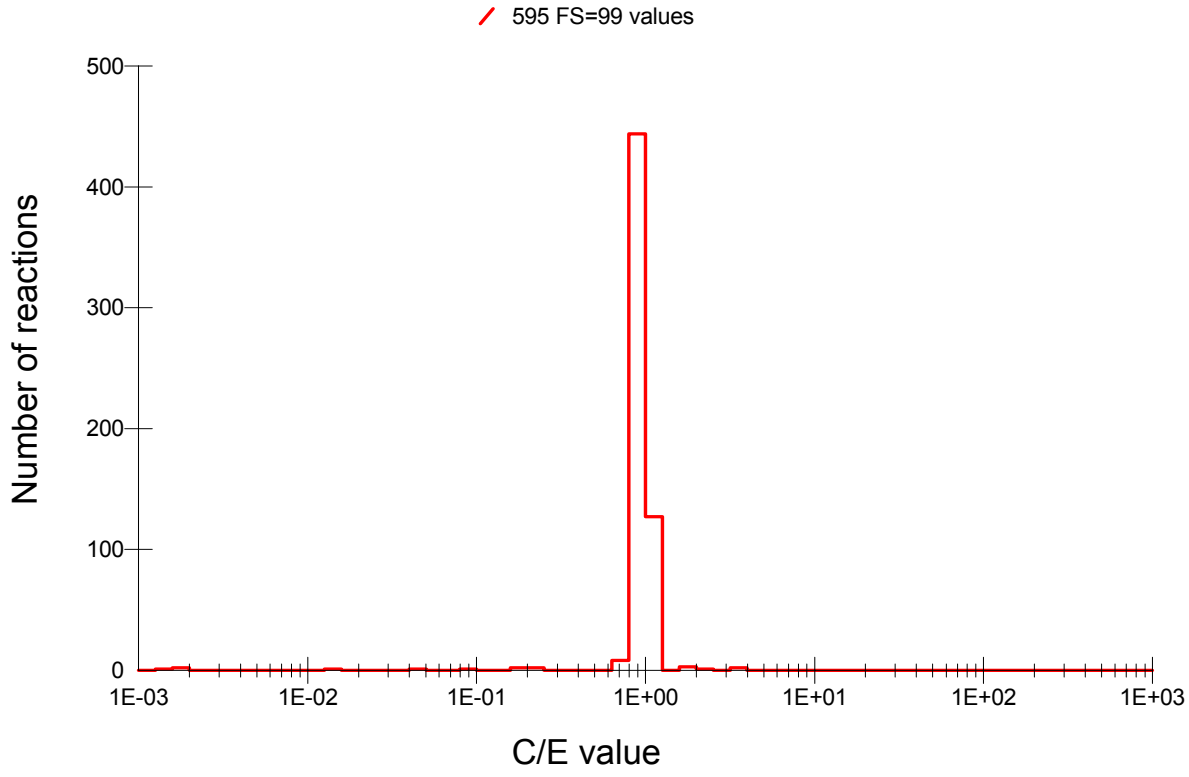

Figure 25. C/E histogram at E = 0.0253 eV using TALYS-5 calculations.

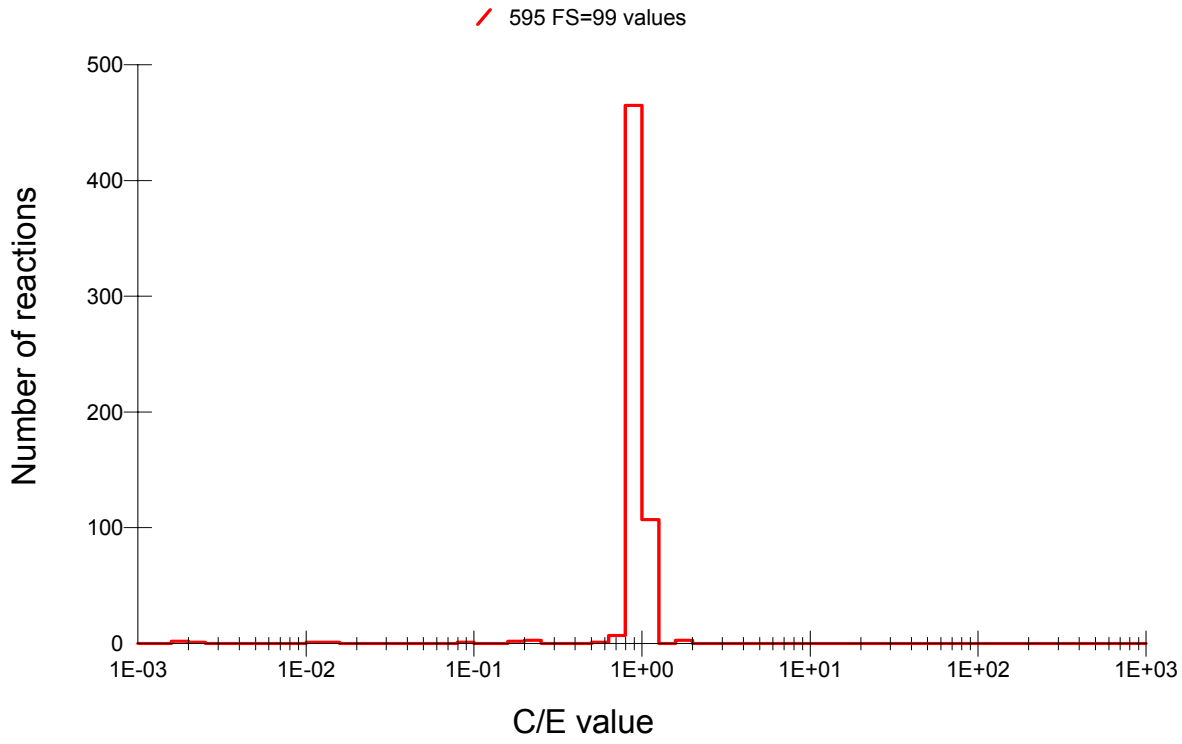

Figure 26. C/E histogram at E = 0.0253 eV using TALYS-6 calculations.

4.1.2 Validation at 30 keV

The agreement of the calculated statistical compound nucleus component is tested at an energy of 30 keV. The histograms shown in Figures 27 and 28 weakly support the observation on the importance of D_0 for the results, since for TALYS-5 (with adjusted D_0) the histogram is well centred around C/E = 1, while for TALYS-6 (with global D_0) a small shift to values C/E about 1.5 can be seen. It is worth noting, that the eventual adjustment of the derived Γ_γ(tot) to experimental or recommended values would probably improve the fit further. C/E values deviating significantly from 1 correspond to reactions in which the 30 keV energy point lies in the resolved resonance region.

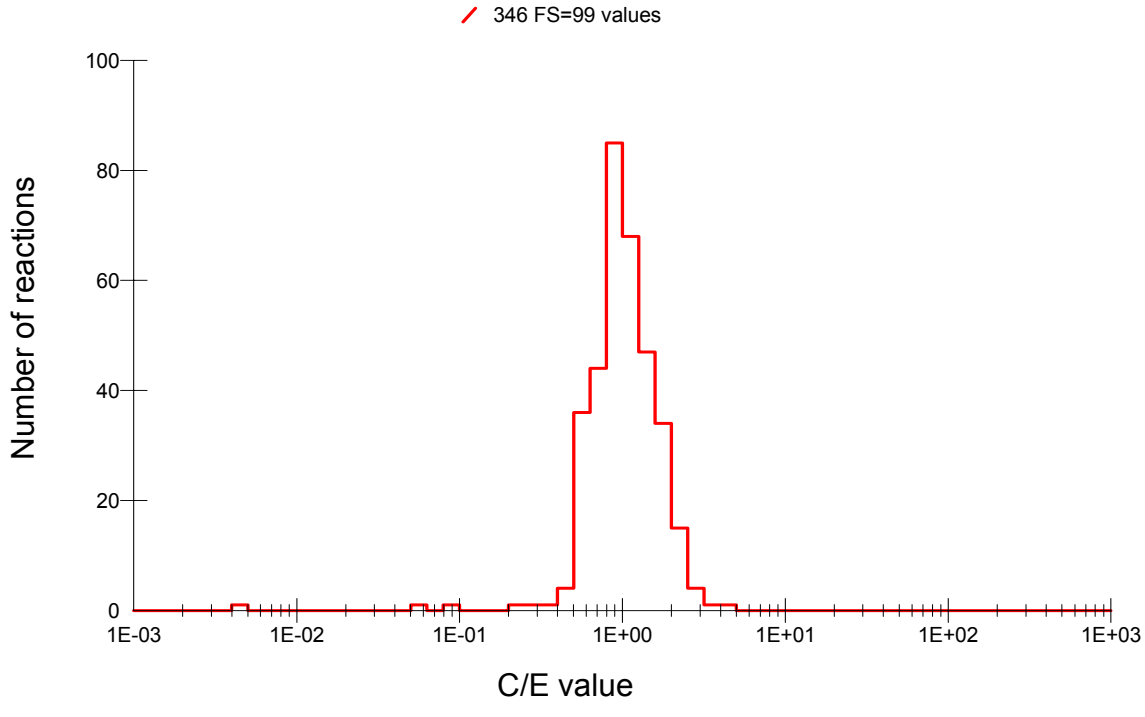

Figure 27. C/E for 30 keV cross sections for TALYS-5 calculations.

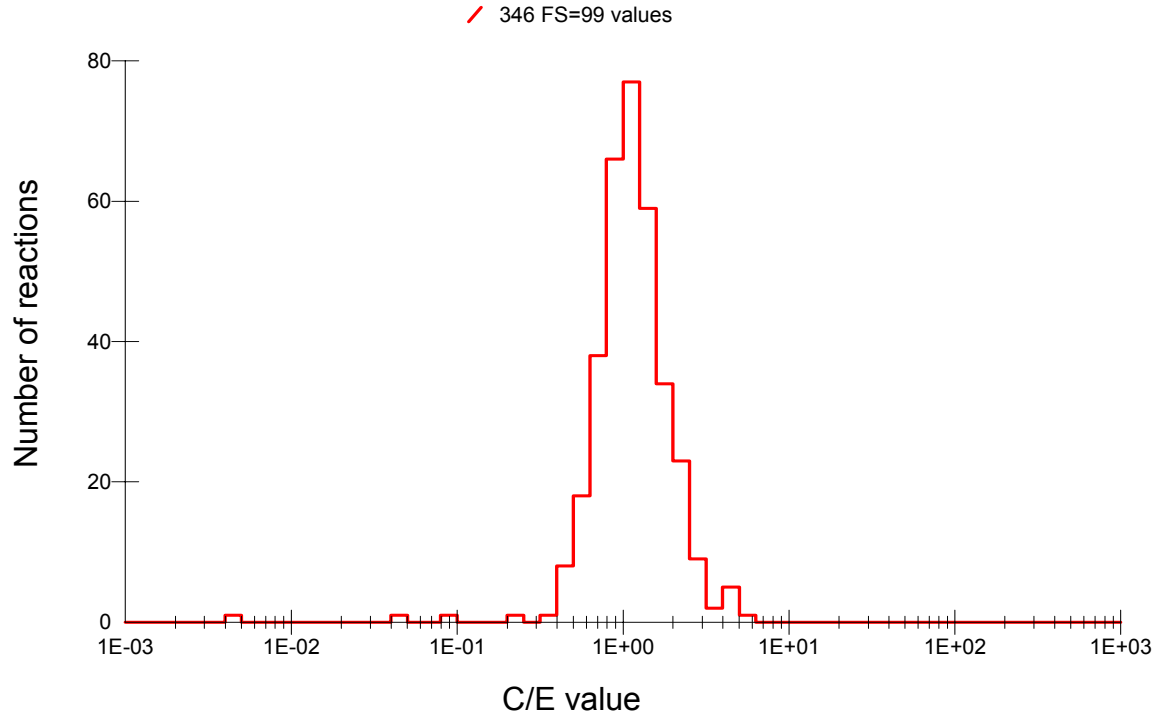

Figure 28. C/E for 30 keV cross sections for TALYS-6 calculations. Note the slight shift of the peak above C/E = 1.

Another test for the statistical compound nucleus component can be performed by the comparison of 30keV values of TALYS and EAF-2007 data files for Score = 1–6 reactions, assuming that the EAF-2007 data are used as a reference. These two histograms are shown in Figures 29 and 30.

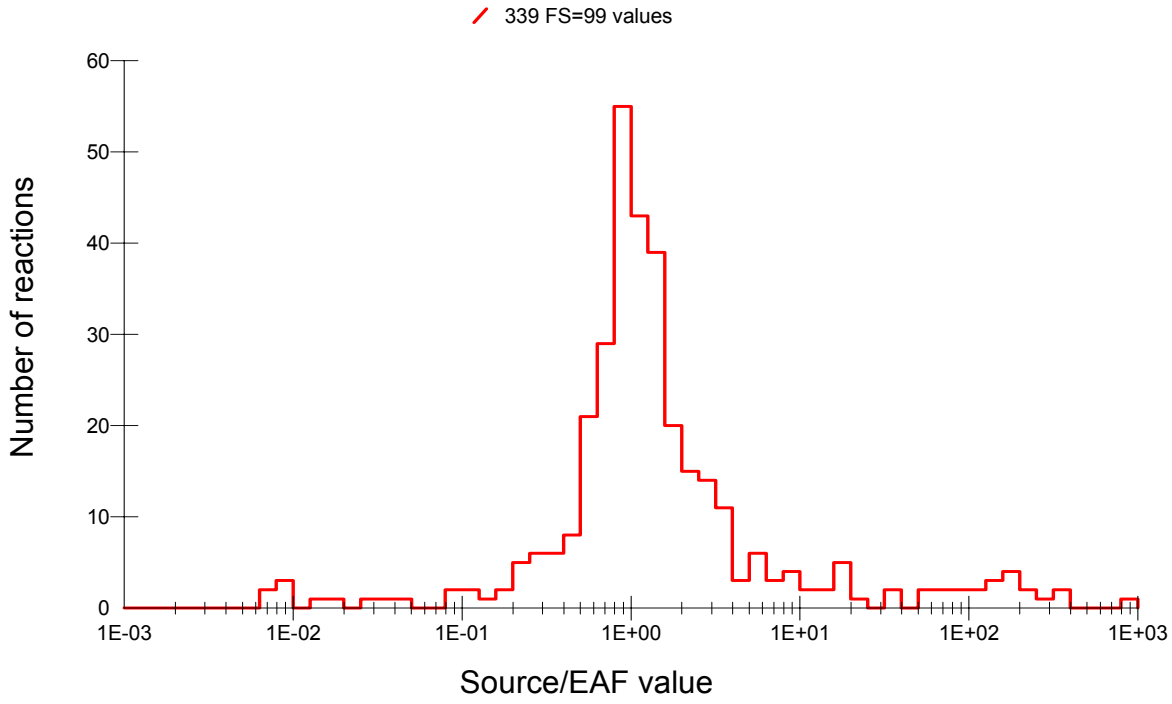

Figure 29. Ratio of TALYS-5 to EAF-2007 data at 30 keV. Ratios far from unity are for reactions where the 30 keV energy point lies in the resolved resonance region.

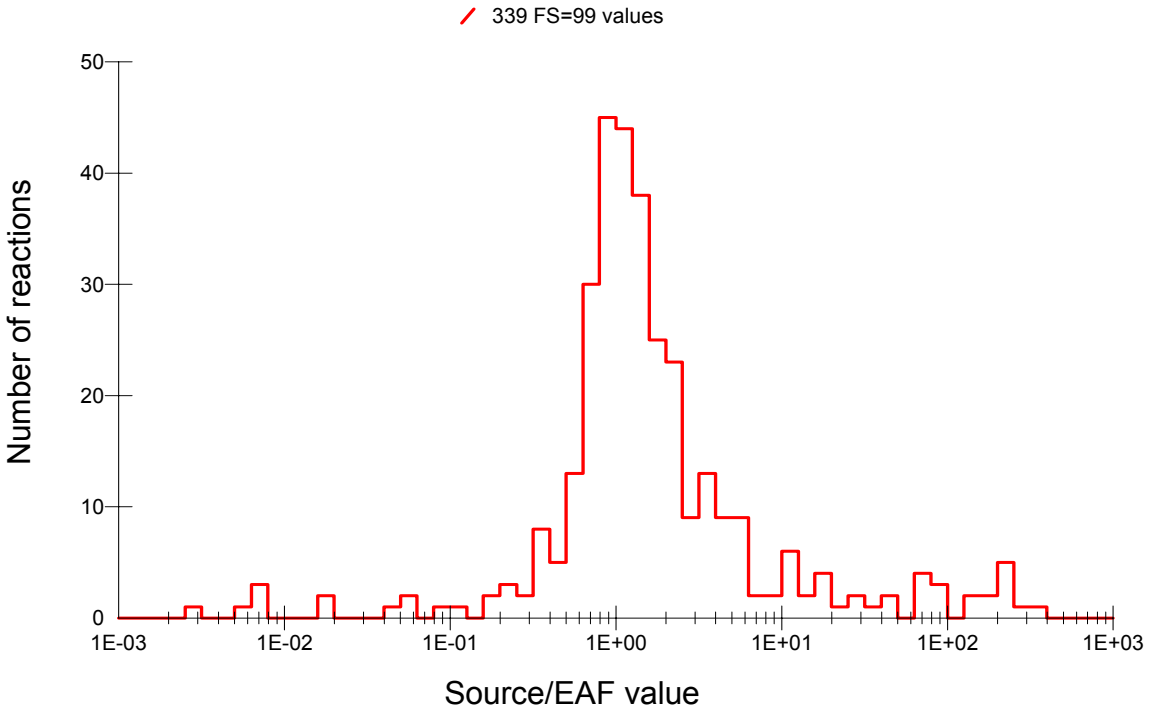

Figure 30. Ratio of TALYS-6 to EAF-2007 data at 30 keV. Note the slight shift of the peak above 1. Ratios far from unity are for reactions where the 30 keV energy point lies in the resolved resonance region.

4.1.3 Validation at 14.5 MeV

The pre-equilibrium component, as calculated with TALYS, is in good agreement with the relatively limited 14.5 MeV experimental database as shown in Figures 31 and 32. There are limited differences between the two sets of TALYS calculations, thus the influence of level density prescription is not as relevant at this energy as at 30 keV. The scatter of the C/E values can be largely explained by the spread of the energies of measured data, which lie between 14 and 15 MeV.

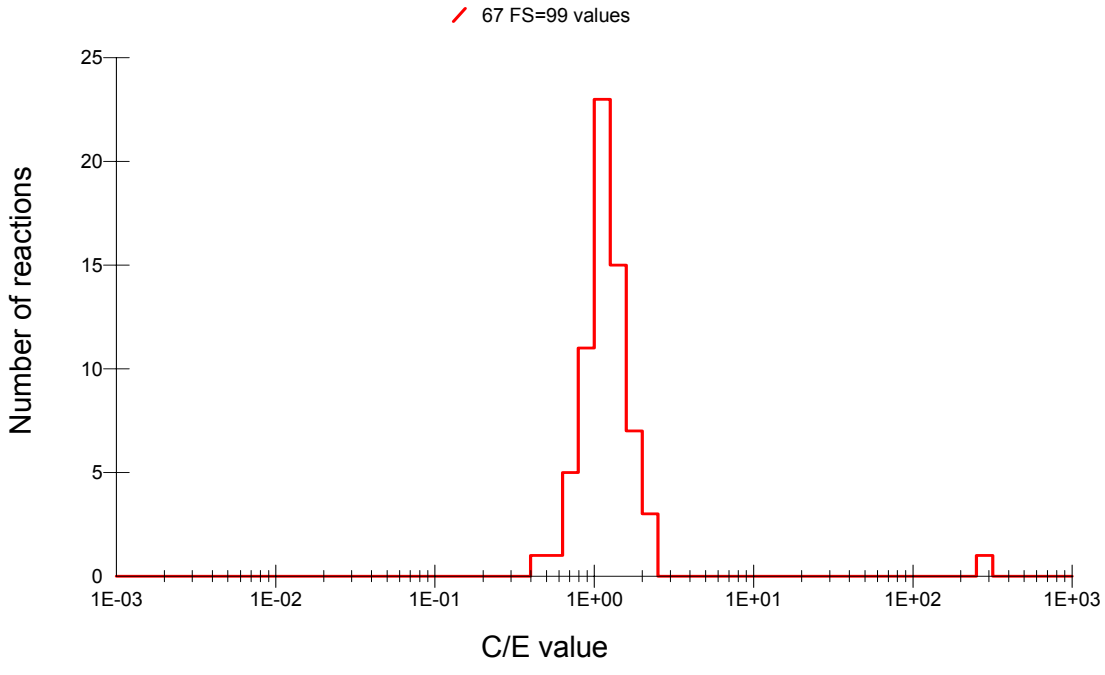

Figure 31. C/E at 14.5 MeV for data from for TALYS-5 calculations. Note the slight shift of the peak above C/E = 1.

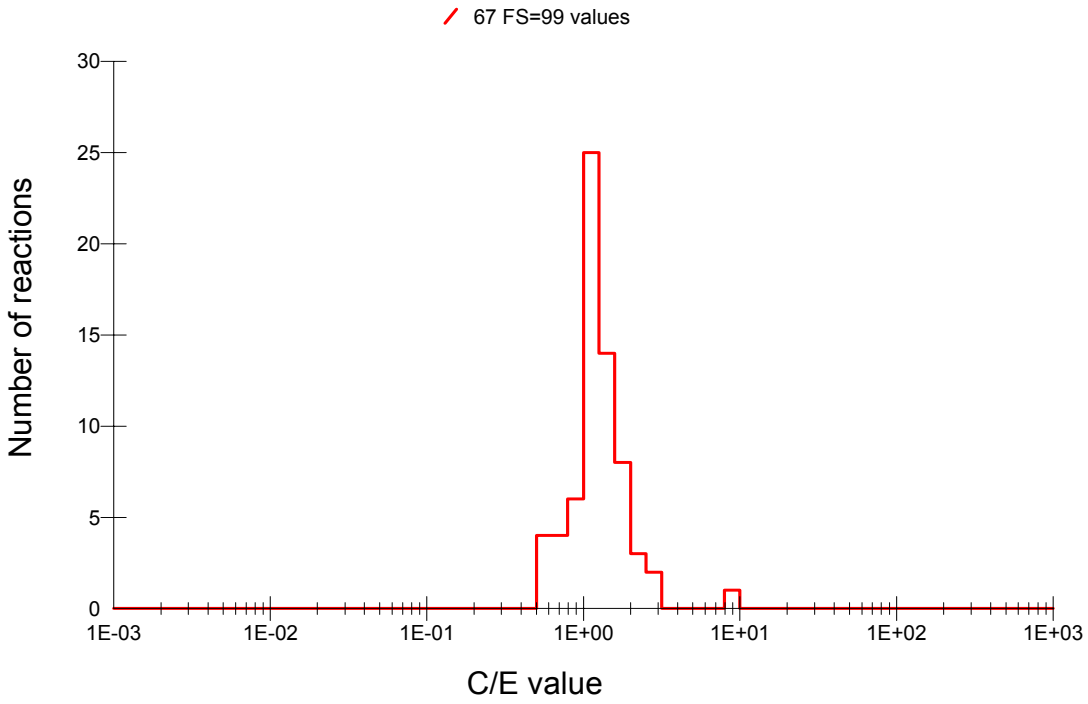

Figure 32. C/E at 14.5 MeV for data from TALYS-6 calculations. Note the slight shift of the peak above C/E = 1.

In conclusions, for the EAF-2007 data with Score = 1-6 a generally good agreement is found for the statistical component of cross sections, with the C/E peak closed to unity. However, a number of improvements are proposed for some reactions, to improve both the statistical or pre-equilibrium parts of the excitation curve (see Appendices 1-3). Both sets of TALYS calculations have a tendency slightly to overestimate the statistical component, with the C/E peak at about 1.5. The calculation with local D_0 values shows a better agreement with experiment, which is to be expected and it is recommended that this D_0 adjustment be used for all future TALYS calculations.

4.2 Data with no experimental support

4.2.1 Validation at 30 keV

The same C/S analysis has been carried out for TALYS-6 calculations as was done for the EAF-2007 data. There is no difference between TALYS-5 and -6 calculations for Score = 0 targets, since in both cases global D_0 adjustment is applied (local D_0 values do not exist). The result of the C/S validation for TALYS-6 data is shown in Figure 33 for all targets. This shows a reasonably narrow distribution with the peak centred at about C/S = 2, indicating a slight overestimation of the calculations.

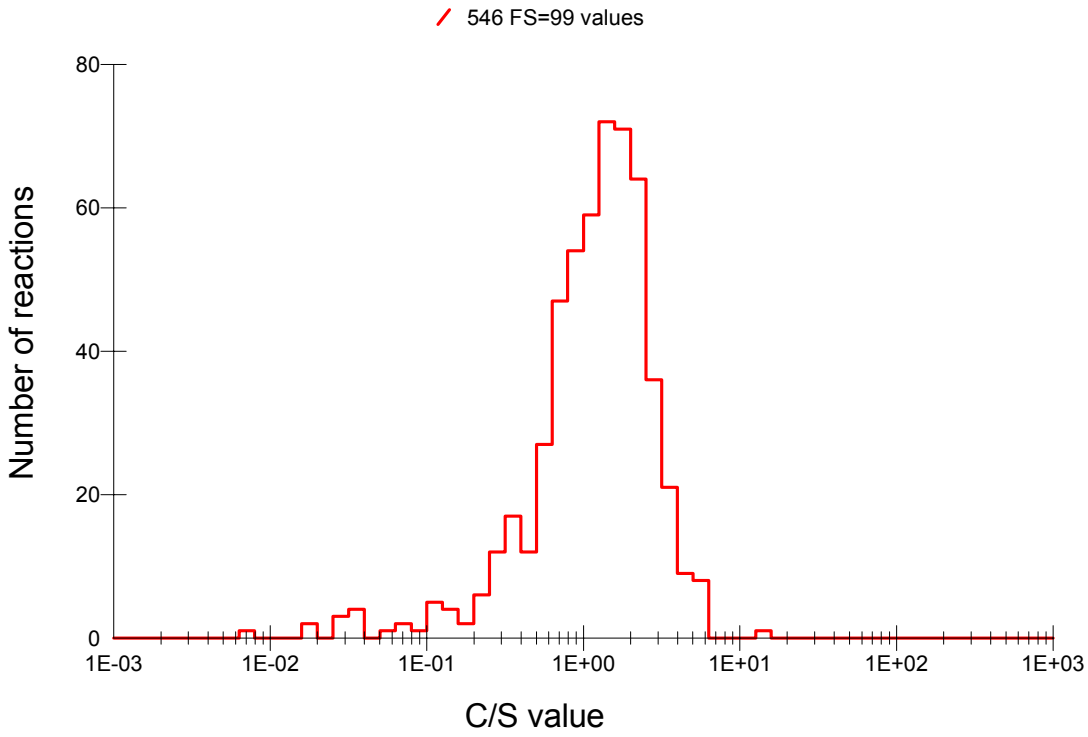

Figure 33. C/S at 30 keV for data from TALYS-6 calculations. Reaction data for all targets are plotted. Values of C/S < 0.1 correspond to reactions where the 30 keV data point lies in the resolved resonance region.

The C/S analysis has been repeated for targets with Score = 1-6 and the result is shown in Figure 34. It can be seen that the slight overestimation of the systematic cross section is also present, with the peak centred at about C/S = 1.8. This supports the overestimation seen in the C/E results for TALYS-6 (Figure 31), where the peak is centred at about 1.5. These two results show, that TALYS calculation with *global level density parameters* over-predict the statistical cross section component.

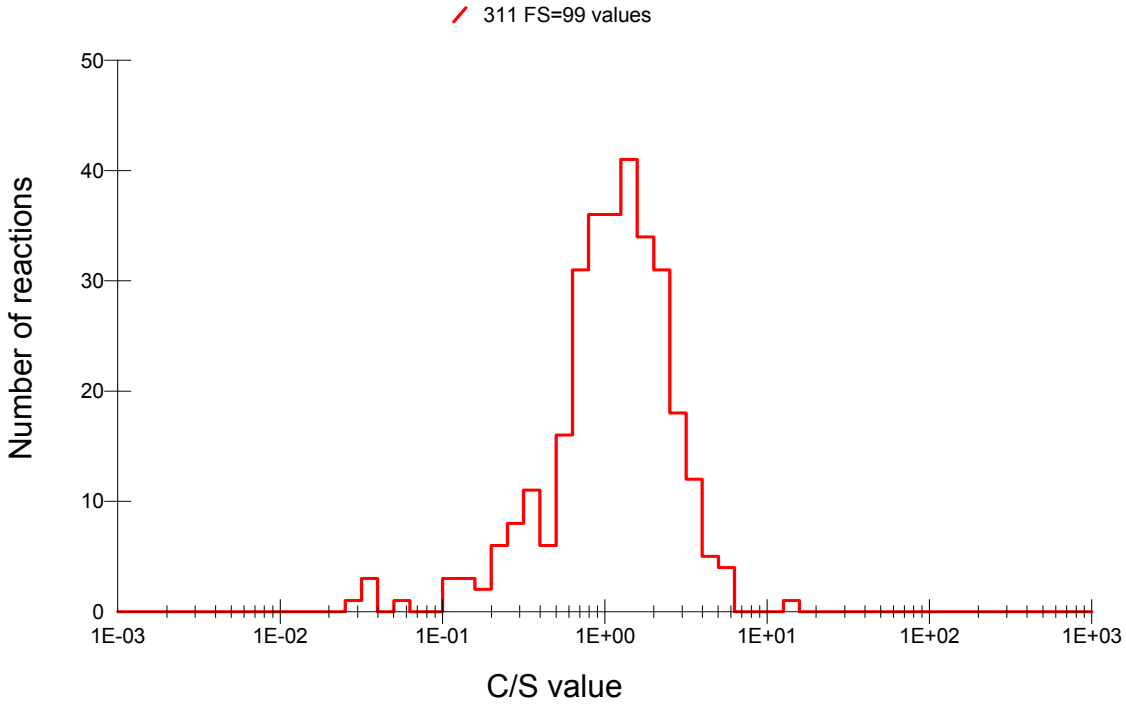

Figure 34. C/S at 30 keV for data from TALYS-6 calculations, for targets with Score = 1-6.

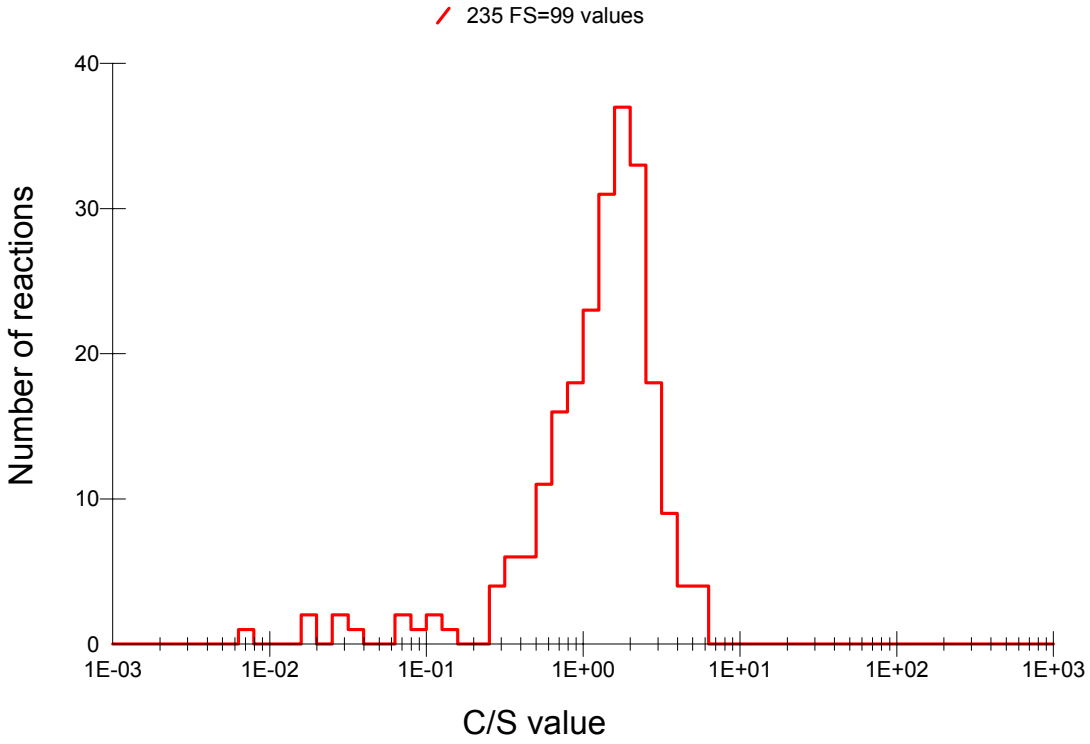

Figure 35. C/S at 30 keV for data from TALYS-6 calculations, for targets with Score = 0.

The same result of an overestimation of the C/S peak is found for targets with no experimental cross section data, as can be seen in Figure 35. This overestimation tends to increase slightly with the mass number A (as long as the actinide targets with $A > 225$ are ignored), as demonstrated in Figure 36, where the same data are plotted as a function of A.

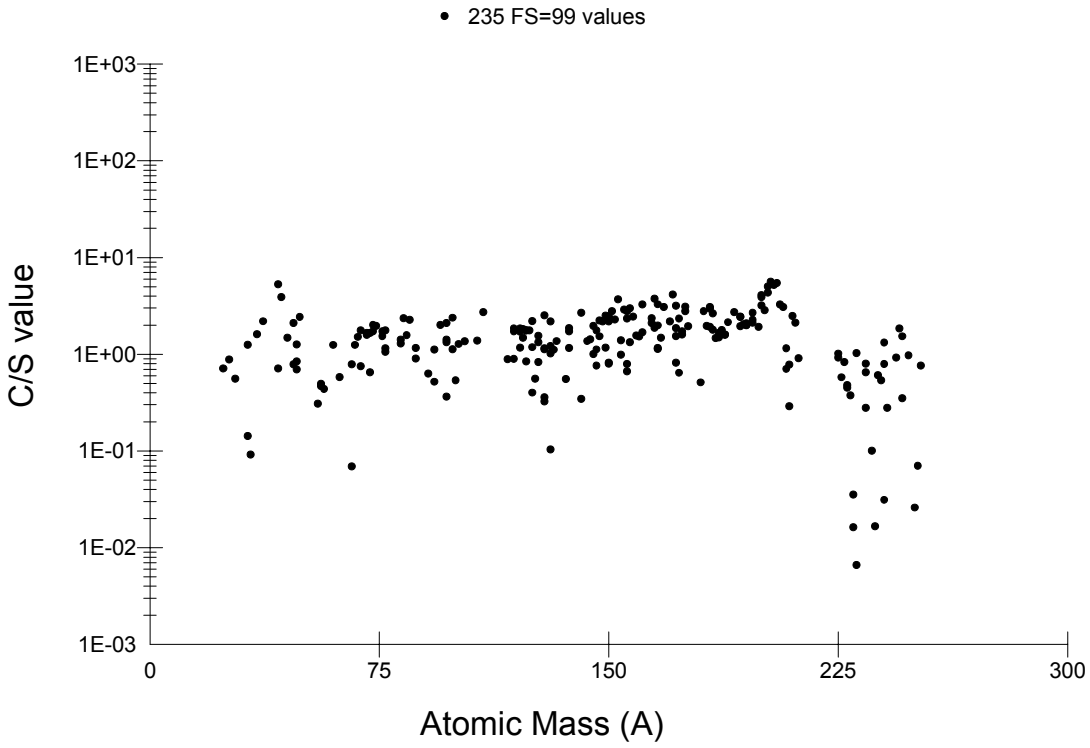

Figure 36. C/S at 30 keV for data from TALYS-6 calculations for targets with Score = 0 plotted as a function of A. Note the increasing trend of C/S with A and problems for actinide targets arising from a large uncertainty of E_H values (often above 30 keV).

In conclusions, for EAF-2007 data with Score = 0 a general good agreement is found for the statistical component of cross sections, with the C/S peak value closed to unity. However, a number of changes are proposed for some reactions, to improve both the statistical or pre-equilibrium parts of the excitation curve (see Appendix 3). Both sets of TALYS calculations (here only TALYS-6 results are shown) have a tendency slightly to overestimate the statistical component, with the C/S peak centred at about 2. Such a result is expected, since for all Score = 0 targets the TALYS calculations are performed with global level density parameters, which have been shown to be less good than the local parameters.

4.2.2 Validation at 14.5 MeV

The results of C/S analysis for 14.5 MeV data show a significant over-prediction of calculated values against the 14.5 MeV systematic by a factor of 1.5 - 2. This is demonstrated in Figure 37 for TALYS-6 results. This over-prediction can be accounted for by the two-component exciton model used in TALYS, since the C/E results in Figure 32 also show a peak centred above C/E = 1. However, the over-prediction is still at the same level as the uncertainty of the derived $\sigma_{14.5}$ systematic, which is estimated to be f = 1.5 (see Section 2.2.3).

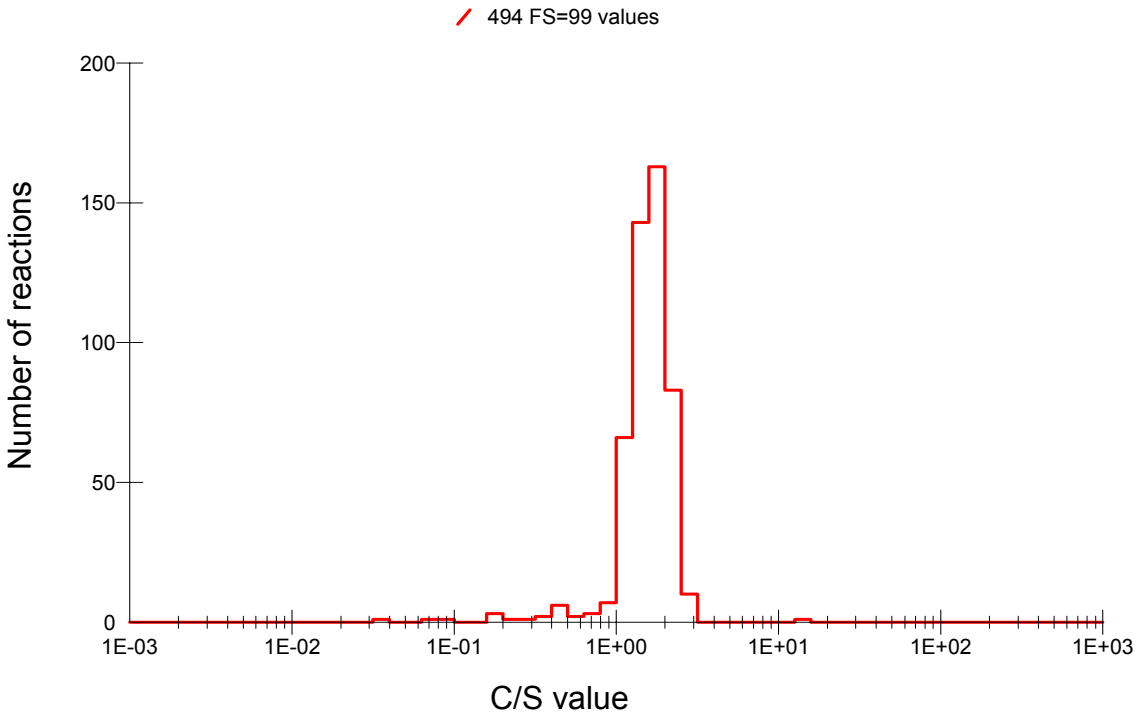

Figure 37. C/S analysis for data from TALYS-6 calculations at 14.5 MeV.

In order to obtain more information on the pre-equilibrium data behaviour, the 14.5 MeV cross section values from EAF-2007 and TALYS-6 have been plotted as a function of the mass A as shown in Figures 38 and 41.

A closer inspection of Figure 38 reveals the following facts. EAF-2007 data at 14.5 MeV are in reasonable agreement with the systematic prediction. In fact, a large number of MASGAM calculations in EAF-2007 have been normalized to this prediction, as can be seen in the figure. The slight overestimation of the trend curve at high A is primarily due to a number of adopted data from JEFF and JENDL evaluations, where the direct/semi-direct model [4] has been used for the representation of the pre-equilibrium component. These calculations extended in energy up to 20 MeV and typically have non-physical increasing values above the statistical part. This is demonstrated in Figure 39 for the ^{143}Ce target where the Final (EAF-2007) curve corresponds to original data from JEF-2.2 merged at 20 MeV with the

renormalized TALYS-6 calculation. The TALYS-6 result has a more physical shape and gives a good agreement with the systematic at 14.5 MeV.

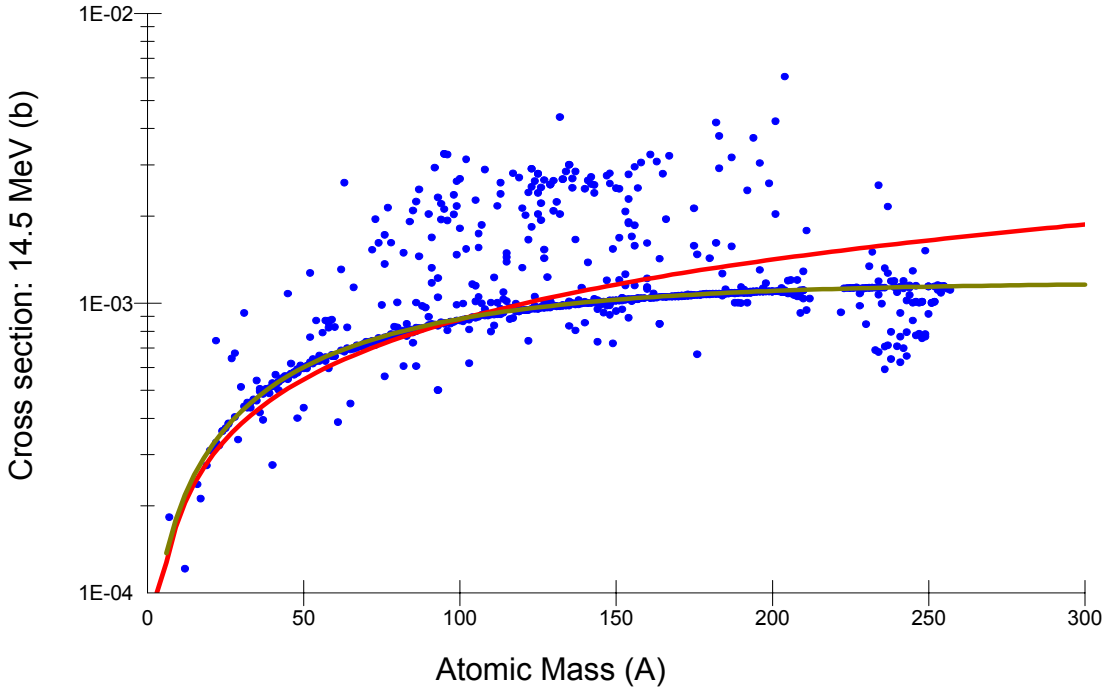

Figure 38. 14.5 MeV cross section values from EAF-2007. The red curve is the trend of the displayed data, while the green curve corresponds to the 14.5 MeV systematic predictions.

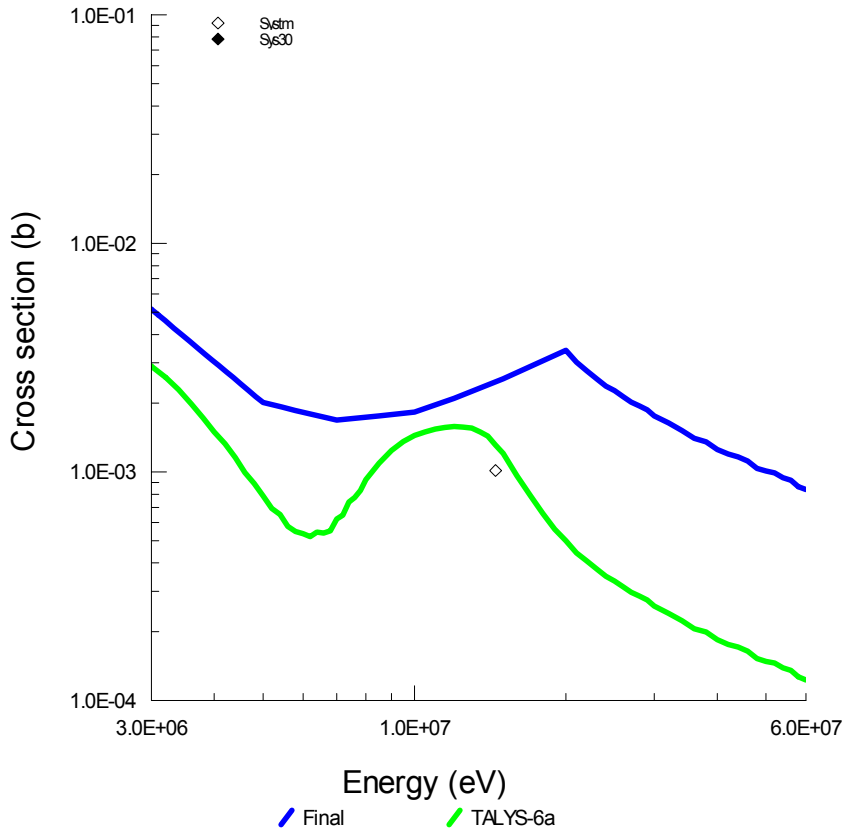

Figure 39. The pre-equilibrium region in the $^{143}Ce(n,\gamma)^{144}Ce$ reaction for EAF-2007 (Final) and TALYS-6.

This non-physical local maximum in the cross section at 20 MeV can be demonstrated by SACS analysis. Figure 40 show the E_{max} values for capture data in EAF-2007 for energies above 10 MeV. Many reactions have a local maximum at 20 MeV caused by the merging of data at 20 MeV. However, even for these reactions the cross sections are typically 2 – 4 mb which is physical even though the shape of the curve could be improved.

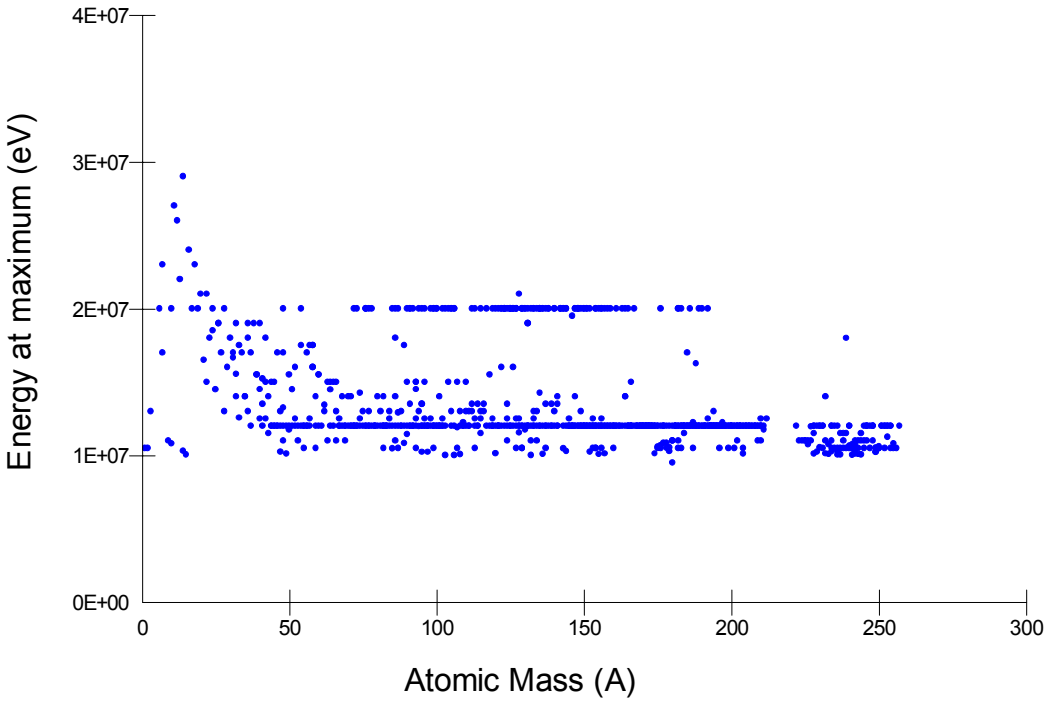

Figure 40. $E_{max}(A)$ data for capture reactions in EAF-2007. Note that only local maxima > 10 MeV are shown.

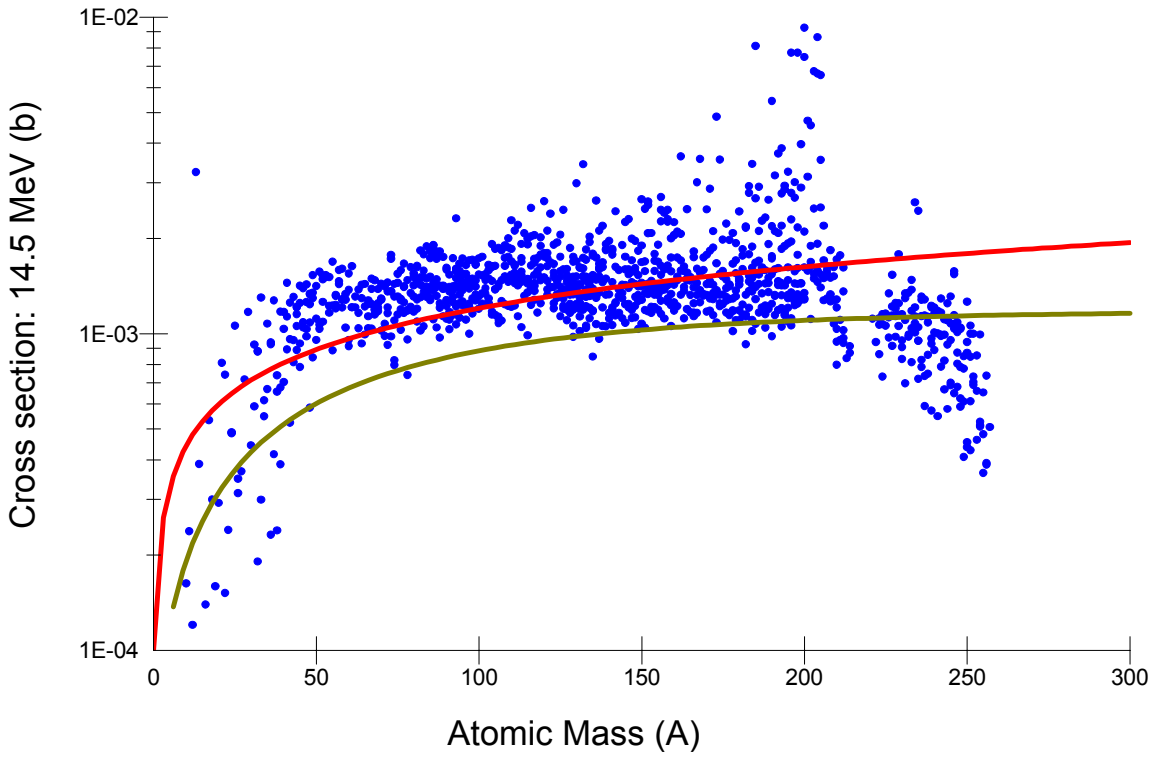

Figure 41. 14.5 MeV cross section values from TALYS-6. The red curve is the trend of the displayed data, while the green curve corresponds to the 14.5 MeV systematic predictions.

A similar analysis for 14.5 MeV data from TALYS-6 is shown in Figure 41. There are two main regions, where the calculated data are significantly different from the trend. Firstly, the narrow set of points at $190 < A < 210$ which are above the trend, corresponding to targets with closed shell structure. Secondly, the points with $A > 210$ which are below the trend, corresponding to the heavier actinides. The remaining points have a trend parallel to the systematic prediction, with about a 50 % over-prediction. This confirms the over-prediction observed already earlier in the C/E and C/S analyses.

A comparison with the other major data sources, MASGAM and NGAMMA used in EAF-2007 for capture reactions shows good agreement with TALYS in the shape of the pre-equilibrium component, as well as the energy at which the cross section has its maximum. This is rather surprising for reactions based on MASGAM since this code uses the systematic for the whole pre-equilibrium region [5], where the shape of the curve above 7 MeV is calculated. Examples for these data source are shown in Figures 42 and 43. The $E_{max}(A)$ analysis for TALYS-6, shown in Figure 44, demonstrates a very good predictive power of the exciton model used in TALYS.

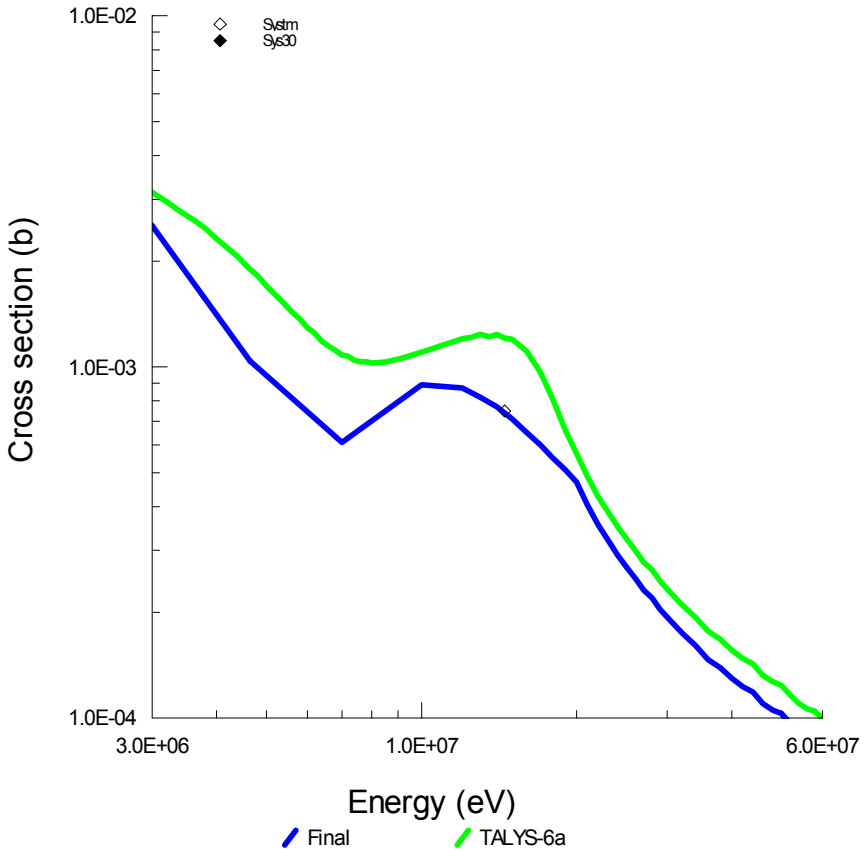

Figure 42. The pre-equilibrium region in the ^{72}Ga(n,γ)^{73}Ga reaction for EAF-2007 (Final) and TALYS-6. EAF-2007 data are taken from MASGAM (optionally renormalized to 14.5 MeV systematic).

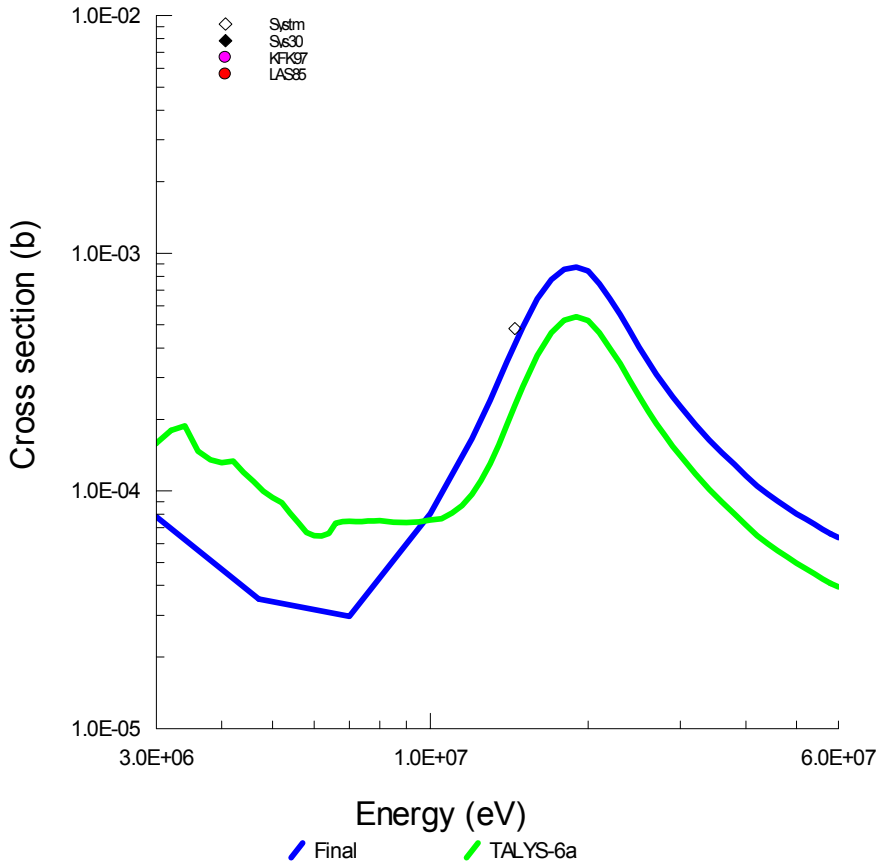

Figure 43. The pre-equilibrium region in the $^{36}S(n,\gamma)^{37}S$ reaction for EAF-2007 (Final) and TALYS-6. EAF-2007 data are taken from NGAMMA (optionally renormalized to 14.5 MeV systematic).

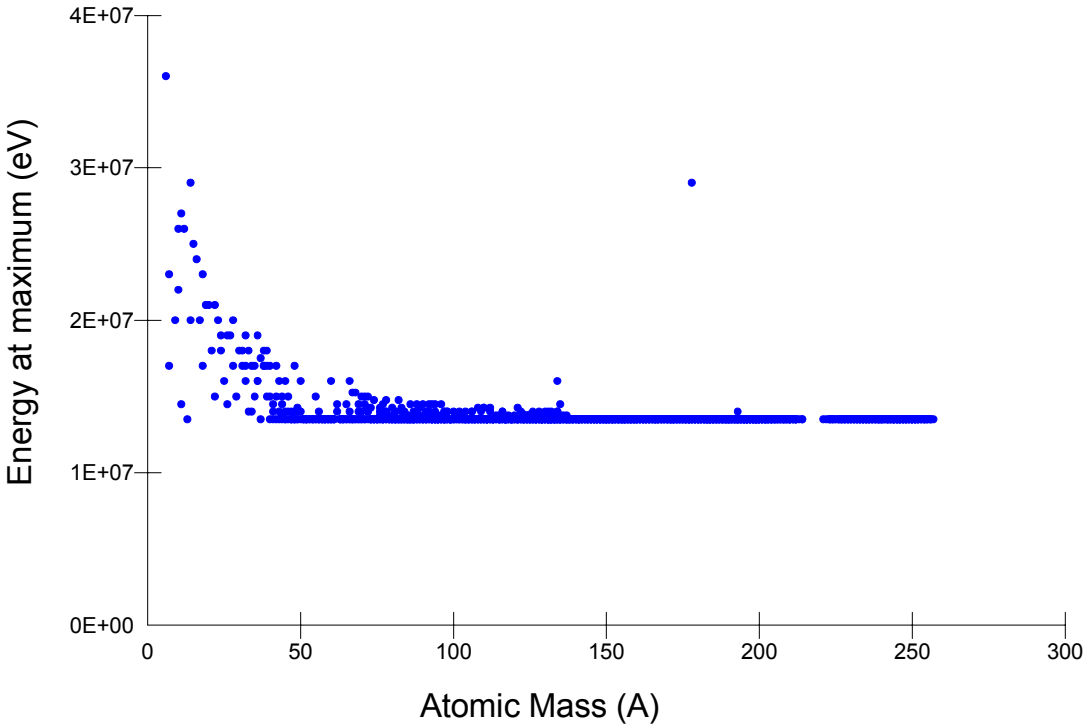

Figure 44. $E_{max}(A)$ data for capture reactions in TALYS-6. Note that only local maxima > 10 MeV are shown. The strongly deviating point below A = 200 corresponds to the isomeric radioactive target ^{179n}Hf, with its energy in the continuum, where TALYS calculations have difficulties.

5. EAF-2007 Score = 0 data validation and improvements

Based on the recent improvements described above, the 30 keV cross section systematic can now be considered as sufficiently good when compared to the original experimental data. Therefore it can be used as a tool for direct data validation of the statistical cross section component and in reactions with a strong C/S disagreement also for a renormalization modification. The present study is the first where this systematic is used to validate EAF-2007 data for reactions with no experimental support and to propose modifications for EAF-2009. This may also be combined with an inter-comparison of two or more independent calculations carried out with different modelling codes and input parameters. This gives another degree of validation, based on how well the calculated results agree with each other. Here the EAF-2007 cross sections are compared with TALYS-6 calculations. The data sources of all the Score = 0 capture reactions in EAF-2007 are given in Table 2.

Table 2. Data sources of Score = 0 reactions as adopted in EAF-2007.

Data source	Number	Data origin
MASGAM	238	Calculations
SIGECN- MASGAM	3	Calculations
NGAMMA	18	Calculations
TALYS-5a	10	Calculations
TALYS-6a (-6)	39	Calculations
JEF-2.2	25	Evaluations
ADL-3	6	Evaluations
ENDF/B-VI	1	Evaluations
ENDF/B-VII.2	2	Evaluations
JENDL-3.1	4	Evaluations
JENDL-3.3	1	Evaluations
Total	337	

It can be seen, that the majority of entries (MASGAM and NGAMMA) are also based on global input parameters, as discussed above, and therefore a comparison with TALYS-6 calculations can give information on the behaviour of these two completely independent calculations and can thus serve as an indirect validation, in cases where the results reasonably agree. This argument is based on the fact that different level density models, gamma-ray strength functions and pre-equilibrium treatment as well as independently chosen input parameters have been applied in the two calculations. Since in these global calculations (MASGAM, NGAMMA and TALYS) no attempt to improve the fit to the data by adjusting model parameters has been applied, the agreement between them conveys a feeling for the accuracy of these model calculations. Only in the first set of MASGAM calculations, in 1992 for the EAF-3 library [1], was the 30 keV systematic from reference [1] used for renormalization of the statistical component, for reactions where there was strong disagreement between the calculated and systematic values.

In the visual validation, a quality judgment has been assigned to each reaction, based on the agreement between both data sources (EAF and TALYS) and the fit to the 30 keV cross section systematic. Further the estimates of D_0 (= E_H in calculated excitation curves) and σ_{th} can also be compared, since these are derived from level density models and so give an indication of their agreement. The thermal cross section is dependent on the level density parameters (a, U), since the systematic formula (equation 1) has been used in all calculations.

An example of the excellent agreement between both MASGAM and TALYS calculations and the σ_{30} value is shown in Figure 45. In contrast a poor agreement both of cross sections and level density parameters (indicated by the large $1/v$ disagreement) is shown in Figure 46.

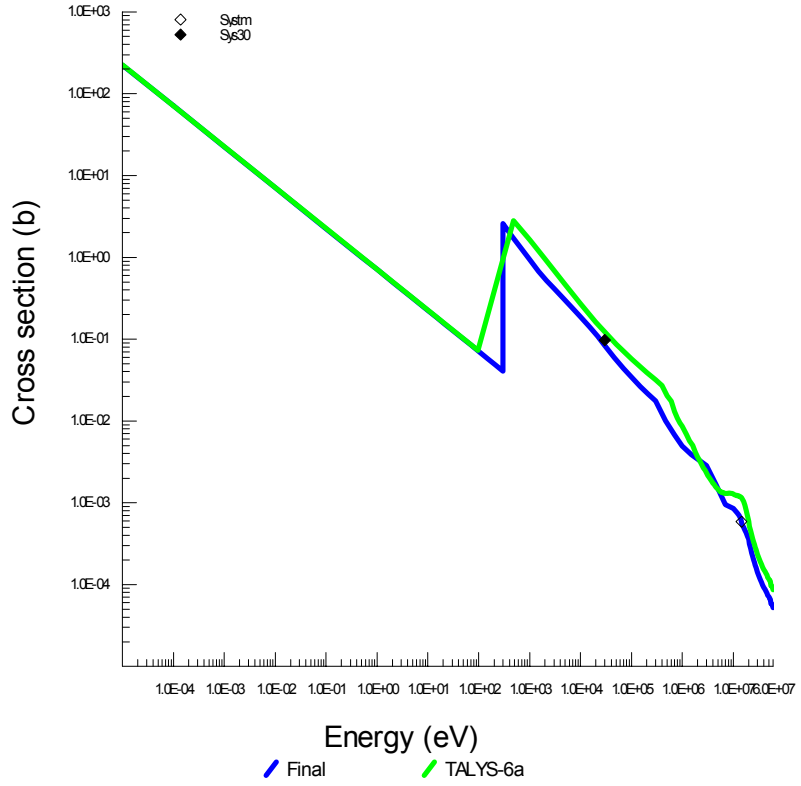

Figure 45. ^{48}V(n,γ)^{49}V data from EAF-2007 (Final) and TALYS-6. The excellent agreement with σ_{30}, similar D_0 values and the same thermal cross sections suggest that similar *a*, *U* parameters were used in both calculations.

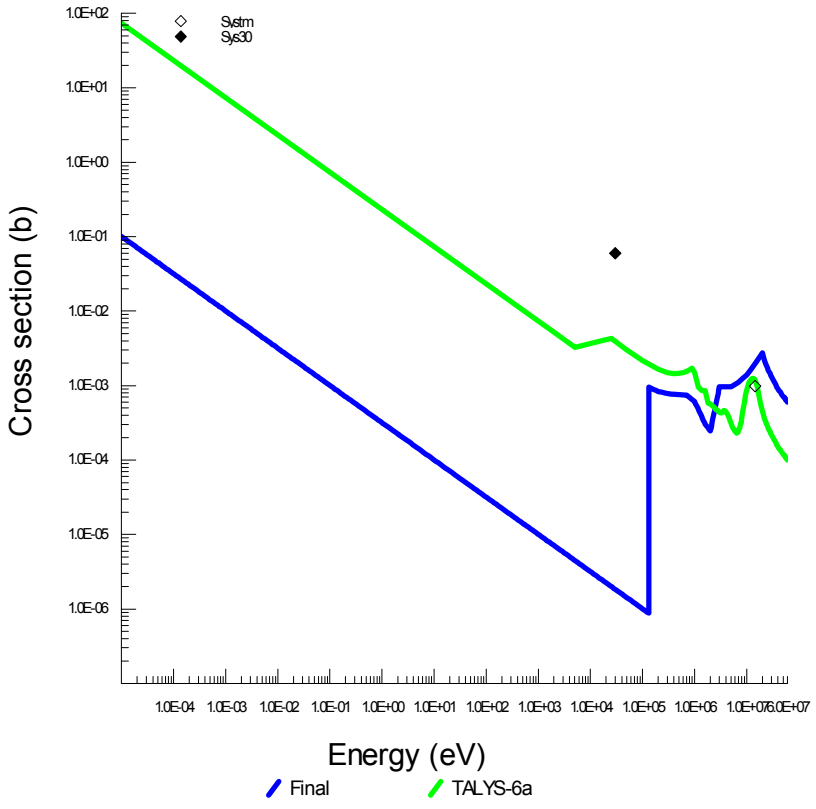

Figure 46. $^{132}Te(n,\gamma)^{133}Te$ data from EAF-2007 (Final) and TALYS-6. The poor agreement with σ_{30}, dissimilar D_0 values and the discrepant thermal cross sections (factor 10 or more difference) suggest that different *a*, *U* parameters were used for the calculations.

To summarise the results of the validation for EAF-2007 and TALYS-6 it is convenient to consider numbers of reactions agreeing/disagreeing within a factor of 2. This corresponds to an estimated 95% confidence level based on the estimated accuracy of the 30 keV systematic. Table 3 gives the statistics for EAF-2007 and TALYS-6.

Table 3. C/S statistics (σ_{30}) for studied Score = 0 reactions, for details see Appendix 3.

Quality score	Number of reactions (%) EAF-2007	Number of reactions (%) TALYS-6
C/S < 0.5	57(17)	22 (9)
0.5 < C/S < 2	257(76)	145 (63)
C/S > 2	23(7)	68 (28)
Total	337	235

From these results an interesting observation can be made, which demonstrates the high quality of both data sources. The number of evaluations or calculations in EAF-2007, which agree with the 30 keV cross section systematic within a factor of two, is very satisfactory. The slightly smaller agreement for TALYS-6 data reflects the observation noted above, that the TALYS global calculations over-predict both the C/E and the C/S at 30 keV (see Figures 34 and 35). The visual inspection of plotted data shows that the majority of EAF-2007 and TALYS-6 calculation agree in the shape of the statistical component for energies > E_H. This is a rather surprising result, when the differences in the modelling codes (the physics) as well as the quality and completeness of the input parameters (essentially the discrete levels) are considered. Even more amazing is that a reasonable agreement of both E_H and σ_{th} values are found, since they are completely dependent on the assumed level densities, which are very different both in models and parameters in the various calculations.

All these observation suggest an additional validation argument, that the available calculations are basically physically correct (regarding the shape of the excitation curves), and correctly normalised in the low energy ($1/v$) energy region. The observation that 'blind' calculations of the statistical component of capture reactions in EAF-2007 are in reasonable agreement with the expected trend, has been found in all validation procedures in this study. In the comparison of the EAF-2007 and TALYS-6 data, entries for which TALYS calculations have been already adopted in EAF-2007, have been only compared with the 30 keV systematic.

The reactions in EAF-2007 with C/S < 0.5 or > 2 are listed in Table 4 with comments for modifications to be implemented for EAF-2009.

Table 4. C/S (σ_{30}) for EAF-2007 Score = 0 reactions.

No RPL = *the selected source gives the best fit or EAF-2007 data source agree with TALYS-6a and no other data source is currently available*
Only TALYS-X = *only TALYS-X calculation exists for this reaction channel*

57 reactions with C/S < 0.5 (17%)	C/S	Comment	Modification
Te-132(n,γ)Te-133	0.00003	D_0 > 30 keV	RPL-TALYS-6a
Po-210(n,γ)Po-211	0.00285		RPL-TALYS-6a

Pa-230(n,γ)Pa-231	0.01619	Only TALYS-6a	
Es-250(n,γ)Es-251	0.02594	Only TALYS-6a	
Eu-156(n,γ)Eu-157	0.02823		RPL-TALYS-6a
Eu-157(n,γ)Eu-158	0.04010		RPL-TALYS-6a
I-135(n,γ)I-136	0.04804	Only TALYS-6a	
P-32(n,γ)P-33	0.05214		RPL-TALYS-6a
Bk-246(n,γ)Bk-247	0.05353	No RPL	
P-33(n,γ)P-34	0.05546	D_0 > 30 keV	
Al-26(n,γ)Al-27	0.05963		RPL-TALYS-6a
Bk-248(n,γ)Bk-249	0.06478	No RPL	
Bk-248m(n,γ)Bk-249	0.06478	Only MASGAM	
Ga-66(n,γ)Ga-67	0.06904	Only TALYS-6a	
U-231(n,γ)U-232	0.09528	No RPL	
Cm-240(n,γ)Cm-241	0.09564	Only TALYS-6a	
Bk-245(n,γ)Bk-246	0.09665	No RPL	
Np-236m(n,γ)Np-237	0.10086	Only TALYS-6a	
U-230(n,γ)U-231	0.10136	No RPL	
Np-234(n,γ)Np-235	0.12534		RPL-TALYS-6a
Pb-209(n,γ)Pb-210	0.13041		RPL-TALYS-6a
Bk-247(n,γ)Bk-248	0.13203	No RPL	
Fm-252(n,γ)Fm-253	0.13427		RPL-TALYS-6a
Am-240(n,γ)Am-241	0.13888	No RPL	
Si-32(n,γ)Si-33	0.14275	Do > 30 keV	
Pa-229(n,γ)Pa-230	0.14413		RPL-TALYS-6a
Sn-126(n,γ)Sn-127	0.14613	No RPL	
Cf-246(n,γ)Cf-247	0.14923		RPL-TALYS-6a
Sn-119m(n,γ)Sn-120	0.15393		RPL-TALYS-6a (>EH)
Es-251(n,γ)Es-252	0.16650	No RPL	
Pa-228(n,γ)Pa-229	0.17637		RPL-TALYS-6a
Pu-237(n,γ)Pu-238	0.18453	No RPL	
Cm-241(n,γ)Cm-242	0.18623		RPL-TALYS-6a
Hf-178n(n,γ)Hf-179	0.19954	Only JEF-2.2	
Cf-248(n,γ)Cf-249	0.21885		RPL-TALYS-6a
Sn-125(n,γ)Sn-126	0.24209	No RPL	
Zn-72(n.γ)Zn-73	0.25334		RPL-TALYS-6a
Hf-180m(n,γ)Hf-181	0.26658		RPL-TALYS-6a (>EH)
Ar-37(n,γ)Ar-38	0.27627		RPL-TALYS-6a
Fe-60(n,γ)Fe-61	0.30309		RPL-TALYS-6a
Ni-66(n,γ)Ni-67	0.35232		RPL-TALYS-6a
Ca-47(n,γ)Ca-48	0.36490		RPL-TALYS-6a
Pt-200(n,γ)Pt-201	0.38363	No RPL	
Zr-86(n,γ)Zr-87	0.38793		RPL-TALYS-6a
Zn-69m(n,γ)Zn-70	0.42001		RPL-TALYS-6a
Ti-45(n,γ)Ti-46	0.42144		RPL-TALYS-6a
Sn-123(n,γ)Sn-124	0.44094		RPL-TALYS-6a
Ac-228(n,γ)Ac-229	0.44996	Only TALYS-6a	
Po-209(n,γ)Po-210	0.45471		RPL-TALYS-6a
Po-208(n,γ)Po-209	0.45517		RPL-TALYS-6a
Pd-112(n,γ)Pd-113	0.45824		RPL-TALYS-6a
Os-194(n,γ)Os-195	0.47031	No RPL	

Zr-97(n,γ)Zr-98	0.47129	No RPL	
Ni-56(n,γ)Ni-57	0.48243	No RPL	
Fe-52(n,γ)Fe-53	0.49152	Only TALYS-6a	
Ge-68(n,γ)Ge-69	0.49315		RPL-TALYS-6a
Ge-77(n,γ)Ge-78	0.49380		RPL-TALYS-6a

23 reactions with C/S > 0.5 (7%)	**C/S**	**Comment**	**Modification**
Au-196n(n,γ)Au-197	2.00986	Only TALYS-6	
Cr-48(n,γ)Cr-49	2.19302		RPL-TALYS-6a
Ir-193m(n,γ)Ir-194	2.23505	No RPL	
Re-186m(n,γ)Re-187	2.35797	No RPL	
Tc-99m(n,γ)Tc-100	2.37901	Only TALYS-6a	
Tb-154n(n,γ)Tb-155	2.39825	Only TALYS-6a	
At-211(n,γ)At-212	2.46791	Only TALYS-6a	
At-210(n,γ)At-211	2.47849	Only TALYS-6a	
Ta-184(n,γ)Ta-185	2.64191	Only TALYS-6a	
Pt-202(n,γ)Pt-203	2.77101	No RPL	
Ho-164m(n,γ)Ho-165	2.91114		RPL-TALYS-6a
Mo-99(n,γ)Mo-100	2.91437		RPL-TALYS-6a
Os-183m(n,γ)Os-184	3.07039	Only TALYS-6a	
Ta-175(n,γ)Ta-176	3.09890	Only TALYS-6a	
Au-198m(n,γ)Au-199	3.12742	Only MASGAM	
Pt-195m(n,γ)Pt-196	3.23582		RPL-TALYS-6a >EH
Dy-153(n,γ)Dy-154	3.69429	Only TALYS-6a	
Mo-93m(n,γ)Mo-94	4.13925	Only TALYS-6a	
Ir-192n(n,γ)Ir-193	4.54281		
Bi-204(n,γ)Bi-205	5.19436	Only TALYS-6a	
S-35(n,γ)S-36	14.6635		RPL-TALYS-6a
Pu-246(n,γ)Pu-247	22.4123		RPL-TALYS-6a
Mg-28(n,γ)Mg-29	55.2223		RPL-TALYS-6a

For EAF-2009 37 modifications are proposed, and therefore the total of Score = 0 reaction data validated with C/S within a factor of 2 should be improved to about 87%.

A new Quality Score is proposed for Score = 0 reactions to be applied in the EAF-2009 release. For reactions with values of 0.5 < C/S (30 keV) < 2 a new classification is proposed, namely Score = 0_2, while for the remaining cases Score = 0_1 will be used. This is based on the Score = 1 and 2 definitions for reactions with experimental data.

6. Conclusions

The neutron capture cross section data in EAF-2007, the data sources used and the calculation tools have been thoroughly reviewed. This analysis results in a number of proposed modifications, which should lead to a quality improvement in the EAF-2009 release. Calculations, provided by the TALYS code, have been tested and can serve as a validation of the default calculations of capture cross sections generated by TALYS.

The results can be summarized in the following conclusions (1-5) and proposals (6-7):

1. EAF-2007 (and the future EAF-2009) form the most complete high quality files of capture cross section data in the energy range 10^{-5} eV to 60 MeV. They are based on the best available data sources and use very sophisticated 'internal' tools for data production as well data testing (included in the processing code SAFEPAQ-II).
2. Analysis of the TALYS default calculations demonstrate that both statistical Hauser-Feshbach and pre-equilibrium exciton model results are of a very high quality, producing excitation curves with a physically good shape, but with a slight over estimation (factor < 2), which could be improved by a small global adjustment.
3. Regarding the available tools, the most important result of this exercise is the improvement of *the 30 keV systematic cross section formula*. Inconsistencies between sets of the level density parameters *a*, *U* were discovered which enabled previous disagreements to be explained. The newly derived formula has been successfully tested against the experimental data and can now serve as an additional validation tool for the statistical cross section component for all targets. In addition a new *systematic estimate for thermal cross sections* has been derived, based on the most recent recommended experimental values.
4. All EAF-2007 (n,γ) reactions have been graphically reviewed (plot files are available on request) and tested against the cross section systematics and a number of modification are proposed for the future EAF-2009 (see Appendices 1-3).
5. Reactions with no experimental support have been extensively reviewed, and for the first time their quantitative validation, based on the 30 keV systematic, has been carried out with very consistent results.
6. Three new Quality Score classifications are proposed. Reactions containing a resolved resonance region should be considered to be supported by broad energy information. This may change the Quality Score for a number of reactions from 2 to 4. For split reactions, the experimental data for the total (FS = 99) are proposed to be considered, especially for targets with one dominant reaction channel, and applied as a Score assignment both to the summed reaction (shown in brackets) and also to the dominant reaction. In this connection, inclusion of the summed total cross section to the EAF point-wise file is proposed for consideration. Finally, for the validation of Score = 0 reactions it is recommended that 30 keV validation information be routinely considered, leading to Score = 0_2 and Score = 0_1 assignments.
7. The only remaining action from this study is the possible revision of the included resolved resonance data. In the last few years, there have been a number of new experiments as well as data revisions included in the latest releases of libraries (such as EFDF/B-VII and JEFF-3.1) and the new resonance data from such sources should be considered for EAF-2009. This action is proposed to be completed during 2008.

Acknowledgement

This work, supported by United Kingdom Engineering and Sciences Research Council and the European Communities under the contract of Association between EURATOM and UKAEA, was carried out within the framework of the European Fusion Development Agreement. The views and opinions expressed herein do not necessarily reflect those of the European Commission.

6. References

[1] J Kopecky, MG Delfini, HAJ van der Kamp and D Nierop, *'Revisions and extensions of neutron capture cross-sections in the European Activation File EAF-3'*, **ECN-C-92-051**, 1992 and

J-Ch Sublet, JA Simpson, RA Forrest, J Kopecky and D Nierop, '*The European Activation File EAF-97 Cross section library – (n,γ) reactions*', **UKAEA FUS 352**, June 1997.

[2] RA Forrest, J Kopecky and J-Ch Sublet, *'The European Activation File: EAF-2007 cross section library'*, EASY Documentation Series, **UKAEA FUS 535 ,** March 2007 and
RA Forrest, '*SAFEPAQ-II User manual',* **UKAEA FUS 454**, Issue 7, 2007.

[3] V Benzi, GC Panini and G Reffo, FISPRO II: *A Fortran Code for Fast Neutron Radiative Capture Calculations*, **CNEN RT/FI(44)**, 1969 and
H Gruppelaar, FISPRO-ECN: *A modified and updated version of FISPRO II*, unpublished, 1974.

[4] AM Lane and JE Lynn, Gen. Contr. PUAE, Vol. 15, P/4 (1958) and GE Brown, *Nucl. Phys*. **57,** 339, 1964.

[5] Zhao Zhixiang and Zou Delin, *Chin. J. of Nucl. Physics*, **13**, 139, 1991.

[6] SF Mughabghab, M Divadeenam and NE Holden, *'Neutron cross-sections, Vols. 1 A,B: Neutron resonance parameters and thermal cross-sections'*, Academic Press, Orlando, Florida, 1981; 1984.

[7] PG Young, '*Global and Local Optical Model Parameterisation*' in "Proc. Specialists' Meeting on the Use of the Optical Model for the Calculation of Neutron Cross Sections below 20 MeV", Paris 13-15 November 1985, OECD/NEA Report **NEANDC – 222'U'**, 127, 1986.

[8] G Reffo, *Parameter Systematics for Statistical Calculations of Neutron Reaction Cross Sections*, CNEN Report, **RT/FI(78)**, 1978.

[9] G Reffo, M Blann, T Komoto and RJ Howerton, *Nucl. Instr. Meth*. **A267,** 408, 1988.

[10] DM Brink, Oxford University thesis, (unpublished), 1955.

[11] J Speth and A van der Woude, *Rep.Prog.Phys*. **44,** 719, 1981.

[12] JJ Griffin, *Phys. Rev. Let.*, **17**, 478, 1966.

[13] Shi Xiangjun, H Gruppelaar and JM Akkermans, *Nucl. Phys.*, **A466**, 333, 1987.

[14] Shi Xiangjun, J Kopecky and H Gruppelaar, *'Description of the NGAMMA code and user manual'*, **ECN-NFA-FUS-90-05**, 1990.

[15] B Buck and F Perey, *Phys. Rev. Lett.*, **8**, 444, 1962.

[16] B Buck and F Perey, *Nuc. Phys.*, **32**, 353, 1962.

[17] M Uhl, Private communication.

[18] '*Handbook for calculations of nuclear reaction data – Reference input parameter library'*, **IAEA-TECDOC-1034**, August 1998.

[19] J Kopecky and M Uhl, *Phys. Rev. C*, **41**, 1941, 1990.

[20] J Kopecky, M Uhl and RE Chrien, *Phys. Rev. C*, **47**, 312, 1993.

[21] M Uhl and J Kopecky, *'Gamma-ray strength function models and their parameterization'*, **INDC(NDS)-355**, 157, 1995.

[22] SS Dietrich and BL Berman, *At. Data Nucl. Data Tables*, **38**, 199, 1988.

[23] AV Varlamov *et al*, *'Atlas of Giant Dipole Resonances'*, **INDC(NDS)-394**, 157, 1999.

[23] AJ. Koning, S Hilaire and MC Duijvestijn, '*TALYS: Comprehensive nuclear reaction modeling'*, Proceedings of the International Conference on Nuclear Data for Science and Technology - ND2004, AIP vol. 769, eds. R.C. Haight, M.B. Chadwick, T. Kawano, and P. Talou, Sep. 26 - Oct. 1, 2004, Santa Fe, USA, p. 1154, 2005 and TALYS website: www.talys.eu

[24] AJ Koning and JP Delaroche, *Nucl. Phys*. **A713**, 231, 2003.

[25] JM Akkermans and H Gruppelaar, Phys. Lett. **157B**, 95, 1985.

[26] M Uhl and J Kopecky, *The sensitivity of statistical model capture calculations to model assumptions'*, Proceedings of an International Conference, Jülich, 977, 1991.

[27] M Uhl and J Kopecky, '*Neutron Capture Cross section and Gamma-ray Strength Functions*', presented at 2nd International Symposium on Nuclear Astrophysics – Nuclei in Cosmos – Karlsruhe, July 1992.
[28] M Herman, '*EMPIRE-II and its Application to the Radiative Neutron Capture*', Proceedings of the 11th Int. Symp. Capture Gamma-Ray Spectroscopy and Related Topics, Prague, 2-6 September 2002, (World Scientific 2003).
[29] S Mughabghab, *'Atlas of Neutron Resonances, Resonance parameters and thermal cross-sections Z = 1-100'*, Elsevier, Amsterdam, 2006.
[30] ZY Bao and F Kaeppeler, *At. Data Nucl. Data Tables, **36**, 447, 1987.*
[31] K Niedzwieuk *et al*, *Acta Physica Polonica*, **B13**, 51, 1982.
[32] Zhao Zhixiang *et al.*, *Nuclear data for science and technology*, Proceedings of an International Conference, MITO, 513, 1988.
[33] J Kopecky, GM Delfini and M Uhl, *'Proceedings of specialist meeting on neutron activation cross-sections for fission and fusion energy applications'*, **NEANDC-259 U**, 201, 1990.
[34] ZY Bao et al., *At. Data Nucl. Data Tables*, **76**, 70-154, 2000.
[35] A Gilbert and AGW Cameron*, Can. J. Physics*, **43**, 1445, 1965.
[36] RA Forrest and J Kopecky, *'The European Activation File: EAF-2001 cross section library'*, EASY Documentation Series, **UKAEA FUS 451,** March 2001.
[37] '*Handbook for calculations of nuclear reaction data – RIPL-2'***, IAEA-TECDOC-1506**, August 2006.
[38] H Gruppelaar, HAJ van der Kamp, J Kopecky and D Nierop, '*The REAC-ECN-3 data library with activation cross sections for use in fusion reactor technology'*, **ECN-207**, May 1988.
[39] M Wagner and H Warhanek, *Acta Phys. Austriaca*, **52**, 23, 1980.
[40] R. Forrest *et al*., '*Validation of EASY-2005 using integral measurements'*, **UKAEA FUS 526,** January 2006.

Appendix 1.

Reactions of type (n,γ) with IS = All and FS = 99 and Score = 3-6 (254 reactions)

Reaction Score notations and modification comments:

*	FS=99 data plotted, FS=0, 1 and/or 2 data exist in EAF-2007
Resonance region	taken from the data source
No resonance region	data source in brackets
SRA	Single Resonance Approximation applied in EAF
Score in brackets	Scores for g/m/n/(Total) reaction shown
RPL-TALYS-6a	replace by TALYS-6a data in the whole energy range
RPL-TALYS-6a >EH	replace by TALYS-6a data above energy E_H (end of the resonance range)

Reaction		Data source	QS	Modification for EAF-2009
H-1(n,γ)H-2		(ENDF/B-VI.8)	5	
H-2(n,γ)H-3		(ENDF/B-VI.8)	5	
He-3(n,γ)He-4		(IEAF-2001)	5	
Li-7(n,γ)Li-8		(EFF-2.4)	4	
B-10(n,γ)B-11		(JENDL-3.2)	4	
C-12(n,γ)C-13		(ENEA(MENGONI))	4	
C-13(n,γ)C-14		SIG-ECN	4	
N-14(n,γ)N-15		(BROND-2.2)	5	
N-15(n,γ)N-16		JENDL-3.3	4	
O-16(n,γ)O-17		(ENEA(MENGONI))	4	
O-18(n,γ)O-19		(JENDL-3.2/A)	4	
F-19(n,γ)F-20		JEF-2.2	4	
Ne-20(n,γ)Ne-21		SIGECN-MASGAM	3	
Ne-21(n,γ)Ne-22		SIGECN-MASGAM	3	
Ne-22(n,γ)Ne-23		SIGECN-MASGAM	3	
Na-22(n,γ)Na-23		JEF-2.2	5	
Na-23(n,γ)Na-24	*	JEF-2.2	2/2/(4)	
Mg-26(n,γ)Mg-27		LANL-2000	4	
Al-27(n,γ)Al-28		JEFF-3.0	4	
Si-28(n,γ)Si-29		JENDL-3.1	4	
Si-29(n,γ)Si-30		JENDL-3.1	3	
Si-30(n,γ)Si-31		JENDL-3.1	4	
P-31(n,γ)P-32		JEF-2.2	4	
Cl-35(n,γ)Cl-36		SIGECN-MASGAM	4	
Cl-37(n,γ)Cl-38	*	JENDL-3.2	4/2/(4)	
Ar-40(n,γ)Ar-41		JEF-2.2	4	
K-39(n,γ)K-40		JENDL-3.1	4	
K-41(n,γ)K-42		JENDL-3.1	4	
Ca-40(n,γ)Ca-41		JENDL-3.1	4	
Ca-42(n,γ)Ca-43		JENDL-3.1	4	
Ca-43(n,γ)Ca-44		JENDL-3.1	4	RPL-TALYS-6a >EH RN-EXP
Ca-46(n,γ)Ca-47		(JENDL-3.1)	4	RPL-TALYS-6a >EH RN-EXP
Ca-48(n,γ)Ca-49		JENDL-3.1	4	
Sc-45(n,γ)Sc-46	*	JENDL-3.2	3/3/(3)	
Ti-46(n,γ)Ti-47		JENDL-3.1	4	

Ti-47(n,γ)Ti-48		JENDL-3.1	4	
Ti-48(n,γ)Ti-49		JENDL-3.1	4	
Ti-49(n,γ)Ti-50		JENDL-3.1	4	
Ti-50(n,γ)Ti-51		JENDL-3.1	4	
V-51(n,γ)V-52		JENDL-3.1	6	
Cr-50(n,γ)Cr-51		EFF-2.4	4	
Cr-52(n,γ)Cr-53		EFF-2.4	4	
Cr-53(n,γ)Cr-54		EFF-2.4	4	
Cr-54(n,γ)Cr-55		EFF-2.4	4	
Mn-52(n,γ)Mn-53		MASGAM	5	SRA
Mn-55(n,γ)Mn-56		IRDF-P	6	
Fe-54(n,γ)Fe-55		ENDF/B-VI	4	
Fe-56(n,γ)Fe-57		ENDF/B-VI	4	
Fe-57(n,γ)Fe-58		ENDF/B-VI	4	
Fe-58(n,γ)Fe-59		ENDF/B-VI	6	
Co-59(n,γ)Co-60	*	JEF-2.2	0/5/(5)	
Ni-60(n,γ)Ni-61		EFF-2.4	4	
Ni-64(n,γ)Ni-65		JENDL-3.2	4	
Cu-63(n,γ)Cu-64		ENDF/B-VI	5	
Cu-65(n,γ)Cu-66		ENDF/B-VI	6	
Zn-64(n,γ)Zn-65		JEF-2.2	4	
Zn-66(n,γ)Zn-67		SIGECN-MASGAM	4	
Zn-68(n,γ)Zn-69	*	SIGECN-MASGAM	4/5/(4)	
Ga-69(n,γ)Ga-70		SIGECN-MASGAM	4	
Ga-71(n,γ)Ga-72		SIGECN-MASGAM	4	
Ge-70(n,γ)Ge-71		SIGECN-MASGAM	4	
Ge-74(n,γ)Ge-75	*	JENDL-3.2	2/2/(4)	
As-75(n,γ)As-76		JENDL-3.2	4	
Se-74(n,γ)Se-75		JEF-2.2	4	
Se-80(n,γ)Se-81	*	JEF-2.2	4/3/(4)	
Br-79(n,γ)Br-80	*	JEF-2.2	4/4/(4)	
Kr-83(n,γ)Kr-84		JEF-2.2	4	
Kr-86(n,γ)Kr-87		(JEF-2.2)	4	SRA
Rb-85(n,γ)Rb-86	*	JEF-2.2	4/4/(4)	
Rb-87(n,γ)Rb-88		JEF-2.2	4	
Sr-84(n,γ)Sr-85	*	JEF-2.2	2/6/(6)	
Sr-86(n,γ)Sr-87	*	JENDL-3.2	2/5/(5)	
Sr-87(n,γ)Sr-88		JEF-2.2	4	
Sr-88(n,γ)Sr-89		JENDL-3.2	4	
Y-89(n,γ)Y-90	*	LANL-2000	4/6/(4)	
Zr-90(n,γ)Zr-91		JEF-2.2	4	
Zr-91(n,γ)Zr-92		JEF-2.2	4	
Zr-92(n,γ)Zr-93		JEF-2.2	4	
Zr-93(n,γ)Zr-94		JENDL-3.3	4	
Zr-94(n,γ)Zr-95		JEF-2.2	6	RPL-TALYS-6a >EH
Zr-96(n,γ)Zr-97		JEF-2.2	5	
Nb-93(n,γ)Nb-94	*	ENDF/B-VI	4/6/(4)	
Mo-92(n,γ)Mo-93	*	JEF-2.2	1/3/(4)	
Mo-94(n,γ)Mo-95		JEF-2.2	4	
Mo-95(n,γ)Mo-96		JEF-2.2	4	

Mo-96(n,γ)Mo-97		JEF-2.2	4	
Mo-97(n,γ)Mo-98		JEF-2.2	4	
Mo-98(n,γ)Mo-99		JEF-2.2	6	
Mo-100(n,γ)Mo-101		JEF-2.2	6	
Tc-99(n,γ)Tc-100		JENDL-3.2	4	
Ru-96(n,γ)Ru-97		(JEF-2.2)	4	
Ru-100(n,γ)Ru-101		JEF-2.2	4	RPL-TALYS-6a >EH
Ru-101(n,γ)Ru-102		JEF-2.2	4	
Ru-102(n,γ)Ru-103		JEF-2.2	4	RPL-TALYS-6a E>0.4 MeV
Ru-104(n,γ)Ru-105		JEF-2.2	4	RPL-TALYS-6a E>0.4 MeV
Rh-103(n,γ)Rh-104	*	JEF-2.2	5/5/(5)	
Pd-104(n,γ)Pd-105		JEF-2.2	4	RPL-TALYS-6a >EH
Pd-105(n,γ)Pd-106		JENDL-3.3	4	
Pd-106(n,γ)Pd-107	*	JEF-2.2	2/2/(4)	
Pd-107(n,γ)Pd-108		JEF-2.2	4	
Pd-108(n,γ)Pd-109	*	JEF-2.2	2/3/(4)	
Pd-110(n,γ)Pd-111	*	JEF-2.2	4/4/(4)	
Ag-107(n,γ)Ag-108	*	JEF-2.2	4/2/(4)	
Ag-109(n,γ)Ag-110	*	JENDL-3.2	4/4/(4)	
Cd-106(n,γ)Cd-107		ENDF/B-VII.2	4	
Cd-108(n,γ)Cd-109		JENDL-3.1	4	RPL-TALYS-6a >EH RN
Cd-110(n,γ)Cd-111	*	JEF-2.2	4/3/(4)	
Cd-111(n,γ)Cd-112		JEF-2.2	4	RPL-TALYS-6a >EH
Cd-112(n,γ)Cd-113	*	JEF-2.2	2/2/(4)	RPL-TALYS-6a >EH
Cd-113(n,γ)Cd-114		JEF-2.2	4	
Cd-114(n,γ)Cd-115	*	JEF-2.2	4/2/(4)	
Cd-116(n,γ)Cd-117	*	JEF-2.2	4/2/(4)	
In-113(n,γ)In-114	*	JEF-2.2	1/3/(4)	
In-115(n,γ)In-116	*	TALYS-5a	2/5/2/(5)	
Sn-112(n,γ)Sn-113	*	JEF-2.2	1/2/(4)	
Sn-114(n,γ)Sn-115		JENDL-3.2	4	
Sn-115(n,γ)Sn-116		JENDL-3.3	4	
Sn-116(n,γ)Sn-117	*	JEF-2.2	4/4/(4)	
Sn-117(n,γ)Sn-118		JENDL-3.2	4	
Sn-118(n,γ)Sn-119	*	JENDL-3.2	4/2/(4)	
Sn-119(n,γ)Sn-120		JEF-2.2	4	
Sn-120(n,γ)Sn-121	*	JEF-2.2	4/2/(4)	
Sn-122(n,γ)Sn-123	*	JEF-2.2	2/3/(3)	
Sn-124(n,γ)Sn-125	*	JEF-2.2	2/4/(4)	RPL-TALYS-6a >EH
Sb-121(n,γ)Sb-122	*	JEF-2.2	3/3/(3)	
Sb-123(n,γ)Sb-124	*	JEF-2.2	4/2/(4)	RPL-TALYS-6a >8MeV
Te-122(n,γ)Te-124	*	JEF-2.2	2/1/(4)	RPL-TALYS-6a >EH
Te-123(n,γ)Te-124		JEF-2.2	4	RPL-TALYS-6a >EH
Te-124(n,γ)Te-125	*	JEF-2.2	4/2/(4)	
Te-125(n,γ)Te-126		JEF-2.2	4	RPL-TALYS-6a >EH
Te-126(n,γ)Te-127	*	JEF-2.2	4/2/(4)	RPL-TALYS-6a >EH
Te-128(n,γ)Te-129	*	JEF-2.2	4/2/(4)	
Te-130(n,γ)Te-131	*	JEF-2.2	2/4/(4)	
I-127(n,γ)I-128		JEF-2.2	5	
I-129(n,γ)I-130	*	JEF-2.2	2/2/(4)	

Xe-128(n,γ)Xe-129	*	JEF-2.2	2/2/(4)	
Xe-129(n,γ)Xe-130		JEF-2.2	4	RPL-TALYS-6a >EH
Xe-130(n,γ)Xe-131	*	JEF-2.2	2/2/(4)	RPL-TALYS-6a >EH
Cs-133(n,γ)Cs-134	*	JEF-2.2	4/3/(4)	
Cs-134(n,γ)Cs-134	*	JEF-2.2	2/0/(4)	RPL-TALYS-6a >EH
Cs-135(n,γ)Cs-134	*	JEF-2.2	2/0/(4)	RPL-TALYS-6a >EH
Cs-137(n,γ)Cs-134	*	JEF-2.2	2/0/(4)	
Ba-134(n,γ)Ba-135	*	JEF-2.2	4/4/(4)	
Ba-135(n,γ)Ba-136	*	JEF-2.2	4/2/(4)	RPL-TALYS-6a >EH
Ba-136(n,γ)Ba-137	*	JEF-2.2	4/2/(4)	RPL-TALYS-5a >EH
Ba-137(n,γ)Ba-138		JEF-2.2	4	RPL-TALYS-5a >EH
Ba-138(n,γ)Ba-139		JEF-2.2	4	RPL-TALYS-6a >EH
La-139(n,γ)La-140		JEF-2.2	4	
Ce-140(n,γ)Ce-141		JEF-2.2	4	RPL-TALYS-6a >EH
Ce-142(n,γ)Ce-143		JENDL-3.2	4	
Pr-141(n,γ)Pr-142	*	JEF-2.2	2/2/(4)	
Nd-142(n,γ)Nd-143		JEF-2.2	4	RPL-TALYS-5a >EH
Nd-143(n,γ)Nd-144		BROND-2.2	4	
Nd-144(n,γ)Nd-145		JEF-2.2	4	RPL-TALYS-6a >EH
Nd-145(n,γ)Nd-146		JEF-2.2	4	
Nd-146(n,γ)Nd-147		JEF-2.2	4	
Nd-148(n,γ)Nd-149		JEF-2.2	4	
Nd-150(n,γ)Nd-151		JEF-2.2	4	RPL-TALYS-6a >EH RN
Pm-147(n,γ)Pm-148	*	JEF-2.2	2/2/(4)	RPL-TALYS-6a >EH
Pm-148(n,γ)Pm-149		(JEF-2.2)	4	SRA
Pm-149(n,γ)Pm-150		(TALYS-6)	4	SRA
Sm-144(n,γ)Sm-145		(JEF-2.2)	4	
Sm-147(n,γ)Sm-148		JEF-2.2	4	
Sm-148(n,γ)Sm-149		(JEF-2.2)	4	RPL-TALYS-6a
Sm-149(n,γ)Sm-150		JEF-2.2	4	
Sm-150(n,γ)Sm-151		JEF-2.2	4	RPL-TALYS-6a >EH
Sm-152(n,γ)Sm-153		JEF-2.2	5	
Sm-154(n,γ)Sm-155		JEF-2.2	4	RPL-TALYS-6a >EH
Eu-151(n,γ)Eu-152	*	JEF-2.2	2/5/2/(5)	
Eu-153(n,γ)Eu-154	*	JEF-2.2	4/0/(4)	
Gd-152(n,γ)Gd-153		JENDL-3.2	4	
Gd-154(n,γ)Gd-155		JEF-2.2	4	RPL-TALYS-6a >EH
Gd-155(n,γ)Gd-156		JEF-2.2	4	
Gd-156(n,γ)Gd-157		JEF-2.2	4	RPL-TALYS-6a >EH
Gd-157(n,γ)Gd-158		JEF-2.2	4	RPL-TALYS-6a >30keV
Gd-158(n,γ)Gd-159		JEF-2.2	4	
Gd-160(n,γ)Gd-161		JEF-2.2	6	
Tb-159(n,γ)Tb-160		JEF-2.2	4	
Dy-160(n,γ)Dy-161		JEF-2.2	4	
Dy-161(n,γ)Dy-162		JEF-2.2	4	RPL-TALYS-6a >10MeV
Dy-162(n,γ)Dy-163		JEF-2.2	4	
Dy-163(n,γ)Dy-164		JEF-2.2	4	RPL-TALYS-6a >8MeV
Dy-164(n,γ)Dy-165	*	ENDF/B-VI.7	5/6/(5)	
Ho-165(n,γ)Ho-166	*	JEF-2.2	4/2/(4)	RPL-TALYS-6a >8MeV
Er-164(n,γ)Er-165		SIGECN-MASGAM	3	

Er-166(n,γ)Er-167	*	JENDL-3.3	2/2(4)	
Er-167(n,γ)Er-168		JEF-2.2	4	RPL-TALYS-6a >8MeV
Er-168(n,γ)Er-169		SIGECN-MASGAM	4	
Er-170(n,γ)Er-171		SIGECN-MASGAM	4	
Tm-169(n,γ)Tm-170		SIGECN-MASGAM	4	
Yb-168(n,γ)Yb-170	*	SIGECN-MASGAM	1/0/(4)	
Yb-170(n,γ)Yb-171		SIGECN-MASGAM	4	
Yb-171(n,γ)Yb-172		SIGECN-MASGAM	4	
Yb-172(n,γ)Yb-173		SIGECN-MASGAM	4	
Yb-173(n,γ)Yb-174		SIGECN-MASGAM	4	
Yb-174(n,γ)Yb-175		SIGECN-MASGAM	4	
Yb-176(n,γ)Yb-177	*	SIGECN-MASGAM	4/2/(4)	
Lu-175(n,γ)Lu-176	*	ENDF/B-VI.7	2/6/(6)	
Lu-176(n,γ)Lu-177	*	ENDF/B-VI.7	4/2/(4)	RPL-TALYS-6a >8MeV
Hf-174(n,γ)Hf-175		JEF-2.2	4	RPL-TALYS-6a >EH
Hf-176(n,γ)Hf-177	*	JEF-2.2	4/0/0/(4)	
Hf-177(n,γ)Hf-178	*	JENDL-3.3	4/2/2/(4)	
Hf-178(n,γ)Hf-179	*	JEF-2.2	2/2/2/(4)	
Hf-179(n,γ)Hf-180	*	JEF-2.2	4/2/(4)	
Hf-180(n,γ)Hf-181		JEF-2.2	5	
Ta-180(n,γ)Ta-181		TALYS-6	4	
Ta-181(n,γ)Ta-182	*	JEF-2.2	6/2/5/(6)	
Ta-182(n,γ)Ta-183		JEF-2.2	4	RPL-TALYS-6a >4MeV
W-180(n,γ)W-181		SIGECN-MASGAM	4	
W-182(n,γ)W-183	*	JEF-2.2	4/0/(4)	
W-183(n,γ)W-184		JEF-2.2	4	RPL-TALYS-6a >8MeV
W-184(n,γ)W-185	*	LANL	4/2/(4)	RPL-TALYS-6a >EH
W-186(n,γ)W-187		JEF-2.2	6	RPL-TALYS-6a >10MeV
Re-185(n,γ)Re-186	*	LANL	4/2/(4)	
Re-187(n,γ)Re-188	*	JEF-2.2	4/5/(4)	RPL-TALYS-6a >EH
Os-186(n,γ)Os-187		SIGECN-MASGAM	4	
Os-187(n,γ)Os-188		SIGECN-MASGAM	4	RPL-TALYS-6a >EH
Os-188(n,γ)Os-199	*	FISPRO	0/0/(4)	RPL-TALYS-6a >8MeV
Os-189(n,γ)Os-190	*	FISPRO	4/2/(4)	RPL-TALYS-6a >EH
Os-190(n,γ)Os-191	*	FISPRO	2/2/(4)	
Os-192(n,γ)Os-193		FISPRO	4	
Ir-191(n,γ)Ir-192	*	SIGECN-MASGAM	2/2/2/(4)	
Ir-193(n,γ)Ir-194		SIGECN-MASGAM	4	
Pt-194(n,γ)Pt-195	*	LANL-2000	4/2/(4)	RPL-TALYS-6a >8MeV
Pt-196(n,γ)Pt-197	*	LANL-2000	4/4/(4)	RPL-TALYS-6a >8MeV
Pt-198(n,γ)Pt-199	*	LANL-2000	4/2/(4)	
Au-197(n,γ)Au-198	*	IRDF-P	4/2/(4)	Correct dropped channels
Hg-198(n,γ)Hg-199	*	SIGECN-MASGAM	4/2/(4)	RPL-TALYS-5a >EH
Hg-199(n,γ)Hg-200		SIGECN-MASGAM	4	RPL-TALYS-5a >EH
Hg-200(n,γ)Hg-201		SIGECN-MASGAM	4	
Hg-201(n,γ)Hg-202		LANL-2000	4	
Hg-202(n,γ)Hg-203		SIGECN-MASGAM	4	
Hg-204(n,γ)Hg-205		(MASGAM)	4	SRA
Tl-203(n,γ)Tl-204		SIGECN-MASGAM	4	
Tl-205(n,γ)Tl-206	*	SIGECN-MASGAM	4/0/(4)	

Pb-204(n,γ)Pb-205		JENDL-3.1	4	
Pb-206(n,γ)Pb-207	*	ENDF/B-VI	4/2/(4)	
Pb-207(n,γ)Pb-208		ENDF/B-VI	4	RPL-TALYS-6a >EH
Pb-208(n,γ)Pb-209		ENDF/B-VI	4	
Bi-209(n,γ)Bi-210		ENDF/B-VI	4	
Th-232(n,γ)Th-233		ENDF/B-VI.7	4	
U-233(n,γ)U-234		JENDL-3.3	4	
U-235(n,γ)U-236		JEF-2.2	4	TALYS-6a wrong
U-236(n,γ)U-237		JENDL-3.3	4	RPL-TALYS-6a >8MeV
U-237(n,γ)U-238		JENDL-3.2	4	
U-238(n,γ)U-239		JEF-2.2	4	
Np-237(n,γ)Np-238		JENDL-3.3	4	
Pu-238(n,γ)Pu-239		JENDL-3.3	4	
Pu-239(n,γ)Pu-240		JEF-2.2	4	
Pu-240(n,γ)Pu-241		JENDL-3.3	4	
Pu-241(n,γ)Pu-242		JEF-2.2	4	RPL-TALYS-6a >EH
Pu-242(n,γ)Pu-243		JEF-2.2	4	
Am-241(n,γ)Am-242	*	JENDL-3.3	4/2/(4)	
Am-243(n,γ)Am-244	*	JENDL-3.3	2/4/(4)	

Appendix 2.

Reactions of type (n,γ) with IS = All and FS = 99 and Score = 1, 2 (221 reactions)
(Experimental data at 0.0253 eV and/or 30 keV)

Reaction Score notations and modification comments:

*	FS=99 data plotted, FS=0,1 and/or 2 data exist in EAF-2007
Resonance region	taken from the data source and denoted by R in source description
SRA	Single Resonance Approximation applied in EAF
Score in brackets	Score for total cross section is shown
RPL-TALYS-6a	replace by TALYS-6a data in the whole energy range
RPL-TALYS-6a >EH	replace by TALYS-6a data above energy E_H (end of the resonance range)
2/4R	Score = 2 in EAF-2007, a new Score = 4R is assigned, based on the existence of resolved resonance region (experimentally based)

Reaction		Data source	QS	Modification for EAF-2009
Li-6(n,γ)Li-7		JENDL-3.2	2	
Be-9(n,γ)Be-10		KOPECKY-2000	2	
Be-10(n,γ)Be-11		ENEA(MENGONI)	2	
B-11(n,γ)B-12		JEF-2.2	2/4R	
C-14(n,γ)C-15		ENEA(MENGONI)	2	
O-17(n,γ)O-18		ENDF/B-VI	2	
Mg-24(n,γ)Mg-25		JENDL-3.1	2/4R	
Mg-25(n,γ)Mg-26		JENDL-3.1	2/4R	
Si-31(n,γ)Si-32		TALYS-6	2	
S-32(n,γ)S-33		JEF-2.2	2/4R	
S-33(n,γ)S-34		JEF-2.2	2/4R	
S-34(n,γ)S-35		JEF-2.2	2/4R	
S-36(n,γ)S-37		NGAMMA	2	
Cl-36(n,γ)Cl-37		MASGAM	2	SRA
Ar-36(n,γ)Ar-37		JEF-2.2	2	
Ar-38(n,γ)Ar-39		JEF-2.2	2	
Ar-39(n,γ)Ar-40		MASGAM	2	
Ar-41(n,γ)Ar-42		MASGAM	2	
K-40(n,γ)K-41		MASGAM	2	SRA
Ca-41(n,γ)Ca-42		MASGAM	2	
Ca-44(n,γ)Ca-45		JENDL-3.1	2/4R	
Ca-45(n,γ)Ca-46		MASGAM	2	SRA
Sc-46(n,γ)Sc-47		MASGAM	2	SRA
Ti-44(n,γ)Ti-45		MASGAM	2	
V-50(n,γ)V-51		SIGECN-MASGAM	2/4R	
Cr-51(n,γ)Cr-52		MASGAM	2	
Mn-53(n,γ)Mn-54		MASGAM	2	
Mn-54(n,γ)Mn-55		MASGAM	2	
Fe-55(n,γ)Fe-56		MASGAM	2	SRA
Fe-59(n,γ)Fe-60		MASGAM	2	SRA
Co-57(n,γ)Co-58	*	MASGAM	(2)	SRA
Co-58(n,γ)Co-59		JEF-2.2(MDF)	2	SRA
Co-58m(n,γ)Co-59		JEF-2.2	2	SRA

Co-60(n,γ)Co-61		MASGAM	2	SRA	
Ni-58(n,γ)Ni-59		EFF-2.4	2/4R		
Ni-59(n,γ)Ni-60		JEF-2.2	2/4R		
Ni-61(n,γ)Ni-62		EFF-2.4	2/4R		
Ni-62(n,γ)Ni-63		JENDL-3.2	2/4R		
Ni-63(n,γ)Ni-64		MASGAM	2	SRA	
Cu-64(n,γ)Cu-65		MASGAM	2	SRA	
Zn-65(n,γ)Zn-66		MASGAM	2	SRA	
Zn-67(n,γ)Zn-68		SIGECN-MASGAM	2/4R		
Zn-70(n,γ)Zn-71	*	SIGECN-MASGAM	(2/4R)		
Ge-72(n,γ)Ge-73	*	JEF-2.2	(2/4R)		RPL-TALYS-6a >EH
Ge-73(n,γ)Ge-74		JEF-2.2	2/4R		
Ge-76(n,γ)Ge-77	*	JEF-2.2	(2/4R)		
Se-75(n,γ)Se-76		MASGAM	2	SRA	
Se-76(n,γ)Se-77	*	JEF-2.2	(2/4R)		
Se-77(n,γ)Se-78		JEF-2.2	2/4R		RPL-TALYS-6a >EH
Se-78(n,γ)Se-79	*	JEF-2.2	(2/4R)		
Se-79(n,γ)Se-80	*	MASGAM	(2)		
Se-82(n,γ)Se-83	*	JEF-2.2	(2/4R)		
Br-81(n,γ)Br-82	*	JEF-2.2	(2/4R)		
Kr-78(n,γ)Kr-79	*	JEF-2.2	(2)		
Kr-79(n,γ)Kr-80		MASGAM	2		
Kr-80(n,γ)Kr-81	*	JEF-2.2	(2/4R)		
Kr-81(n,γ)Kr-82		MASGAM	2		
Kr-82(n,γ)Kr-83	*	JEF-2.2	(2/4R)		
Kr-84(n,γ)Kr-85	*	JEF-2.2	(2/4R)		
Kr-85(n,γ)Kr-86		JEF-2.2	2		
Rb-86(n,γ)Rb-87		JEF-2.2	2	SRA	RPL-TALYS-6a >EH
Sr-89(n,γ)Sr-90		JEF-2.2	2		
Sr-90(n,γ)Sr-91		KOPECKY-2000	2	SRA	RPL-TALYS-6a >EH
Y-90(n,γ)Y-91		JEF-2.2	2		
Y-91(n,γ)Y-92		JEF-2.2	2		
Zr-95(n,γ)Zr-96		JEF-2.2	2/4R		
Nb-94(n,γ)Nb-95	*	JEF-2.2	(2/4R)		
Nb-95(n,γ)Nb-96		JEF-2.2	2/4R		
Tc-98(n,γ)Tc-99	*	MASGAM	(2)		
Ru-98(n,γ)Ru-99		JEF-2.2	2		
Ru-99(n,γ)Ru-100		JEF-2.2	2/4R		
Ru-103(n,γ)Ru-104		JEF-2.2(MDF)	2/4R		
Ru-105(n,γ)Ru-106		JEF-2.2	2		
Ru-106(n,γ)Ru-107		JEF-2.2	2		
Rh-105(n,γ)Rh-106	*	TALYS-6	(2)		
Pd-102(n,γ)Pd-103		JEF-2.2	2	SRA	
Ag-110m(n,γ)Ag-111	*	MASGAM	(2)	SRA	
Ag-111(n,γ)Ag-112		TALYS-6	2		
Cd-109(n,γ)Cd-110		MASGAM	2	SRA	
Cd-113m(n,γ)Cd-114		JEF-2.2	2/4R		
Cd-115(n,γ)Cd-116		TALYS-6	2		
Cd-115m(n,γ)Cd-116		TALYS-6	2		
In-114m(n,γ)In-115	*	MASGAM	(2)		

Sn-113(n,γ)Sn-114		MASGAM	2	SRA	RPL-TALYS-6a E>10 eV
Sb-124(n,γ)Sb-125		JEF-2.2	2	SRA	RPL-TALYS-6a E>10 eV
Te-120(n,γ)Te-121	*	JEF-2.2	(2)	SRA	
Te-127m(n,γ)Te-128		JENDL-3.2	2		RPL-TALYS-6a >EH
I-125(n,γ)I-126		MASGAM	2		RPL-TALYS-6a
I-126(n,γ)I-127		MASGAM	2	SRA	
I-128(n,γ)I-129		MASGAM	2	SRA	RPL-TALYS-6a
I-130(n,γ)I-131		JEF-2.2	2	SRA	RPL-TALYS-6a
I-131(n,γ)I-132	*	JEF-2.2	(2)		RPL-TALYS-6a >EH
Xe-124(n,γ)Xe-125	*	JEF-2.2	(2/4R)		
Xe-126(n,γ)Xe-127	*	JEF-2.2	(2/4R)		RPL-TALYS-6a >EH
Xe-131(n,γ)Xe-132	*	JEF-2.2	(2/4R)		
Xe-132(n,γ)Xe-133	*	JEF-2.2	(2/4R)		
Xe-133(n,γ)Xe-134	*	JEF-2.2	(2)	SRA	RPL-TALYS-6a >EH
Xe-134(n,γ)Xe-135	*	JEF-2.2	(2)	SRA	RPL-TALYS-6a >EH
Xe-135(n,γ)Xe-136		JENDL-3.2	2	SRA	
Xe-136(n,γ)Xe-137	*	JENDL-3.2	(2/4R)		
Ba-130(n,γ)Ba-131	*	SIGECN-MASGAM	(2/4R)		
Ba-132(n,γ)Ba-133	*	JENDL-3.3	(2)		RPL-TALYS-6a
Ba-133(n,γ)Ba-134		MASGAM	2	SRA	
Ba-139(n,γ)Ba-140		MASGAM	2	SRA	
Ba-140(n,γ)Ba-141		JEF-2.2	2/4R		RPL-TALYS-6a >EH
La-138(n,γ)La-139		JENDL-3.1	2/4R		
La-140(n,γ)La-141		JEF-2.2	2		RPL-TALYS-6a >EH
Ce-134(n,γ)Ce-135	*	MASGAM	(2)		
Ce-135(n,γ)Ce-136		MASGAM	2		RPL-TALYS-6a
Ce-136(n,γ)Ce-137	*	SIGECN-MASGAM	(2/4R)		
Ce-137(n,γ)Ce-138		TALYS-6a	2		
Ce-138(n,γ)Ce-139	*	MASGAM	(2)	SRA	RPL-TALYS-6a >E3
Ce-139(n,γ)Ce-140		MASGAM	2	SRA	
Ce-141(n,γ)Ce-142		JEF-2.2	2	SRA	RPL-TALYS-5a
Ce-143(n,γ)Ce-144		JEF-2.2	2	SRA	RPL-TALYS-6a
Ce-144(n,γ)Ce-145		JEF-2.2	2/4R		
Pr-142(n,γ)Pr-143		JEF-2.2	2	SRA	RPL-TALYS-6a
Pr-143(n,γ)Pr-144	*	JEF-2.2	(2)		RPL-TALYS-6a
Nd-147(n,γ)Nd-148	*	JEF-2.2	(2/4R)		RPL-TALYS-6a >EH
Pm-146(n,γ)Pm-147		MASGAM	2	SRA	
Pm-148m(n,γ)Pm-149		JEF-2.2	2	SRA	RPL-TALYS-6a >EH
Pm-151(n,γ)Pm-152		MASGAM	2	SRA	RPL-TALYS-6a
Sm-145(n,γ)Sm-146		MASGAM	2	SRA	
Sm-151(n,γ)Sm-152		JEF-2.2	2/4R		RPL-TALYS-6a >EH
Sm-153(n,γ)Sm-154		JEF-2.2	2	SRA	
Eu-152(n,γ)Eu-153		ENDF/B-VI	2/4R		
Eu-152m(n,γ)Eu-153		JEF-2.2	2/4R		
Eu-154(n,γ)Eu-155		ENDF/B-VI.8	2/4R		
Eu-155(n,γ)Eu-156		JENDL-3.2	2/4R		
Gd-148(n,γ)Gd-149		MASGAM	2	SRA	
Gd-153(n,γ)Gd-154		MASGAM	2	SRA	
Tb-160(n,γ)Tb-161		NGAMMA	2		
Dy-156(n,γ)Dy-157		SIGECN-MASGAM	2/4R		

Dy-158(n,γ)Dy-159		SIGECN-MASGAM	2/4R		
Dy-159(n,γ)Dy-160		MASGAM	2	SRA	
Dy-165(n,γ)Dy-166		MASGAM	2	SRA	
Ho-163(n,γ)Ho-164	*	MASGAM	(2)		
Ho-166m(n,γ)Ho-167		MASGAM	2	SRA	
Er-162(n,γ)Er-163		SIGECN-MASGAM	2/4R		
Er-169(n,γ)Er-170		MASGAM	2		
Er-171(n,γ)Er-172		MASGAM	2		
Tm-170(n,γ)Tm-171		SIGECN-MASGAM	4-2		
Tm-171(n,γ)Tm-172	*	SIGECN-MASGAM	2/4R		RPL-TALYS-6a >EH RN
Yb-169(n,γ)Yb-176		SIGECN-MASGAM	2/4R		
Yb-175(n,γ)Yb-176	*	MASGAM	(2)		RPL-TALYS-6a
Lu-177(n,γ)Lu-178	*	MASGAM	(2)	SRA	
Lu-177m(n,γ)Lu-178	*	MASGAM	(2)		RPL-TALYS-6
Hf-178(n,γ)Hf-179		JEF-2.2	2(4)		
Hf-181(n,γ)Hf-182	*	MASGAM	(2)	SRA	
Hf-182(n,γ)Hf-183		MASGAM	2		
Ta-179(n,γ)Ta-180	*	MASGAM	(2)		
W-185(n,γ)W-186		MASGAM	2	SRA	
W-187(n,γ)W-188		MASGAM	2	SRA	
W-188(n,γ)W-189		MASGAM	2	SRA	
Re-184(n,γ)Re-185		MASGAM	2	SRA	
Re-186(n,γ)Re-187		MASGAM	2		
Re-188(n,γ)Re-189		MASGAM	2		
Os-184(n,γ)Os-185		MASGAM	2	SRA	RPL-TALYS-6a
Os-191(n,γ)Os-192	*	MASGAM	(2)		
Os-193(n,γ)Os-194		MASGAM	2		
Ir-192(n,γ)Ir-193		SIGECN-MASGAM	2/4R		RPL-TALYS-6a >EH
Ir-194(n,γ)Ir-195	*	MASGAM	(2)	SRA	
Pt-190(n,γ)Pt-191		SIGECN-MASGAM	2/4R		
Pt-192(n,γ)Pt-193	*	FISPRO	(2/4R)		
Pt-193(n,γ)Pt-194		MASGAM	2		
Pt-195(n,γ)Pt-196		SIGECN-MASGAM	2/4R		RPL-TALYS-6a >EH
Au-198(n,γ)Au-199		MASGAM	2	SRA	RPL-TALYS-6a >EH
Au-199(n,γ)Au-200	*	MASGAM	(2)	SRA	
Hg-203(n,γ)Hg-204		MASGAM	2		
Hg-196(n,γ)Hg-197		SIGECN-MASGAM	2/4R		
Tl-204(n,γ)Tl-205		MASGAM	2	SRA	
Pb-205(n,γ)Pb-206		MASGAM	4		Change score to 2
Pb-210(n,γ)Pb-211		TALYS-6	2		RPL-TALYS-6a >EH
Bi-210(n,γ)Bi-211		MASGAM	2		RPL-TALYS-6a >EH
Bi-210m(n,γ)Bi-211		MASGAM	2	SRA	RPL-TALYS-6a
Po-210(n,γ)Po-211	*	MASGAM	(2)		RPL-TALYS-6a
Rn-222(n,γ)Rn-223		TALYS-6a	2		
Ra-223(n,γ)Ra-224		JENDL-3.1	2	SRA	
Ra-224(n,γ)Ra-225		JENDL-3.1	2	SRA	
Ra-226(n,γ)Ra-227		JENDL-3.1	2/4R		
Ra-228(n,γ)Ra-229		TALYS-6	2		
Ac-227(n,γ)Ac-228		JENDL-3.1	2	SRA	RPL-TALYS-6a >EH
Th-228(n,γ)Th-229		JENDL-3.1	2		RPL-TALYS-6a >EH

Th-229(n,γ)Th-230		JENDL-3.1	2/4R		
Th-230(n,γ)Th-231		JENDL-3.3	2/4R		
Th-234(n,γ)Th-235		JENDL-3.1	2		
Pa-231(n,γ)Pa-232		JENDL-3.2	2/4R		
Pa-232(n,γ)Pa-233		JENDL-3.1	2	SRA	
Pa-233(n,γ)Pa-234	*	JENDL-3.3	(2/4R)		
U-232(n,γ)U-233		ENDF/B-VI.8	2/4R		
U-234(n,γ)U-235	*	JENDL-3.3	(2/4)		
Np-235(n,γ)Np-236	*	MASGAM	(2)	SRA	RPL-TALYS-6a >EH
Np-236(n,γ)Np-237		MASGAM	2		
Np-239(n,γ)Np-240	*	JEF-2.2	(2)	SRA	RPL-TALYS-6a >EH
Pu-236(n,γ)Pu-237	*	JENDL-3.3	(2/4R)		
Pu-243(n,γ)Pu-244		TALYS-6a	2		
Pu-244(n,γ)Pu-245		JENDL-3.3	2/4R		
Am-242(n,γ)Am-243		JEF-2.2	2	SRA	
Am-242m(n,γ)Am-243		JEF-2.2	2/4R		
Cm-245(n,γ)Cm-246		JENDL-3.3	2/4R		
Cm-246(n,γ)Cm-247		JENDL-3.3	2/4R		
Cm-247(n,γ)Cm-248		JENDL-3.3	2/4R		
Cm-248(n,γ)Cm-249		JENDL-3.3	2/4R		
Cm-249(n,γ)Cm-250		JENDL-3.3	2/4R		
Cm-250(n,γ)Cm-251		JENDL-3.1	2	SRA	
Bk-249(n,γ)Bk-250		JENDL-3.2	2/4R		
Bk-250(n,γ)Bk-251		JENDL-3.1	2/4R		
Cf-249(n,γ)Cf-250		JENDL-3.3	2/4R		
Cf-250(n,γ)Cf-251		JENDL-3.3	2/4R		
Cf-251(n,γ)Cf-252		JEF-2.2	2/4R		
Cf-252(n,γ)Cf-253		JENDL-3.3	2/4R		
Cf-253(n,γ)Cf-254		KOPECKY-2000	2	SRA	RPL-TALYS-5a >EH
Cf-254(n,γ)Cf-255		JENDL-3.1	2		RPL-TALYS-6a
Es-253(n,γ)Es-254	*	JEF-2.2(MDF)	(2/4R)		
Es-254(n,γ)Es-255		KOPECKY-2000	2		RPL-TALYS-6a
Es-254m(n,γ)Es-255		KOPECKY-2000	2		
Es-255(n,γ)Es-256	*	JENDL-3.1	(2)	SRA	
Fm-255(n,γ)Fm-256		JENDL-3.1	2		
Cm-242(n,γ)Cm-243		JEF-2.2	2/4R		
Cm-243(n,γ)Cm-244		JENDL-3.3	2/4R		
Cm-244(n,γ)Cm-245		JENDL-3.2	2/4R		

Appendix 3.

Reactions of type (n,γ) with IS = All and FS = 99 and Score = 0 (337 reactions)

Reaction Score notations and modification comments:

Reaction entry	0.5 < C/S < 2 at 30 keV
Reaction entry (italics)	C/S < 0.5 or C/S > 2 at 30 keV
*	FS=99 data plotted, FS=0, 1 and/or 2 data exist in EAF-2007
RR	resolved resonance region
RRC	resolved resonance region from ground state target used in isomeric target
GRR	random generated resolved resonance region
SRA	single reaction approximation
?	no σ_{30} systematic can be calculated (no parameters)
RPL-TALYS-6a	replace by TALYS-6a data in the whole energy range
RPL-TALYS-6a >EH	replace by TALYS-6a data above the energy E_H (the end of the resonance range
Modifications (italics)	to improve C/S at 30 keV
Modifications	to improve the shape of the excitation curve, especially between statistical- and PEQ- components

Reaction		**Data source**	**Modification for EAF-2009**	
Be-7(n,γ)Be-8		TALYS-5a	?	Strange shape
Na-24(n,γ)Na-25		NGAMMA		
Mg-28(n,γ)Mg-29		NGAMMA		*RPL-TALYS-6a*
Al-26(n,γ)Al-27		NGAMMA		*RPL-TALYS-6a*
Si-32(n,γ)Si-33		TALYS-6a		
P-32(n,γ)P-33		MASGAM		*RPL-TALYS-6a*
P-33(n,γ)P-34		MASGAM		
S-35(n,γ)S-36		NGAMMA		*RPL-TALYS-6a*
Ar-37(n,γ)Ar-38		MASGAM		*RPL-TALYS-6a*
Ar-42(n,γ)Ar-43		NGAMMA		
K-42(n,γ)K-43		MASGAM		
K-43(n,γ)K-44		MASGAM		
Ca-47(n,γ)Ca-48		MASGAM		*RPL-TALYS-6a*
Sc-44m(n,γ)Sc-45	*	MASGAM		
Sc-47(n,γ)Sc-48		MASGAM		
Sc-48(n,γ)Sc-49		MASGAM		
Ti-45(n,γ)Ti-46		MASGAM		*RPL-TALYS-6a*
V-48(n,γ)V-49		MASGAM		
V-49(n,γ)V-50		MASGAM		
Cr-48(n,γ)Cr-49		ADL-3		*RPL-TALYS-6a*
Fe-52(n,γ)Fe-53	*	TALYS-6a		
Fe-60(n,γ)Fe-61		MASGAM		*RPL-TALYS-6a*
Co-55(n,γ)Co-56		MASGAM		
Co-56(n,γ)Co-57		MASGAM		
Ni-56(n,γ)Ni-57		MASGAM		
Ni-57(n,γ)Ni-58		MASGAM		
Ni-66(n,γ)Ni-67		MASGAM		*RPL-TALYS-6a*
Cu-67(n,γ)Cu-68	*	MASGAM		

Zn-62(n,γ)Zn-63		TALYS-6a		
Zn-69m(n,γ)Zn-70		MASGAM		*RPL-TALYS-6a*
Zn-72(n,γ)Zn-73	*	MASGAM		*RPL-TALYS-6a*
Ga-66(n,γ)Ga-67		TALYS-6a		
Ga-67(n,γ)Ga-68		MASGAM		
Ga-72(n,γ)Ga-73		MASGAM		
Ge-68(n,γ)Ge-69		MASGAM		*RPL-TALYS-6a*
Ge-69(n,γ)Ge-70		MASGAM		
Ge-71(n,γ)Ge-72		MASGAM		
Ge-77(n,γ)Ge-78		MASGAM		*RPL-TALYS-6a*
As-71(n,γ)As-72		MASGAM		
As-72(n,γ)As-73		MASGAM		
As-73(n,γ)As-74		MASGAM		
As-74(n,γ)As-75		MASGAM		
As-76(n,γ)As-77		MASGAM		
As-77(n,γ)As-78		MASGAM		
Se-72(n,γ)Se-73	*	MASGAM		
Se-73(n,γ)Se-74		MASGAM		
Br-76(n,γ)Br-77	*	MASGAM		
Br-77(n,γ)Br-78		MASGAM		
Br-82(n,γ)Br-83		MASGAM		
Kr-76(n,γ)Kr-77		ADL-3		RPL-TALYS-6a
Rb-82m(n,γ)Rb-83		TALYS-6a		
Rb-83(n,γ)Rb-84	*	MASGAM		
Rb-84(n,γ)Rb-85		MASGAM		
Sr-82(n,γ)Sr-83	*	MASGAM		
Sr-83(n,γ)Sr-84		MASGAM		
Sr-85(n,γ)Sr-86		MASGAM		
Sr-91(n,γ)Sr-92		TALYS-6a		
Y-86(n,γ)Y-87	*	MASGAM		
Y-87(n,γ)Y-88		MASGAM		
Y-87m(n,γ)Y-88		TALYS-5a		
Y-88(n,γ)Y-89		MASGAM		
Y-93(n,γ)Y-94		TALYS-6a		
Zr-86(n,γ)Zr-87	*	ADL-3		*RPL-TALYS-6a*
Zr-88(n,γ)Zr-89	*	MASGAM		
Zr-89(n,γ)Zr-90	*	MASGAM		
Zr-97(n,γ)Zr-98	*	MASGAM		
Nb-90(n,γ)Nb-91	*	MASGAM		
Nb-91(n,γ)Nb-92	*	MASGAM		
Nb-91m(n,γ)Nb-92	*	MASGAM		
Nb-92(n,γ)Nb-93	*	MASGAM		
Nb-92m(n,γ)Nb-93	*	MASGAM		
Nb-93m(n,γ)Nb-94	*	ENDF/B-VI(MDF)	RRC	
Nb-95m(n,γ)Nb-96		JEF-2.2	RRC	
Nb-96(n,γ)Nb-97	*	MASGAM		
Mo-93(n,γ)Mo-94		MASGAM		
Mo-93m(n,γ)Mo-94		TALYS-6		
Mo-99(n,γ)Mo-100		JEF-2.2		*RPL-TALYS-6a*
Tc-95(n,γ)Tc-96	*	MASGAM		

Tc-95m(n,γ)Tc-96	*	MASGAM		
Tc-96(n,γ)Tc-97	*	MASGAM		
Tc-97(n,γ)Tc-98		MASGAM		
Tc-97m(n,γ)Tc-98		MASGAM		
Tc-99m(n,γ)Tc-100		TALYS-6a		
Ru-97(n,γ)Ru-98		MASGAM		
Rh-99(n,γ)Rh-100	*	MASGAM		
Rh-99m(n,γ)Rh-100	*	MASGAM		
Rh-100(n,γ)Rh-101	*	MASGAM		
Rh-101(n,γ)Rh-102	*	MASGAM		
Rh-101m(n,γ)Rh-102	*	MASGAM		
Rh-102(n,γ)Rh-103	*	MASGAM		
Rh-102m(n,γ)Rh-103		MASGAM		
Pd-100(n,γ)Pd-101		MASGAM		RPL-TALYS-6a
Pd-101(n,γ)Pd-102		MASGAM		
Pd-103(n,γ)Pd-104		MASGAM		
Pd-109(n,γ)Pd-110		MASGAM		
Pd-112(n,γ)Pd-113	*	MASGAM		*RPL-TALYS-6a*
Ag-105(n,γ)Ag-106	*	MASGAM		
Ag-106m(n,γ)Ag-107	*	MASGAM		
Ag-108m(n,γ)Ag-109	*	MASGAM		
Cd-107(n,γ)Cd-108		TALYS-6a		
In-111(n,γ)In-112	*	MASGAM		
Sn-117m(n,γ)Sn-118		JEF-2.2	RRC	
Sn-119m(n,γ)Sn-120		JEF-2.2	RRC	*RPL-TALYS-6a >EH*
Sn-121m(n,γ)Sn-122		MASGAM		
Sn-123(n,γ)Sn-124		JEF-2.2		*RPL-TALYS-6a*
Sn-125(n,γ)Sn-126		JEF-2.2		RPL-TALYS-6a
Sn-126(n,γ)Sn-127	*	JEF-2.2		RPL-TALYS-6a
Sb-119(n,γ)Sb-120	*	MASGAM		
Sb-120m(n,γ)Sb-121		MASGAM		
Sb-122(n,γ)Sb-123		MASGAM		
Sb-125(n,γ)Sb-126	*	JEF-2.2		RPL-TALYS-6a
Sb-126(n,γ)Sb-127		JEF-2.2		RPL-TALYS-6a
Sb-127(n,γ)Sb-128	*	MASGAM		
Sb-128(n,γ)Sb-129	*	TALYS-6a		
Te-118(n,γ)Te-119	*	MASGAM		
Te-119(n,γ)Te-120		MASGAM		
Te-119m(n,γ)Te-120		MASGAM		
Te-121(n,γ)Te-122		MASGAM		
Te-121m(n,γ)Te-122		MASGAM		
Te-123m(n,γ)Te-124		JEF-2.2	RRC	RPL-TALYS-6a >EH
Te-125m(n,γ)Te-126		JEF-2.2	RRC	RPL-TALYS-6a >EH
Te-127(n,γ)Te-128		JEF-2.2		RPL-TALYS-6a
Te-129(n,γ)Te-130		JEF-2.2		RPL-TALYS-6a
Te-129m(n,γ)Te-130		JEF-2.2		RPL-TALYS-6a
Te-131m(n,γ)Te-132		MASGAM		
Te-132(n,γ)Te-133	*	JEF-2.2		*RPL-TALYS-6a*
I-123(n,γ)I-124		MASGAM		
I-124(n,γ)I-125		MASGAM		

I-133(n,γ)I-134	*	MASGAM		
I-135(n,γ)I-136	*	TALYS-6a		
Xe-122(n,γ)Xe-123		ADL-3		RPL-TALYS-6a
Xe-125(n,γ)Xe-126		MASGAM		
Xe-127(n,γ)Xe-128		MASGAM		
Xe-129m(n,γ)Xe-130		JEF-2.2	RRC	
Xe-131m(n,γ)Xe-132		JEF-2.2	RRC	
Xe-133m(n,γ)Xe-134	*	JEF-2.2		RPL-TALYS-6a
Cs-127(n,γ)Cs-128		TALYS-6a		
Cs-129(n,γ)Cs-130		MASGAM		
Cs-131(n,γ)Cs-132		MASGAM		
Cs-132(n,γ)Cs-133		MASGAM		
Cs-136(n,γ)Cs-137	*	JEF-2.2	RRC	RPL-TALYS-6a >EH
Ba-128(n,γ)Ba-129	*	MASGAM		
Ba-129(n,γ)Ba-130		MASGAM		
Ba-131(n,γ)Ba-132		MASGAM		
Ba-133m(n,γ)Ba-134		MASGAM		
Ba-135m(n,γ)Ba-136	*	JEF-2.2	RRC	
La-135(n,γ)La-136	*	MASGAM		
La-137(n,γ)La-138		MASGAM		
La-141(n,γ)La-142		MASGAM		
Ce-137m(n,γ)Ce-138		MASGAM		
Nd-140(n,γ)Nd-141	*	MASGAM		
Nd-141(n,γ)Nd-142		MASGAM		
Nd-149(n,γ)Nd-150		MASGAM		
Pm-143(n,γ)Pm-144		MASGAM		
Pm-144(n,γ)Pm-145		MASGAM		
Pm-145(n,γ)Pm-146		MASGAM		
Pm-150(n,γ)Pm-151		MASGAM		
Sm-146(n,γ)Sm-147		MASGAM		
Sm-156(n,γ)Sm-157		TALYS-6a		
Eu-145(n,γ)Eu-146		MASGAM		
Eu-146(n,γ)Eu-147		MASGAM		
Eu-147(n,γ)Eu-148		MASGAM		
Eu-148(n,γ)Eu-149		MASGAM		
Eu-149(n,γ)Eu-150	*	MASGAM		
Eu-150(n,γ)Eu-151		MASGAM		
Eu-150m(n,γ)Eu-151		MASGAM		
Eu-156(n,γ)Eu-157		JEF-2.2		*RPL-TALYS-6a*
Eu-157(n,γ)Eu-158		JEF-2.2		*RPL-TALYS-6a*
Gd-146(n,γ)Gd-147		MASGAM		
Gd-147(n,γ)Gd-148		MASGAM		
Gd-149(n,γ)Gd-150		MASGAM		
Gd-150(n,γ)Gd-151		MASGAM		
Gd-151(n,γ)Gd-152		MASGAM		
Gd-159(n,γ)Gd-160		MASGAM		
Tb-151(n,γ)Tb-152	*	MASGAM		
Tb-152(n,γ)Tb-153		MASGAM		
Tb-153(n,γ)Tb-154	*	MASGAM		
Tb-154(n,γ)Tb-155		MASGAM		

Tb-154m(n,γ)Tb-155		TALYS-5a		
Tb-154n(n,γ)Tb-155		TALYS-5a		
Tb-155(n,γ)Tb-156	*	MASGAM		
Tb-156(n,γ)Tb-157		MASGAM		
Tb-156m(n,γ)Tb-157		TALYS-5a		
Tb-156n(n,γ)Tb-157		MASGAM		
Tb-157(n,γ)Tb-158	*	MASGAM		
Tb-158(n,γ)Tb-159		MASGAM		
Tb-161(n,γ)Tb-162		MASGAM		
Dy-153(n,γ)Dy-154		TALYS-6a		
Dy-154(n,γ)Dy-155		MASGAM		
Dy-155(n,γ)Dy-156		MASGAM		
Dy-157(n,γ)Dy-158		MASGAM		
Dy-166(n,γ)Dy-167		MASGAM		RPL-TALYS-6a
Ho-164(n,γ)Ho-165		ADL-3		RPL-TALYS-6a
Ho-164m(n,γ)Ho-165		ADL-3		*RPL-TALYS-6a*
Ho-166(n,γ)Ho-167		MASGAM		
Er-160(n,γ)Er-161		TALYS-5a		
Er-161(n,γ)Er-162		MASGAM		
Er-165(n,γ)Er-166		MASGAM		
Er-172(n,γ)Er-173		MASGAM		
Tm-165(n,γ)Tm-166		MASGAM		
Tm-166(n,γ)Tm-167		MASGAM		
Tm-167(n,γ)Tm-168		MASGAM		
Tm-168(n,γ)Tm-169		MASGAM		
Tm-172(n,γ)Tm-173		MASGAM		
Tm-173(n,γ)Tm-174		TALYS-6a		
Yb-166(n,γ)Yb-167		MASGAM		
Lu-169(n,γ)Lu-170	*	MASGAM		
Lu-170(n,γ)Lu-171	*	MASGAM		
Lu-171(n,γ)Lu-172	*	MASGAM		
Lu-172(n,γ)Lu-173		MASGAM		
Lu-173(n,γ)Lu-174	*	MASGAM		
Lu-174(n,γ)Lu-175		MASGAM		
Lu-174m(n,γ)Lu-175		MASGAM		
Hf-170(n,γ)Hf-171		MASGAM		
Hf-171(n,γ)Hf-172		MASGAM		
Hf-172(n,γ)Hf-173		MASGAM		
Hf-173(n,γ)Hf-174		MASGAM		
Hf-175(n,γ)Hf-176		MASGAM		
Hf-178n(n,γ)Hf-179	*	JEF-2.2	RRC	
Hf-179n(n,γ)Hf-180	*	JEF-2.2	RRC	
Hf-180m(n,γ)Hf-181		JEF-2.2	RRC	*RPL-TALYS-6a >EH*
Ta-175(n,γ)Ta-176		TALYS-6a		
Ta-176(n,γ)Ta-177		TALYS-6a		
Ta-177(n,γ)Ta-178	*	MASGAM		
Ta-183(n,γ)Ta-184		MASGAM		
Ta-184(n,γ)Ta-185		TALYS-6a		
W-178(n,γ)W-179	*	MASGAM		
W-181(n,γ)W-182		MASGAM		

Re-181(n,γ)Re-182	*	MASGAM		
Re-182(n,γ)Re-183		MASGAM		
Re-182m(n,γ)Re-183		TALYS-5a		
Re-183(n,γ)Re-184	*	MASGAM		
Re-184m(n,γ)Re-185		MASGAM		
Re-186m(n,γ)Re-187		MASGAM		
Re-189(n,γ)Re-190	*	MASGAM		
Os-182(n,γ)Os-183	*	MASGAM		
Os-183(n,γ)Os-184		MASGAM		
Os-183m(n,γ)Os-184		TALYS-6a		
Os-185(n,γ)Os-186		MASGAM		
Os-191m(n,γ)Os-192	*	MASGAM		
Os-194(n,γ)Os-195		MASGAM		
Ir-185(n,γ)Ir-186	*	MASGAM		
Ir-186(n,γ)Ir-187		MASGAM		
Ir-187(n,γ)Ir-188		TALYS-6a		
Ir-188(n,γ)Ir-189		MASGAM		
Ir-189(n,γ)Ir-190	*	MASGAM		
Ir-190(n,γ)Ir-191	*	MASGAM		
Ir-192n(n,γ)Ir-193		SIGECN-MASGAM	RRC	
Ir-193m(n,γ)Ir-194		SIGECN-MASGAM	RRC	
Ir-194m(n,γ)Ir-195	*	MASGAM		
Ir-196m(n,γ)Ir-197	*	MASGAM		
Pt-188(n,γ)Pt-189		MASGAM		
Pt-189(n,γ)Pt-190		MASGAM		
Pt-191(n,γ)Pt-192		MASGAM		
Pt-193m(n,γ)Pt-194		MASGAM		
Pt-195m(n,γ)Pt-196		SIGECN-MASGAM	RRC	*RPL-TALYS-6a >EH*
Pt-197(n,γ)Pt-198		MASGAM		
Pt-200(n,γ)Pt-201		MASGAM		RPL-TALYS-6a
Pt-202(n,γ)Pt-203		TALYS-5a		
Au-193(n,γ)Au-194	*	MASGAM		
Au-194(n,γ)Au-195	*	MASGAM		
Au-195(n,γ)Au-196	*	MASGAM		
Au-196(n,γ)Au-197	*	MASGAM		
Au-196n(n,γ)Au-197	*	TALYS-6		
Au-198m(n,γ)Au-199		MASGAM		
Au-200m(n,γ)Au-201		MASGAM		
Hg-193(n,γ)Hg-194		MASGAM		
Hg-193m(n,γ)Hg-194		MASGAM		
Hg-194(n,γ)Hg-195	*	MASGAM		
Hg-195(n,γ)Hg-196		MASGAM		
Hg-195m(n,γ)Hg-196		MASGAM		
Hg-197(n,γ)Hg-198		MASGAM		
Hg-197m(n,γ)Hg-198		MASGAM		
Tl-199(n,γ)Tl-200		TALYS-6a		
Tl-200(n,γ)Tl-201		MASGAM		
Tl-201(n,γ)Tl-202		MASGAM		
Tl-202(n,γ)Tl-203		MASGAM		
Pb-200(n,γ)Pb-201	*	MASGAM		

Pb-201(n,γ)Pb-202	*	TALYS-6a		
Pb-202(n,γ)Pb-203	*	MASGAM		
Pb-203(n,γ)Pb-204	*	MASGAM		
Pb-209(n,γ)Pb-210		MASGAM		*RPL-TALYS-6a*
Pb-212(n,γ)Pb-213		TALYS-6a		
Bi-203(n,γ)Bi-204		MASGAM		
Bi-204(n,γ)Bi-205		TALYS-6a		
Bi-205(n,γ)Bi-206		MASGAM		
Bi-206(n,γ)Bi-207		MASGAM		
Bi-207(n,γ)Bi-208	*	MASGAM		
Bi-208(n,γ)Bi-209		MASGAM		
Po-206(n,γ)Po-207	*	MASGAM		
Po-207(n,γ)Po-208		MASGAM		
Po-208(n,γ)Po-209		MASGAM		*RPL-TALYS-6a*
Po-209(n,γ)Po-210		MASGAM		*RPL-TALYS-6a*
Po-210(n,γ)Po-211		MASGAM		*RPL-TALYS-6a*
At-210(n,γ)At-211	*	TALYS-6a		
At-211(n,γ)At-212		TALYS-6a		
Rn-211(n,γ)Rn-212		NGAMMA		
Ra-225(n,γ)Ra-226		JENDL-3.1		
Ac-225(n,γ)Ac-226		JENDL-3.1		
Ac-226(n,γ)Ac-227		JENDL-3.1		
Ac-228(n,γ)Ac-229		TALYS-6a		
Th-227(n,γ)Th-228		JENDL-3.1		
Th-231(n,γ)Th-232		TALYS-6a		
Pa-228(n,γ)Pa-229		MASGAM		*RPL-TALYS-6a*
Pa-229(n,γ)Pa-230		MASGAM		*RPL-TALYS-6a*
Pa-230(n,γ)Pa-231		TALYS-6a		
Pa-234(n,γ)Pa-235		TALYS-6a		
U-230(n,γ)U-231		MASGAM		RPL-TALYS-6a
U-231(n,γ)U-232		MASGAM		
U-240(n,γ)U-241		ENDF/B-VII.2	RR	
U-241(n,γ)U-242		ENDF/B-VII.2	GRR	
Np-234(n,γ)Np-235		MASGAM		*RPL-TALYS-6a*
Np-236m(n,γ)Np-23		TALYS-6a		
Np-238(n,γ)Np-239		TALYS-5a		
Pu-234(n,γ)Pu-235		TALYS-6a		
Pu-237(n,γ)Pu-238		JENDL-3.3		
Pu-245(n,γ)Pu-246		TALYS-6a		
Pu-246(n,γ)Pu-247		MASGAM		*RPL-TALYS-6a*
Am-239(n,γ)Am-240		TALYS-6a		
Am-240(n,γ)Am-241		MASGAM		
Am-244(n,γ)Am-245		TALYS-6a		
Cm-240(n,γ)Cm-241		MASGAM		
Cm-241(n,γ)Cm-242		TALYS-5a		*RPL-TALYS-6a*
Bk-245(n,γ)Bk-246		NGAMMA		
Bk-246(n,γ)Bk-247		NGAMMA		
Bk-247(n,γ)Bk-248	*	NGAMMA		
Bk-248(n,γ)Bk-249		NGAMMA		
Bk-248m(n,γ)Bk-249		NGAMMA		

Cf-246(n,γ)Cf-247	NGAMMA		*RPL-TALYS-6a*
Cf-248(n,γ)Cf-249	NGAMMA		*RPL-TALYS-6a*
Es-250(n,γ)Es-251	TALYS-6a		
Es-251(n,γ)Es-252	NGAMMA		
Es-252(n,γ)Es-253	NGAMMA	?	
Es-256m(n,γ)Es-257	TALYS-6	?	
Fm-252(n,γ)Fm-253	NGAMMA		*RPL-TALYS-6a*
Fm-253(n,γ)Fm-254	NGAMMA		
Fm-257(n,γ)Fm-258	NGAMMA	?	